University of California
Santa Barbara

Discovery of *Klebsiella aerogenes* CDI Receptor and Investigation of the Binding in the Receptor

A dissertation submitted in partial satisfaction
of the requirements for the degree Doctor of Philosophy

in
Molecular, Cellular, and Developmental Biology

by

Nicole Ashley Chan

Committee in charge:

Professor Christopher S. Hayes, Chair
Professor David Low
Professor Max Wilson

June 2023

The Dissertation of Nicole Ashley Chan is approved.

Professor David Low

Professor Max Wilson

Professor Christopher S. Hayes, Committee Chair

March 2023

Discovery of *Klebsiella aerogenes* CDI Receptor and Investigation of the Binding in the Receptor

by

Nicole Ashley Chan

For my Mom, Dad, and Loren (Best Sister Ever)

Acknowledgements

To my family, thank you for the everlasting support and love in everything I do. Mom and Dad, you guys are great in every way. You have supported me in every decision and words cannot explain how much I appreciate and love you. Loren, you are the best sister there ever is/was. I love calling you for anything at all, topics ranging clothes to the most important document and presentation in my entire life. I appreciate all the help you've given me since you've been born. I wouldn't be here without you and I'd do anything for you.

Megan and Will, you guys are my best friends that all started with going on a run. Thank you for all of the fun times in the past, present, and future. Your support during this time was incredible. It was a lot, a lot of the times. Tiffany, I wouldn't have made it without you. I knew you were an excellent role model from the start. You've helped me so much with many of the mental struggles as a grad student and I am forever thankful. Shane, I definitely wouldn't have made it without you in my first year. Thank you for all of your support, patience, kindness, and advice over the years. To all of my best friends over the years, I am finally out of school and thank you for hanging with me until the end. We can actually do stuff now that I am done. To all of my undergrads, thank you so much for joining me on this journey. You have all helped me and I hope I have helped you guys as well. I will never forget any of you and the part of the journey we shared. I would like to thank my Seventh Dimension family. I would like to thank Harmony for allowing me to try out one afternoon and the rest is history. I would not have made it without you guys. All the time spent in the studio, the safe space, and the camaraderie made this journey possible. Rhys, thank you for being the most supportive, nice, and caring. You are truly the best.

Curriculum Vitæ

Nicole Ashley Chan

Education

2023	**Ph.D. in Molecular, Cellular, and Developmental Biology** (Expected), University of California, Santa Barbara.
2019	**M.A. in Molecular, Cellular, and Developmental Biology**, University of California, Santa Barbara.
2012	**B.S. in Biochemistry and Cell Biology**, University of California, San Diego

Research

2017-2023	**Graduate Student Researcher**, Department of Molecular, Cellular, and Developmental Biology, University of California, Santa Barbara

Teaching

2018-2022	**Teaching Assistant**, General Microbiology Lab, Department of Molecular, Cellular, and Developmental Biology, University of California, Santa Barbara
2022	**Teaching Assistant**, Medical Microbiology, Department of Molecular, Cellular, and Developmental Biology, University of California, Santa Barbara
2017	**Teaching Assistant**, Introduction to Biology Lab, Department of Molecular, Cellular, and Developmental Biology, University of California, Santa Barbara

Publications

Roberts, D., Estrada, D., Yagi, N., Anglin, E., Chan, N. and Sailor, M., (2017). Preparation of Photoluminescent Porous Silicon Nanoparticles by High-Pressure Microfluidization. Particle Particle Systems Characterization, 34(3), 1600326. https://doi.org/10.1002/ppsc.201600326

Kumeria, T., Wang, J., Chan, N., Harris, T. J., Sailor, M. J. (2018). Visual Sensor for Sterilization of Polymer Fixtures Using Embedded Mesoporous Silicon Photonic Crystals. ACS sensors, 3(1), 143–150. https://doi.org/10.1021/acssensors.7b00764

Zuidema, J. M., Kumeria, T., Kim, D., Kang, J., Wang, J., Hollett, G., Zhang, X., Roberts, D. S., Chan, N., Dowling, C., Blanco-Suarez, E., Allen, N. J., Tuszynski, M. H., Sailor, M. J. (2018). Oriented Nanofibrous Polymer Scaffolds Containing Protein-Loaded Porous Silicon Generated by Spray Nebulization. Advanced materials (Deerfield Beach, Fla.), 30(12), e1706785. https://doi.org/10.1002/adma.201706785

Halvorsen, T. M., Garza-Sánchez, F., Ruhe, Z. C., Bartelli, N. L., Chan, N. A., Nguyen, J. Y., Low, D. A., Hayes, C. S. (2021). Lipidation of Class IV CdiA Effector Proteins Promotes Target Cell Recognition during Contact-Dependent Growth Inhibition. mBio, 12(5), e0253021. https://doi.org/10.1128/mBio.02530-21

Kim, D., Fang, C., Joo, J., Chan, N., Chen, M.Y., Sciacca, B., Miskelly, G. M., Sailor, M. J. The Effect of Thermal Oxidation on the Optical Spectra of Rugate Porous Silicon (*Manuscript*)

Abstract

Discovery of *Klebsiella aerogenes* CDI Receptor and Investigation of the Binding in the Receptor

by

Nicole Ashley Chan

Klebsiella aerogenes is a nosocomial infectious bacteria that can become multidrug-resistant to drugs saved as the last line of defense, such as colistins and carbapenems, leading to septicemia. It has two contact dependent inhibition (CDI) systems that promote antagonistic toxin transfer among closely related bacteria. These delivery systems are used in a proximity dependent manner. Bacteria that possess the CDI phenotype utilize a large cell surface protein called CdiA, which binds to an outer membrane (OM) receptor to intoxicate neighboring cells. The toxin is the last $\sim$ 200 residues at the C-terminus of CdiA that enter the target cell and translocate across the outer and inner membrane into the cytoplasm. In previous studies, three OM receptors for CdiA in *Enterobacteria* have been identified: BamA, OmpC/F, Tsx, and the lipopolysaccharide layer. The *K. aerogenes* CDI receptor has been revealed as a Class II receptor and only utilizes OmpC for binding. In Chapter 2, I discuss the discovery of this receptor and mutations in loop 3 of OmpC which has implications in antibiotic resistance. These mutations were then duplicated in another species to confer the effect of the mutation in binding to the barrel wall and its electrostatic effect on the transport of small molecules through this non-selective porin. The mutations affect the transport of antibiotics into the cells rendering them useless. In Chapter 3, I investigate the topology of CdiB and its interaction with CdiA. The topology mapping of CdiB suggests interaction with CdiA, which is further supported with crosslinking data. Upon further investigation, the pre-

sentation of CdiA on the exterior of the cell is very robust. These results suggest that the mutations in OmpC can affect the uptake of antibiotics in the cell, therefore increasing their effectiveness and ultimately help reduce the 270,000 deaths by septicemia.

Contents

List of Tables

List of Figures

Chapter 1

Introduction

Bacteria are viewed as small individuals living in a microscopic part of the big place we call Earth. Although they are small, they make up a large part of the biomass on planet Earth. Comparing total biomass of the kingdoms measured in tons of carbon, respectively plants are 450 gigatons, bacteria are 70 gigatons, and the animal kingdom as a whole is 2 gigatons. If the animal kingdom is further segmented, people are 0.06 gigatons, terrestrial arthropods are 0.2 gigatons, and annelids are 0.2 gigatons [1]. Bacteria has the second most in terms of carbon mass. This allows them to create and dictate their local environment leading to change in the large scale for the biome as a whole. Without bacteria we may not be the oxygen breathing organisms humans are today. One of the ways they dictate the human body is through their presence of 40 trillion bacterial cells living in and around the human body that is comprised of 30 trillion eukaryotic cells. The number of bacterial cells greatly predominates human cells, but their small size only allots them 1-3% of our biomass [2]. Our microbiome provides many benefits and some disadvantages. Some advantages are absorbing nutrients, synthesizing nutrients, aiding in digestion, and space filling to prevent other more dangerous bacteria from utilizing the space [3]. Opportunistic bacteria are able to cause serious health consequences in

imbalanced natural flora environments; and possibly leading to serious and other chronic issues like irritable bowel syndrome, gastritis, and persistent bacterial bronchitis [4, 5, 6].

For bacteria to be so small to enforce a large change on us and the environment, they must collaborate and communicate with one another. Bacteria often communicate with their environment both indirectly and directly. Through quorum sensing, bacterial cells release signaling molecules called autoinducers as a form of indirect contact [7]. This communication enhances their survivorship regarding food, living in a habitable environment, and defense against invaders or other abiotic challenges. The autoinducers will only have an effect with a minimum critical mass, until a "quorum" is reached. Quorum sensing can regulate activities such as virulence factor expression, biofilm formation, sporulation, and mating [8]. They are released and dispersed to neighboring cells however they diffuse. Challenges of this are uneven signals that are sent causing a gradient of action instead of a full reaction in the surrounding cells. This message could also be sent to other cells competing for the same space and provide them with the advantage as well. For sister cells, to maintain an advantage over their competitors, contact dependent signaling is an alternative to deliver direct messages. This was observed in *Myxococcus xanthus* which has a complex signaling system to enhance colony survival using a non-diffuseable surface protein that upon contact initiates a signal cascade to induce sporulation and further surface protein expression [7]. Another example of communication is with F pili in *E. coli*. F pili are from the F plasmid which encodes the genes for the origin of transfer, origin of vegatative replication, transfer genes, and insertion elements. F pili are responsible for horizontal gene transfer, specifically the transfer of antibiotic resistance among a population of bacteria [9].

1.1 Secretion Systems

1.1.1 Type I Secretion System

The Type I Secretion Sytstem (T1SS) was found upon the discovery of a pore-forming toxin hemolysin A (HlyA) from *E. coli*. This system has large RTX proteins which are adhesins with a nonapeptide-binding sequence with the motif of GGxGxDxUx, where x can be any amino acid and U is a large hydrophobic amino acid. The sequence stands for repeats in toxins (RTX) as the name for the family. The RTX domain is located before the secretion signal at the extreme C terminus. This domain acts as an internal chaperone that keeps the polypeptide unfolded in the calcium-deprived cytosol and triggers folding in the calcium-rich extracellular matrix [10]. The T1SS consists of TolC, a membrane fusion protein, and an inner membrane protein. T1SS secretes the RTX domain [11]. To become active, HlyA is acylated by acyltransferase, HlyC which is also encoded on the same operon. HlyC catalyzes the post-translational modification of two internal lysine residues and requires an acyl carrier protein. The modification is required to form a pore in the host membrane, but not required for exportation to the extracellular space. The acylation to be active is recorded in other hemolysins and other members of the RTX family. The traditional activity for this toxin is forming pores in the target cells to alter cell permeability [12]. The canonical substrate for T1SS is an uncleavable C terminal signal sequence on the RTX domain [11].

This system is novel in that it is a one-step process to move from the cytosol to the extracellular space. This system is also Sec independent, which means that it does not require the Sec pathway to move its substrate from the inner membrane to the periplasm [13]. The Sec pathway moves proteins in an unfolded state from the cytoplasm to the periplasmic space. The Sec pathway consists of three parts which include a protein targeting component, a motor protein, and a membrane integrated channel. Proteins

that use this pathway have an N terminal, hydrophobic signal sequence that consists of three regions: a positively charged amino terminal, a hydrophobic core, and a polar carboxy termninal. The signal sequence is removed when translocated by the Sec B protein which serves as one of the proteins that guides the exportee to the SecYEG channel. After transport to the periplasm, the protein is folded [14].

T1SS translocates adhesins, iron-scavenger proteins, lipases, proteases, or pore-forming toxins [13, 14]. It utilizes an ABC transporter, ATP-binding cassette, which exports small molecules such as antibiotics and toxins out of the cell. The ABC transporter is the inner membrane component that catalyzes ATP to provide the energy to move the substrate across the membrane [15]. The six transmembrane helices create a concave bowl at the end of the channel crossing the inner membrane leading to the periplasm [16]. T1SS also utilizes a membrane fusion protein (MFP) and an outer membrane factor (OMF). The membrane fusion protein crosses the inner membrane and connects it to the outer membrane factor which generates the pore in the outer membrane to the extracellular matrix. These three proteins are the essential components for T1SS.

T1SS is used by *Serratia marcescens* that secretes hemophore HasA. *Vibrio cholerae* uses this system to secrete the MARTX toxin which is much larger and has a novel repeat section [17, 12]. MARTX causes cell rounding that affects the actin cytoskeleton leading to a loss in cell structure [12]. Uropathogenic *E. coli* secrete HlyA which causes pores to form in target cells. The *E. coli* toxin can also insert into erythrocytes and nucleated eukaryotic cells causing them to rupture [18]. The bursting of these cells help bacteria cross mucosal barriers, thus hindering clearance of the infection [19].

1.1.2 Type II Secretion System:

The Type II secretion system (T2SS) is utilized by pathogenic and non-pathogenic bacteria [20]. The T2SS moves folded proteins from the periplasm to the extracellular matrix and is one of the most conserved systems in Gram-negative bacteria [20, 14]. The exported proteins are moved to the periplasm via the Sec or Tat secretion system [21]. The Sec pathway moves unfolded proteins where as the Tat system moves folded proteins from the cytoplasm to the periplasm [14]. The Tat pathway is important because not all proteins can be secreted in their unfolded state because they may have specific post-translational modifications that cannot be made in the periplasm or in the extracellular space. The Tat system is comprised of a few subunits called TatA, TatB, and TatC. Once the signal peptide binds to TatB and TatC, they recruit TatA to form the membrane spanning channel. The Tat signal sequence has twin arginines that form the S-R-R motif at the N terminus of the protein [22]. Once in the periplasm, the protein can be secreted by T2SS [14].

The T2SS contains 12-15 different proteins encoded in a single operon. The components can be broken down into the pseudopilus, outer membrane complex, inner membrane platform, and the secretion ATPase. The pseudopilus is co-translated and moved into the inner membrane through the Sec pathway [20]. The outer membrane complex is made of the outer membrane protein, GspD. GspD is affiliated with other secretins from other secretion systems. The outer membrane complex is assembled by the GspS, which is also known as the T2SS pilotin. This pilotin is a chaperone that supports oligomerization, assembly, and insertion into the outer membrane [23]. The inner membrane platform is made of four proteins that use transmembrane helices to anchor in the inner membrane. The ATPase is located in the cytoplasm and provides the energy to power the system [14]. The mechanism for this secretion system starts with the recognition of

the N-terminal signal sequence targeting for the periplasm via the Sec or Tat pathway. The exoprotein binds to GspC which has been identified as critical for substrate recognition. The substrate is loaded into the lumen contacting the N0 and N1 domains of the GspD[23]. The pseudopilus assembly is initiated by the minor pseudopilins and GspG is constructed with roughly 24 copies to push the substrate through the central gate to be released extracellularly [24]. There is not a lot of information about the pseudopilus disassembly or retraction, but it is thought to have a disordered disassembly where the pseudopilins remain in the inner membrane [25, 20].

The T2SS contributes to the pathogenicity of *Vibrio cholerae*, enterotoxigenic and enterohemorrhagic *Escherichia coli*, *Pseudomonas aeruginosa*, and *Legionella pneumonphila* to name a few [26, 27, 28, 29]. *V. cholerae* export the cholera toxin and cause watery diarrhea, vomiting, and thirst. *E. coli* EHEC and ETEC release a heat labile toxin which resembles the cholera toxin. EHEC and ETEC can cause cholera-like diarrhea and up to 380,000 deaths annually among children under 5 years of age [30]. *P. aerguinosa* is known for releasing exotoxin A, LasA and LasB proteases, type IV protease, and phospholipase H, as well as lipolytic enzymes causing pneumonia with an increased mortality rate [31]. *L. pneumonphila* secretes many virulence factors that cause damage to lung tissue and Legionnaires' disease [32].

1.1.3 Type III Secretion System:

The Type III secretion system (T3SS) is found in a large number of Gram-negative pathogens and non-pathogenic bacteria alike [33]. This system resembles a molecular syringe. It transports substrates across the inner and outer membrane into the extracellular matrix and can export them into host cells [14]. The T3SS has a core of 9 proteins, which are highly conserved among the systems [34, 35]. This secretion system has evolved from

the flagella and shares eight proteins in common [36]. In combination, T3SS requires over twenty proteins to form its exportation complex. This system is made of three major components consisting of a base complex, a needle component, and a translocon. These components are usually transferred horizontally and are found on pathogenicity islands or on plasmids. The ability to transport effectors into target cells results in increasing the survivorship and colonization. T3SS can deliver to trans-kingdom targets. The effectors can manipulate the host cell immune response, cytoskeleton activity, vesicle transport, and signal transduction[37, 38, 39, 40, 41, 42].

T3SS are related to the flagellar proteins. The base complex is a series of ring structures in the inner and outer membrane consisting of five proteins [43]. The cytosolic ring is located beneath the base complex and is involved in the substrate sorting and recruitment [44]. The cytosolic ring is a substructure common to both the flagella and T3SS [45, 46]. The needle allows the bacteria to inject effectors into the host cells. The needle is arranged from hundreds of proteins with the C-terminal pointing to the needle lumen similar to flagella construction [47]. The needle has a hollow inner core that allows an unfolded effector to be loaded into it [14]. The translocon is assembled upon contact with the host cell and forms a pore that is essential for delivery. This complex is thought to be assembled inside-out starting with the inner membrane similar to flagella assembly. The second model is outside-in starting with the rings forming in the outer membrane first [48].

This secretion system had a significant role in the plague, typhoid fever, and dysentery [49, 50]. Several bacteria use T3SS to establish and maintain intracellular life cycles. *Salmonella* use T3SS from two different pathogenicity islands to invade host cells; pathogenicity island-1 is used to invade the host by creating a vacuole in the cell, and pathogenicity island-2 promotes intracellular survival and replication [37]. *Chlamydia* also use T3SS to invade the host cells by creating a vacuole to support survival [51].

Shigella uses T3SS to deliver its primary virulence factor, invasion plasmid antigen C, which changes the cytoskeleton integrity [52]. *E. coli* that is enteropathogenic and enterohemorrhagic also used this system to attach to the host cells and exploit the epitheilal barrier to increase survivorship [53]. T3SS is also used by *Yersinia pestis* to deliver the plague using *Yersinia* outer proteins that inhibit bacterial phagocytosis and suppress the production of pro-inflammatory cytokines [54].

1.1.4 Type IV Secretion System:

The Type IV secretion system (T4SS) is a secretion system related to bacterial conjugation [14]. T4SS can transport single proteins, protein-protein complexes, and DNA-protein complexes [55]. This systems can also deliver to a variety of target cells such as bacteria of the same species, different species, and eukaryotic cells in a contact-dependent manner [56]. This system is homologous and the model of this system is from *Agrobacterium tunefícans*. *A. tunefícans* uses T4SS to move oncogenic T-DNA into plant cells causing crown galls [57]. This model system is composed of twelve proteins, VirB1-VirB11 and VirD4 [58]. Other T4SS members may contain a complete set of homologous proteins, while others do not. T4SS members can be classified by the effector molecules that are delivered and fall into two major classes of conjugation: baterial uptake and release, and effector delivery [59]. Some systems deliver effectors into host cells that have ulcers, sexually transmitted infections, or fatal pneumonia while others transfer plasmids harboring antibiotic resistance genes [60].

VirB6-10 are found in the periplasm, inner membrane, and outer membrane to form the secretion channel and some accessory proteins [61]. VirB4, VirB11, and VirD4 are located in the inner membrane and are the ATPase that power this system. VirD4 is also a coupling protein that binds to the substrate before secretion through the channel.

VirB5 and VirB2 compose the extracellular pilus extending to the target cell [62]. The crystal structure of this system is largely unresolved but the cryo-electron microscopy has provided some insights. The inner membrane complex was observed by cloning VirB3-VirB10 to show the localization of these proteins. This paper has shown that there is a localization of VirB7, VirB9, and VirB10 in the outer membrane, commonly called the core complex. VirB3 and VirB4 are associated with the inner membrane complex with unconfirmed distribution of VirB5, VirB6, and VirB8 also in the inner membrane complex [63]. The core complex was confirmed to have VirB7, VirB9, and VirB10 in a 1:1:1 ratio with 14 copies of each protein. This forms a complex that is roughly 1100 kDa with a diameter and height of 185 angstroms [60].

The mechanism for T4SS starts with the effectors having a C-terminal signal sequence or having one or more internal signals for docking onto the T4CP receptor [64]. The role of T4CP is to act as the substrate receptor. The ATPases then catalyze the translocation. In our model system, *A. tumefaciens*, VirB4 subunits catalyze the movement of the substrate, but it is still unknown how it works. VirB4 has not been shown to form crosslinks with the substrate and works as a mediator to form crosslinks between the substrate and VirB6 and VirB8. VirB11 is required for substrate transfer and the biogenesis of the pilus [62]. The substrate is then transferred to VirB8 as it moves to the outer membrane complex. VirB10 senses the substrate in the system and acts as a switch to activate the ATPases. The pilus then forms and extends to the target cell, forming a central chamber of 100 angstroms. It is unknown how the ATPases contribute to pilus formation, but there is literature about the substrate only moving through the channel upon contact with the target cell. The receptor for the *A. tumefaciens* T4SS system is unknown and remains a key to understanding how it can deliver to a variety of bacterial, plant, fungal, and human cell types. Some bacteria such as *Helicobacter pylori* deliver CagA that can interfere with host signaling pathways that are the cause of

peptic ulcers and gastric carinomas [58, 65]. Another T4SS from *Neisseria gonorrhoeae* is responsible for the sexually transmitted infection gonorrhea and secretes ssDNA directly into the external environment, which may help with initial biofilm formation [66]. *Legionella pneumophila* causes Legionnaires' disease which is a potentially fatal form of pneumonia that can live and grow in alveolar macrophages to avoid bacteriocidal host activities [67, 55].

1.1.5 Type V Secretion System:

The Type V secretion system (T5SS) is categorized by having two distinct regions referred to as secreted passenger and a β-barrel domain that resides in the outer membrane [68]. This class of systems is also characterized by autotransport meaning that ATP or a proton gradient force does not power the transport of these systems to the exterior of the cell [69]. This system is also known for the dependency on the Sec system for inner membrane transit to the periplasm. The BAM complex then facilitates the folding of the β-barrel in the outer membrane [70]. The T5SS has subclasses labeled type Va to Ve (Fig. 1.1). The subclasses are divided by passenger domain that is exported [71].

Type Va:

Type Va secretion systems (T5aSS) are monomeric autotransporters. They are expressed as a single polypeptide and use the Sec machinery to transport into the periplasm in an unfolded state. These autotransporters have low amounts of cysteine residues in these secreted proteins to minimize complications through the Sec machinery by avoiding disulfide bonds before transport to the extracellular matrix [69]. T5aSS β-barrel domain is 12-stranded and anchors the barrel to the outer membrane. The exported passenger domain usually consists of a β-helical passenger domain and it uses an autochaperone

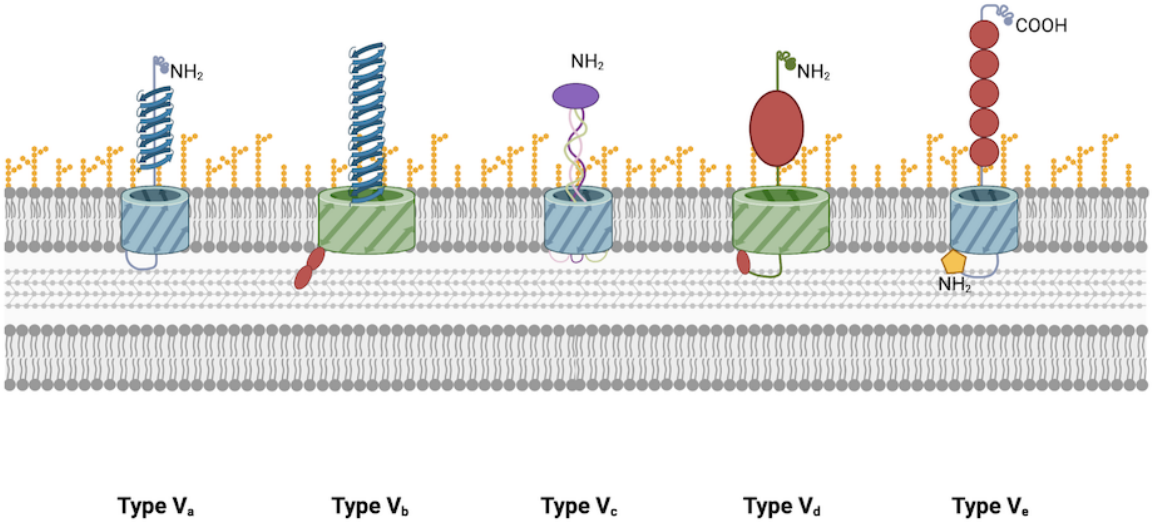

Figure 1.1: Overview of Type 5 secretion systems. Cartoon illustration of the protein components of T5aSS through T5eSS to demonstrate the diversity of these complexes. All figures created with Biorender.

at its C-terminus to properly fold outside of the cell. It is thought to follow the hairpin model where a hairpin loops out of the pore formed by the β-barrel then it starts to fold C- to the N-terminus, pulling out the protein in the process [72, 73].

To begin the secretion, BamA recognizes the C-terminal motif of the β-barrel and is also an essential outer membrane protein. BAM stands for the β-barrel assembly machinery, and BamA in combination with BamB-E export the β-barrel to the outer membrane [74]. The passenger domain may have a wide variety of functions from enzymatic, proteolytic, adhesive, cytotoxic, to contributing to colonization, biofilm formation, and immune evasion [70]. Examples of T5aSS users are IgA proteases from *Neisseria meningitidis*, which cleave antigen binding determinants to allow binding to mucous membranes. AIDA-I is an adhesin from *E. coli* to mediate attachment to epithelial cells, and Per-

tactin from *Bordetella pertussis* is used to attach to ciliated cells in the upper respiratory tract [75, 76, 77, 78, 79]. These virulence factors use this transport system and many of these autotransporters are self cleaved once they have completed secretion into the extracellular matrix [69].

Type Vb:

Type Vb secretion systems (T5bSS) are often called two-partner secretion systems and refer to having a pair of proteins on different polypeptide chains on the same operon involved in the secretion process. The first partner refers to secreted protein (TspA) and the second partner refers to the translocator β-barrel protein (TspB) forming the two-partner secretion (TPS) system [14, 69]. TspB is a 16-strand β-barrel with two polypeptide transport associated (POTRA) domains integrated into the outer membrane [68]. The fate of TspA secretion may differ with some proteins released into extracellular matrix and others remain firmly attached to the outer membrane. TspA is characterized by having a $\sim$300 residue TPS domain in their N-terminal region with the full length of the protein ranging from $\sim$700 to over 5000 amino acids in length [37]. TspA can be referred to as the passenger domain, which can act as a cytotoxin, adhesin, protease, or a heme-binding protein [80, 81, 82]. The structure of TspA is shown to be a β-helical filament that extends away from the outer membrane. The structure is thought to aid in stability, protease resistance, and binding to promote aggregation and receptor binding [83, 84].

The operon is arranged with TspB before TspA. The T5bSS moves from the cytoplasm to the periplasm as a canonical T5SS through the Sec machinery and utilizes the BAM complex for β-barrel insertion into the outer membrane. The β-barrel has two periplasmic POTRA domains that play a role in substrate recognition [85]. TspA also uses the hairpin model to thread through the β-barrel and fold in the extracellular matrix as a

β-helical filament [83, 86]. T5bSS has been observed in a large variety of Gram-negative bacteria. *Bordetella pertussis* makes FHA, filamentous haemagglutinin, a major adhesin and significant contributing factor to whooping cough [87]. *Serratia marcescens* makes the haemolytic ShlA/B system that leads to the lysis of cells by forming pores in the cell membrane [88]. In *Haemophilus influenzae*, it uses HMW1 and HMW2 as adhesins to stick to respiratory epithelial cells. HMW1 and HMW2 stand for high molecular weight 1 and high molecular weight 2 which are proteins that share sequence identity to FHA in *Bordetella pertussis* [81]. This is localized to the respiratory tract and sometimes causes infections in the sinuses, ears, and eyes [89].

Discovery of CDI

CDI stands for contact dependent inhibition and is a T5bSS [90]. TspA corresponds to CdiA which is exported to the extracellular surface by CdiB, a 16-strand β-barrel that corresponds to TspB. The two-partner secretion system is on different polypeptide chains similar to other T5bSS. CDI is an antagonistic system inhibiting cell growth with a toxin upon contact. This was first described by Aoki et al. where *E. coli* with a CDI system were found to regulate the growth of neighboring cells [91]. This system was found in *Escherichia coli* (EC93) and inhibited the growth of *E. coli* MG 1655. MG 1655 and other laboratory strains that did not have a CDI system, therefore, were not able to inhibit other bacteria. The genes were isolated from EC93, CdiA and CdiB, and confirmed inhibitory activity when expressed in the laboratory strains [91]. These two genes are mapped to a 3-gene cluster including CdiI. This gene cluster forms the canonical CdiBAI operon. Using bioinformatics, CdiA can be separated into seven distinct regions. The region at the extreme C-terminus is where the toxin is located. To prevent self-intoxication, an immunity gene, CdiI, is encoded in the operon as well [90].

This system is widespread in α-, β-, and γ- proteobacteria with the *E. coli* and

Burkholderia thailandensis where the CDI systems are described as "*E. coli*"-type or "*Burkholderia*"-type systems [92, 93]. In the *B. thailandensis* system, the genes are arranged CdiAIOB and named bcpAIOB [94]. *B. thailandensis* is studied because it is homologous to *Burkholderia mallei* and *Burkholderia pseudomallei* that have been used in bioterrorism and require a BSL-3 lab, while *B. thailandensis* is a BSL-1 and not a human pathogen [94]. The bcpO gene encodes a lipoprotein required for BcpA function [95]. Inhibition starts with the insertion of the β-barrel, CdiB, into the outer membrane by the BAM complex [96]. CdiB is from the Omp85 family and exports CdiA through the hairpin model [97]. CdiA is roughly $\sim$300-600 amino acids in length and once exported, it enters secretion arrest where the C-terminal half remains sequestered in the periplasm. Activity resumes once the cell binds to its receptor on a target cell and the end result is the toxin being delivered to the target cell [96].

CdiA Architecture, Structure, and Function

CdiA is made of seven distinct regions. In addition to these regions, CdiA carries a signal sequence at the N-terminus for Sec-dependent secretion for transport to the periplasm [98]. The regions going from N to C-terminus are the signal sequence, TPS domain, FHA-1 region, receptor binding domain, YP region, FHA-2 region, pre-toxin domain, and the toxin domain. The transport domain (TPS) is a signal sequence at the N-terminus where CdiA intereacts with CdiB for export to the extracellular matrix [96]. The FHA region stands for filamentous hemagglutinin and this structure repeats to form a β-helical filament [70]. FHA was first identified in the *Bordetella* species and its crystal structure shows a 19 residue repeat forming nine coils [99]. FHA in CdiA forms $\sim$20 residue repeat extending to $\sim$4.8 angstroms in length, which allows the protein to extend 40-140nm from the cell surface [98]. The receptor binding domain (RBD) is the point of contact with the target cells. The sequences of this region differ between the

other sections of this protein and this has led to the discovery of different types of CDI receptors. There are at least four classes of CDI receptors [100, 101].

The YP domain is a conserved region following the RBD with dye-labeling experiments indicating that it crosses the outer membrane [96]. Without this region, the cells do not inhibit in shaking broth, but inhibit on solid agar. This means that in momentary contact, the connection to the target cell is less stable and Ruhe et al. has shown that YP deletions cause CdiA to be ejected into the extracellular matrix. The FHA-2 domain has shown to be required for toxin delivery and is stably associated with the outer membrane of the target cell to deliver the toxin across [102]. The pre-toxin domain contains the canonical cleavage site with the VENN motif or (E/Q)LYN that releases the toxin into the target bacteria [103]. The toxin domain is at the C-terminus and can have RNase, DNase, endonuclease, or pore-forming activity [92, 98]. Previous literature from the lab has shown that the regions are modular between toxins of different species.

This modularity is shown by placing a few toxins on the C-terminus of the same CdiA or "stick". Sequence alignments have shown the canonical VENN motif in the pre-toxin domain which classifies the sequence after VENN as the toxin. Three toxins from different species were made into a chimera of EC 536 CdiA and shown to be effective against their respective species without any cross-species inhibition [104, 105]. *E. coli* EC93, *Yersinia pestis*, *Dickeya dadantii*, and *E. coli* EC 536 in co-culture experiments showed that their CDI system is modular, interchangeable, and provide protection specific immunity genes to each species' toxin [104]. The modular toxins were shown to be effective and other previous work has shown that the RBD is also modular.

The sequence alignments show shared residues in the TPS, FHA-1, YP, and FHA-2 regions between EC 93, EC 536, and *E. coli* STECO31. Although all three species are *E. coli*, their CDI systems use different receptor classes and, thus, have misalignment in the RBD region. In these experiments, the "stick" used is from EC 93, but the RBD of

EC 93 was replaced with the RBD of EC 536 in some of the experiments. EC 93 uses BamA as its CDI receptor and EC 536 uses OmpC as its CDI receptor. The chimeras were able to target their respective target cells and not the *Enterobacter cloacae* controls. The authors were able use co-culture experiments to show binding and functionality and to use flow cytometry to demonstrate binding ability to target cells [106]. Modularity in the CDI system is important because it allows the study of more dangerous bacteria in a more safe manner by engineering specific parts of these bacteria into a nonpathogenic strain. For example, *D. dadantii* which is a BSL-2 bacteria can be experimented outside of a biological safety cabinet if the protein of interest is placed on a nonpathogenic lab strain [94]. The experiments in Chapter 2 are based on the modularity of the CDI system to create a chimera that is functional in co-culture and protein assays.

The first CDI toxin activity was discovered in *Erwinia chrysanthemi* and its CdiA is an adhesin with a C-terminal toxin that closely resembled the rRNase domain of colicin E3 [107]. Colicins are a bacteriocin and may have toxic effects to some strains of *E. coli* [108]. Bacteriocins are a group of antimicrobial peptides produced by bacteria, capable of killing or inhibiting growth of multi-drug resistant bacteria [109]. The purpose of bacteriocins is to inhibit the growth of similar or closely related bacteria by releasing these peptides to form pores, alter gene expression, or protein production in cells [110]. Colicin E3 is from *E. coli* W3110 and prevents protein synthesis by cleaving a single phosphodiester bond in the 16S ribosomal RNA in the 30S subunit [111]. This colicin enters the cell by binding to the BtuB receptor, but the binding does not allow direct entry into the cell and must involve additional outer membrane proteins for entry. Its secondary outer membrane protein is OmpF which forms a heterotrimer that forms an ion-permeable channel that is slightly cation-selective [112]. It is suggested that OmpF provides the channel through which unfolded domains of the colicin can pass into the periplasm [113]. TolB is also required to move colicin E3 from the periplasm to the cytoplasm [114]. Colicin E3 has a

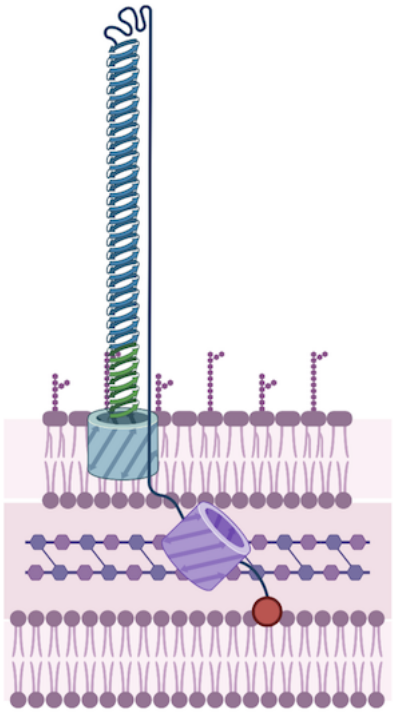

Figure 1.2: Representative illustration of CdiA structure and topology. The RBD is located at the distal tip, extended by FHA-1 repeats, while FHA-2 and toxin remain in the periplasm.

cognate immunity protein to prevent autointoxication [115]. The structural resemblence of *E. chrysanthemi* toxin to colicin E3, sequence identity, and general method of entry into target cells show that these homologs should be actively studied for their applications in antibiotic warfare and biotechnology.

1.1.6 Type VI Secretion System:

The Type VI secretion system (T6SS) is one of the more recent bacterial secretion systems discovered and is similar to a contractile phage tail [14, 116]. It undergoes a rapid conformational change where the sheath protein complex propels the T6SS spike and tube components to deliver toxic effectors into target cells in a contact dependent manner

[14]. The effectors can target eukaryotic cells, other bacteria coinfecting a mammalian host, and neighboring bacteria similar to the T4SS, which can also target prokaryotic and eukaryotic cells [116]. This system is very large and uses up to 38 proteins in *S. marcescens* or a minimum of 13 core components in *Vibrio cholerae* in a contiguous gene cluster [117]. An immunity gene is also encoded alongside the cluster to prevent self intoxication [14]. This system was first discovered in *V. cholerae* in 2006 at Harvard and widely distributed in proteobaceria [118].

The most widely studied T6SS are those from the protein superfamily haemolysin corregulated protein (Hcp) and valine-glycine repeat G (VgrG). They are both secreted and necessary for T6SS function][118]. Some systems have extra copies of Hcp and VgrG which structurally resemble bacteriophage tail tube and tailspike proteins [119]. The core components form two distinct sub assemblies which is the membrane complex that anchors the phage related complex to the cell surface [117]. TssJ, TssK, TssL, and TssM form the membrane complex while TssA, TssB, TssC, Hcp, TssE, TssF, TssG, ClpV, and VgrG form the phage related complex. TssJ, TssL, and TssM form the channel that spans the inner membrane to the outer membrane. TssJ is a lipoprotein that integrates into the outer membrane on the periplasmic side. TssL and TssM are integrated membrane proteins in the inner membrane [119]. TssB and TssC form tubes that resemble a bacteriophage sheath that allows an Hcp tubule to form inside. The assembly and disassembly of TssB and TssC may power the propelling motion before secretion with ClpV required for disassembly [120]. VgrG forms the prism tail-spike of a bacteriophage T4 at the end of the Hcp capped with a PAAR domain, which is a proline–alanine–alanine–arginine repeat [121]. TssA, TssE, TssF, and TssG are thought to form the baseplate [122].

This system is a one step mechanism thought to start with the cytoplasmic and membrane components. The membrane complex may initiate assembly in the inner

membrane to form the channel necessary to form the contractile sheath and T4-like spike [122]. The base plate forms next with TssAEFGK and once the base plate is formed, the spike will be assembled. The Hcp tail is built inside TssBC tube. The mechanism 'fires' and causes the sheath to contract and propels the Hcp-VgrG-PAAR spike into target cells. Effectors are released into the target cells causing peptidoglycan degradation, phospholipase activity, or DNase activity [118]. One of the first T6SS effectors studied was Tae which are peptidoglycan amidase effectors that can be found in *Serratia marcescens*, *Pseudomonas aeruginosa*, and *Vibrio cholerae* [123]. Other toxins are peptidoglycan glycoside hydrolase effectors (Tge) and those with lipase/esterase activity (Tle) which can be found in *Pseudomonas protegens* and *Enterobacter cloacae* [118].

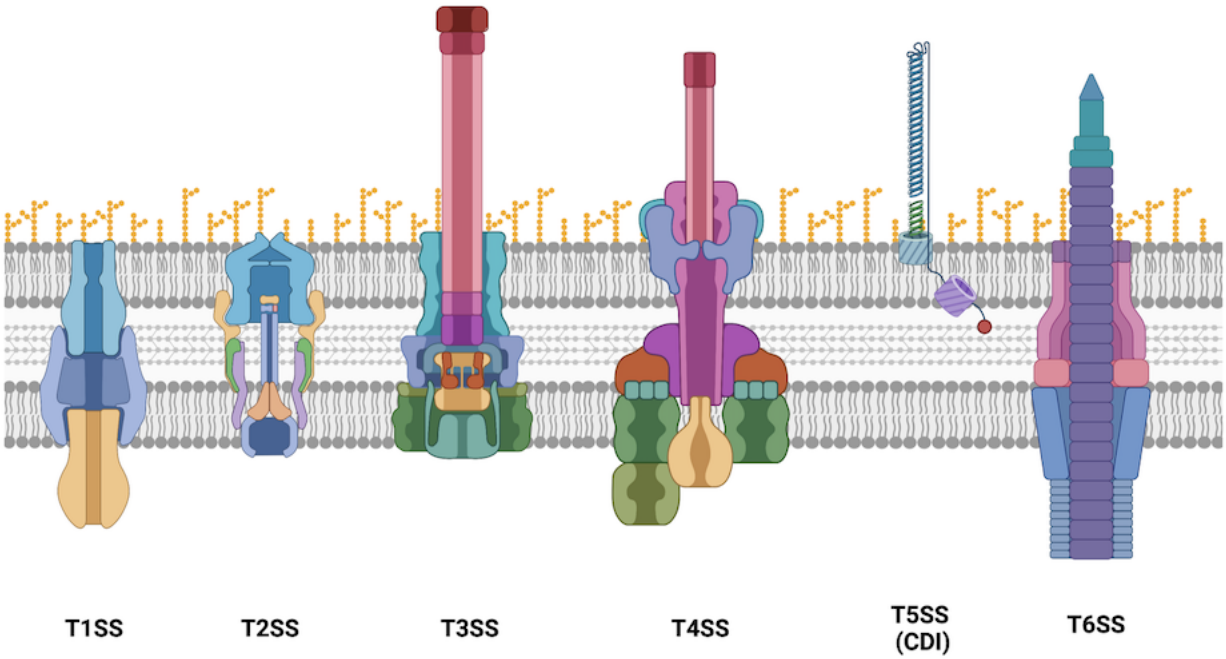

Figure 1.3: Overview of Type I through Type VI secretion in Gram-negative bacteria. Cartoon illustration of the protein components of T1SS through T6SS to demonstrate the diversity and complexity of these complexes. All figures created with Biorender.

1.1.7 Type IX Secretion System:

The Type IX secretion system (T9SS) is a unique system in that it provides mobility or a weapon depending on whether the organism is commensal or a pathogen. This system is only found in some *Bacteriodetes* [124]. *Bacteriodetes* are Gram-negative, non-spore forming, facultative anaerobic, and rod-shaped. *Bacteriodetes* can live in a variety of environments ranging from soil, ocean, freshwater, and the gastrointestinal tract of animals [125]. Two of the most studied species of this system are the *Porphyromonas gingivalis*, known for it's role in periodontitis, and *Flavobacterium johnsoniae*, which is a commensal organism found in water and soil [124]. T9SS cargo proteins are moved to the periplasm through the Sec machinery. The proteins are then recruited to the outer membrane by a C-terminal domain (CTD) sequence [126]. The CTD has been linked to proteins destined for secretion or surface attachment [127]. There are at least 19 proteins necessary for this system that have the conserved CTD to direct towards the outer membrane. The entire system has not been able to be visualized yet, but a few complexes have been seen with cryo-electron microscopy [128].

The inner membrane complex consists of PorL and PorM. The outer membrane proteins are PorE, PorF, PorG, PorK, PorN, PorP, PorQ, PorT, PorU, PorV, PorW, PorZ, and Sov [126]. PorL extends down into the cytoplasm and PorM extends into the periplasm using four domains that also interact with the PorK-N complex. This transport also requires the proton motive force powered by PorL and PorM [129]. PorK-PorN-PorG complex resides in the OM and forms a large ring-shaped structure. This ring structure forms a funnel with the PorL/M inner membrane complex. The T9SS is anchored to the cell surface using the PorU-PorV-PorQ-PorZ [128]. The assembly of this system is very complex including the substrate translocation pathway. The proposed method of substrate delivery to the cell surface involves the substrate moving up the

PorM shaft, passed to PorN, then to PorW, and then to Sov to finally attach to PorV. From here PorV is known to associate with substrates harboring the CTD sequence and anchor PorU and PorZ to the outer membrane through their interaction with PorV. PorU sorts the substrates and cleaves the CTD signal and attaches an A-LPS linking sugar to anchor the substrate to the cell surface [126].

This system can deliver cargo containing the CTD with activity ranging from peptidases, proteases, haemolysins, and adhesins important for many processes in environmental or pathogenic bacteria [124]. The working model of pathogenic mechanisms for this system uses outer membrane vesicles loaded with the virulence factors on the cell surface. The A-LPS forms a virulent coat using the T9SS. Using environmental signals, the cargo proteins are packaged into outer membrane vesicles and can spread their virulence factors to neighboring cells. The goal of the outer membrane vesicles is to dysregulate immune defense systems and generate a positive feedback loop to encourage the spread of diseases such as periodontitis. T9SS is commonly used by *Porphyromonas gingivalis*, *Treponema denticola*, *Tannerella fosythia*, and *Prevotella intermedia* which are common in patients with severe periodontal disease. They secrete virulence factors as well as heme to promote their own growth by disrupting the epithelial barrier through degrading the tight junctions in cells [126].

1.2 Permissions and Attributions

1. The content of Chapter 3 contains data collected in collaboration with Zach Ruhe.

2. The content of Chapter 4 is the result of a collaboration with Tiffany Halvorsen, and has previously appeared in the mBio [101]. It is reproduced here with her permission.

3. Figures were created with BioRender.com

Chapter 2

Discovery of *Klebsiella aerogenes* CDI Receptor and Investigation of the Binding in the Receptor

2.1 Abstract

Contact dependent inhibition is a way for bacteria to communicate with kin and with their surrounding neighbors. *Klebsiella aerogenes* has two CDI systems where each locus has the complete *cdiBAI* gene sequence. Structural differences between the loci are in sequence length where one locus creates a β-helical filament that is 33% longer than the other locus which may affect their functionality. The loci were tested for functionality and locus 1 has shown inhibition capabilities on solid agar. Here we discover OmpC is the locus 1 CDI receptor for *K. aerogenes* which makes it a Class II receptor. We investigated loop 3 in OmpC as a potential binding contact for the receptor binding domain and found that changes to the loop abrogate its ability to deliver the toxin to the target cells. We also tested mutations in a system that uses the same class of receptor, F11, to confer

similar results. Mutants in Tsx which is a smaller β-barrel were inhibited on solid agar and in liquid media, only select mutants were inhibited. The mutations in the exterior loops of Tsx change the ability to deliver a toxin to the target cells. These mutations have implications in antibiotic resistance where clinical isolates with these mutations lock loop 3 in place, rendering the antibiotic useless. The study provides insights into the effector delivery systems of emerging nosocomial infections and suggests alternative approaches to the antibiotic resistance war.

2.2 Introduction

Klebsiella aerogenes is in the *Enterobacteriaceae* family and its original name was *Enterobacter aerogenes*. The *Enterobacter* genus is able to survive in a variety of environments and therefore, can cause various outbreaks in medical settings [130]. This genus is motile, aerobic, Gram-negative, and rod-shaped. *Enterobacter* species are non-fastidious and sometimes encapsulated [131]. They are normally found in soil, water, fruits, meats, eggs, vegetables, grains, flowering plants and trees, and inside animals from insects to humans. They are also known for their ability to colonize and grow rapidly, but mostly known for their pathogenicity [132]. These bacteria are important causes of urinary tract infections (UTIs), septicemia, hospital and health care related pneumonia, intra-abdominal infections, and others. They are known for their nosocomial infections and most notably, their ability to resist antibiotics [133].

In nosocomial infections, these bacteria target those who are immunocompromised, catheterized, and elderly. More recently *E. coli* O157:H7 has emerged as a foodborne pathogen causing hemolytic uremic syndrome leading to bloody diarrhea, vomiting, unexplained bruising, and acute kidney failure in children [134]. *Enterobacteriaceae* are also known to have an economic impact on produce, livestock, and other goods. Salmonellosis

has an impact on poultry, eggs, pigs, cows, sheep, and human disease for example. A few notable instances are *Salmonella* causing Typhoid fever and *Yersinia pestis* causing the bubonic and pneumonic plague. Luckily, they are easy to grow on defined media and thus, easier to study in a lab setting [132].

The overuse and misuse of antibiotics have caused at least 700,000 people worldwide to die each year due to antibiotic resistant bacteria. The World Health Organization predicts that this number could increase to 10 million by 2050 and released a list of pathogens that are high priority in the development of new or alternative drugs to combat these bacteria. These bacteria are part of the ESKAPE pathogens referring to *Enterococcus faecium*, *Staphylococcus aureus*, *Klebsiella pneumoniae*, *Acinetobacter baumannii*, *Pseudomonas aeruginosa*, and *Enterobacter* species [131]. The growing concern with the *Enterobacter* species becoming resistant to more antibiotics which includes the last line of defense in hospitals, carbapenems and colistins. 31% of the of *Enterobacter* species infections in intensive care units in the United States involve strains not susceptible to third generation cephalosporins. This resistance is usually caused by plasmid encoded extended-spectrum β-lactamases along with other resistance genes [133].

Of the acquired infections, *K. aerogenes* and *Enterobacter cloacae* are the most common pathogens found from the *Enterobacteriaceae* family. Differentiation between the two species is done with biochemical tests of lysine decarboxylase and arginine decarboxylase activity [130]. Within the *Enterobacteriaceae* family, *K. aerogenes* has been associated with multidrug-resistance and high mortality rates in intensive care units [135]. This pathogen is acquired through cross-contamination from person to person or contaminated items [130]. Specifically, *K. aerogenes* produces β-lactamase, cephalosporinase, or alters the membrane permeability by changing porin expression or binding affinity [136]. In a study looking at septicemia where *K. aerogenes* and other species from the *Enterobacter* genus were compared for mortality and poor clinical outcomes, *K. aerogenes* was

a contributing factor in poor clinical outcomes where patients experienced acute kidney injury, septic shock, or acute lung injury [137].

The *Enterobacteriaceae* family was originally split into three genera: *Escherichia*, *Aerobacter*, and *Klebsiella*. The *Aerobacter* genus was later changed to the *Enterobacter* genus and whole genome sequencing determined that *Enterobacter aerogenes* should be moved to a different genus. Hormaeche and Edwards originally classified this into the *Enterobacter* genus and it was later re-classified in 2019 due to its higher genotypic similarity with the *Klebsiella* genus [137, 131]. It has the average genome length, number of genes, and %GC content that is in the expected range for *Klebsiella* and with isolates of *K. aerogenes* having over 95% genomic identity to confirm they belong to the same species. In a genomic analysis of the antimicrobial resistance genes in *K. aerogenes*, there are 94 and 95 resistance genes in the core and accessory genomes where the accessory resistance genes are likely acquired by horizontal gene transfer. Some of the core resistance genes confer resistance to aminoglycosides, macrolides, fluoroquinolones, sulfonamides, aminocourmarin, and tetracyclines. The acquired resistance genes involve a large number of efflux pumps and enzymes associated with antibiotic inactivation. Other virulence factors that contribute to *K. aerogenes* pathogenicity are biofilm formation, immune evasion, and toxin production [135]. To further complicate treatment, this species is also known to be resistant to colistin, another last resort antibiotic. This species can also harbor other subpopulations of colistin-resistant bacteria which are undetectable with current diagnostic testing [131].

Efflux pumps play a key role in multidrug resistance. The over expression of Resistance-Nodulation-Division (RND)-type efflux pumps cause antibacterial agents and biocides to move from the periplasm of the target to the exterior of the cell. These pumps are potential targets for novel antibacterial treatments and efflux pump inhibitors could make current antibiotics more effective [138]. The first efflux pump was discovered in

the 1990s and led to finding these pumps in Gram-positive and Gram-negative bacteria. These pumps work to transport substances against a concentration gradient and therefore, consume energy from ATP hydrolysis or chemical gradients [139].

Five major categories of efflux pumps in prokaryotes are ATP binding cassettes, small multidrug resistance family, multidrug and toxin extrusion, major facilitator superfamily, and RND [140]. The major facilitator super family, small multidrug resistance family, multidrug and toxin extrusion, and RND use the proton gradient to drive the extrusion of substrates. ATP binding cassettes (ABC transporters) are primary active transporters that use ATP for substrate extrusion. RND family only exists in Gram-negative bacteria, but are present in prokaryotes and eukaryotes. The RND efflux pump consists of three proteins that span the inner membrane, outer membrane, and the periplasmic space. Examples of the inner membrane protein are AcrB or MexB which have roles in substrate specificity. Outer membrane proteins could be TolC or OprM and the periplasmic membrane fusion protein [140, 141].

K. aerogenes uses the RND efflux pump which is responsible for the multidrug resistant phenotype by utilizing the AcrAB-TolC to export β-lactams [142]. *K. aerogenes* also overexpresses AmpC β-lactamase and modifies OmpC and OmpF expression to combat antibiotics in the environment. OmpC and OmpF reside in the outer membrane and are porins which are water-filled channels. The permeability of these proteins is controlled by their pore size and they are not specific for particular solutes. Since these are not selective, antibiotics are easily let into the cell. *K. aerogenes* modifies its OmpF and OmpC expression in reaction to the presence of antibiotics [143]. OmpC and OmpF are also part of the Class II CDI receptors and will be one of the focal points of this thesis.

CDI Receptor Classes

2.2.1 CDI Class I Receptor

The CDI Class I receptor is BamA. BamA is part of the β-barrel assembly machine in Gram-negative bacteria. Its goal is to insert β-barrel proteins into the outer membrane. BamA is an essential part of this machine, part of the Omp85 superfamily, and well conserved in all Gram-negative bacteria. BamA contains five N-terminal periplasmic polypeptide transport-associated (POTRA) domains that act as a scaffold for interaction with BamB-E [144]. It has two distinct domains consisting of the N-terminal POTRA domains and the C-terminal trans-membrane domain as the β-barrel [145]. BamA is translocated across the inner membrane by the Sec machinery and BamA is predicted to fold proteins by having an interaction of the N- and C-terminus by the open seam in the BamA barrel. Here, the β-hairpins assemble at the seam and the barrel grows into the membrane as each new strand is added [144]. Biogenesis of β-barrels in the outer membrane is complicated due to its hydrophilic pore, hydrophobic exterior, and size which can range from 8 to 24 strands [146]. BamA has 16 strands and a large cavity indicating it plays a role in substrate binding and partial folding [74].

The crystal structure of the BAM complex shows BamA and BamD interaction at POTRA domain 5 to form an extended scaffold to support interaction with BamC, BamD, and BamB. Its central cavity of BamA is approximately 30 x 60 angstroms wide. BamD is also essential in this complex and the mutations result in phenotypes that are more susceptible to membrane permeability [147]. Its crystal structure reveals that its extracellular loops form a capping dome blocking access to the pore and allowing free diffusion across the outer membrane. Loop 6 also has a conserved VRGF/Y motif which has been previously found as important in the two-partner secretion machinery of FhaC [146, 148]. Studies of FhaC have replaced the arginine with alanine causing a drop

in secretion efficiency even though the structure and channel remain unaffected. The replacement of the tyrosine affects the channel suggesting that it stabilizes the loop of FhaC [148]. These extracellular loops, specifically loops 6 and 7 were also found to be the CDI receptor for *E. coli* EC93 [149].

EC 93 has a CDI system and it uses BamA as its receptor. It is species specific where it does not bind to other species such as *Citrobacter freundii*, *K. aerogenes*, or *Proteus mirabilis* even though BamA is highly conserved in enterobacteria and has a sequence identity ranging from 73% to 93%. In an alignment of BamA sequences, loops 4, 6, and 7 had the lowest sequence conservation. These loops are also the longest of the predicted extracellular loops. Mutations were made in these loops and the loop 4 mutation in BamA showed slight resistance compared to wild-type BamA expressing cells in co-culture assays with CDI inhibitor cells. Mutations made in loops 6 and 7 showed complete resistance in co-culture assays with CDI inhibitor cells. To test whether one loop or both loops were essential, EC93 BamA loops 4, 6, and 7 were grafted onto *Enterobacter cloacae* BamA individually and in pairs to confirm the necessity. The individual grafts were unsuccessful at inhibition which meant that one loop was not enough to prohibit binding of CdiA to the target receptor. When EC93 BamA loop 6 and loop 7 were grafted onto *E. cloacae* BamA, inhibition occurred meaning that these were both necessary for binding. This was also confirmed in an aggregation assay where binding was shown by co-localization in a flow cytometer. The sequence variation of these loops is a consequence of exposure to the extracellular matrix to prevent the random binding and exploitation as a receptor from other bacteriocins [100, 149].

2.2.2 CDI Class II Receptor

The Class II CDI receptor is an OmpC and OmpF heterotrimer as shown in Fig. 2.1. These porins are passive transporters that pass small molecules across the outer membrane by facilitated diffusion [150]. OmpC is a 16-strand β-barrel and combines with two other β-barrels to form a trimer. OmpC extracellular loops form a wall to enclose the area common to the three pores with a 14 residue insertion in loop 4 as shown in Fig. 2.2. Its pore is virtually identical to OmpF, but it has an increased number of acidic residues making the lumen more negatively charged. It also has short connections between the β-strands on the periplasmic side, but has long, irregular loops on the extracellular side. These long loops are loop 1, loop 2, and loop 4-8. Loop 3 does not extend out into the extracellular space but folds down inside the barrel constricting the pore, forming a salt bridge [151, 152].

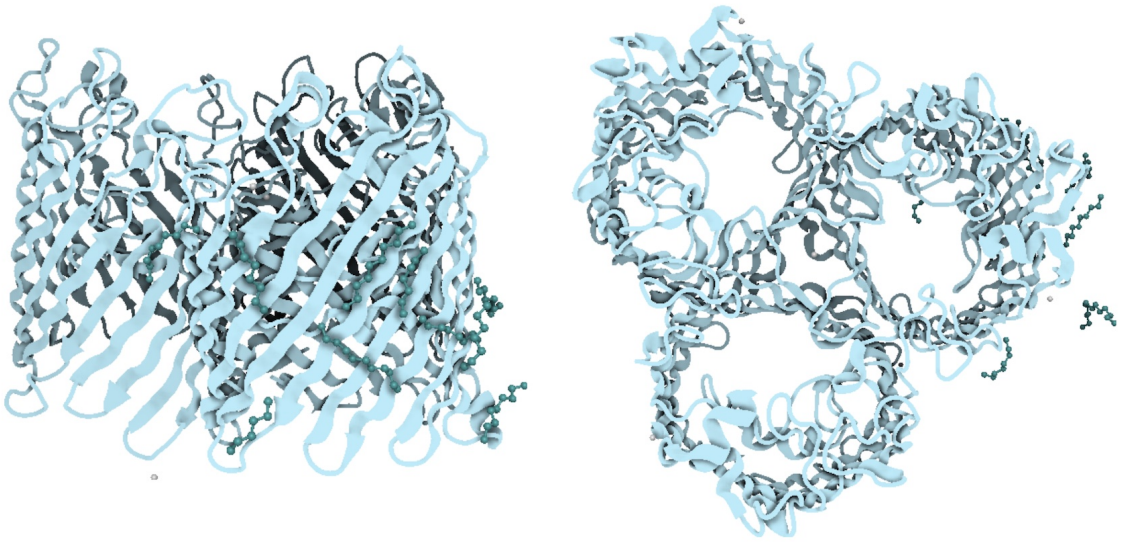

Figure 2.1: **OmpC and OmpF from *E. coli* K-12 showing the complete heterotrimer.** The left is a side view and the right is a view from the top down. All figures created with Biorender.

OmpF is a 16-strand β-barrel and is one part of a trimer. It spans the outer membrane

and has extended loops on the extra cellular side. It also has the short connections between the β-strands on the periplasmic side similar to OmpC. The channel of OmpF has limited access defined by loop 3 which connects β-strands 5 and 6 and is bent inward. This loop can also dictate the size of the pore depending on the fluctuations on the residues [153]. OmpF is widely studied for its ability to transport colicin. The colicins are thought to insert their translocation and active domains through OmpF pores. It is also one of the most abundant proteins in the outer membrane [150]. OmpF and OmpC share a high degree of sequence homology which is roughly 60%. Some of their distinguishing factors are the electrostatics in the pore [123].

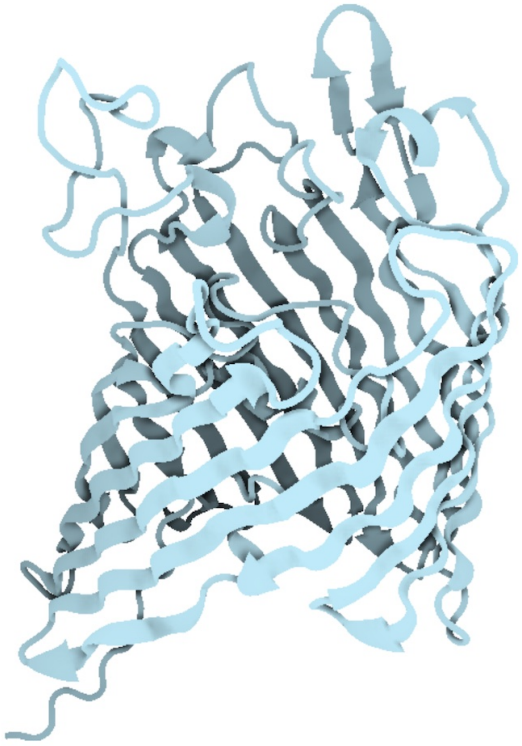

Figure 2.2: **OmpC from *E. coli* K-12 showing the 16 β-strands and the loops on the extracellular surface.** All figures created with Biorender.

E. coli EC 536 OmpC and OmpF in a heterotrimer are used as a CDI receptor because mutations made in these osmoporins resulted in resistance to CdiA from EC 536 [154].

These were found using transposon mutagenesis where cells that were resistant to CdiA from EC 536 indicated that an insertion was made in an important gene for binding. Mutants without OmpC and OmpF were not susceptible to EC 536 CdiA and were only susceptible if both were present. To find the recognition epitopes, mutations were made in loop 4, loop 5, and loop 7. These loops are the longest and may experience the same sequence pressure to avoid exploitation by other bacteria as the external loops in BamA. The same grafting technique was used and other isolates could be inhibited given that loop 4 from EC 536 was grafted on to OmpC. Chimeras made with loop 7 and 8 from EC 536 showed resistance in co-culture assays which means that they do not play a role in binding to EC 536 CdiA. Chimeras made with EC 536 loop 5 were functional CDI receptors and supports recognition to EC 536 CdiA [154].

2.2.3 CDI Class III Receptor

The Class III CDI receptor is Tsx. Tsx stands for receptor for phage T-six and is a nucleoside-specific outer membrane transporter on Gram-negative bacteria. It forms a 12-stranded β-barrel that is substrate specific [155]. The nucleosides that are taken up by the cell are used as carbon and nitrogen sources as precursors for nucleic acid synthesis in submicromolar concentrations [156]. Like other outer membrane proteins, it has long extracellular loops and short periplasmic turns. The crystal structures show the cross section of the pore is shaped like a keyhole [155]. Other substrates take advantage of this channel such as albicidin, which is an inhibitor for DNA replication. Bacteriophages and colicins also use Tsx as a receptor [156]. Mutations in Tsx by Schneider et al. revealed that the mutations were located in the longest external loop. This suggests that the bacteriophages use this loop as the receptor. The mutations did allow colicin K into the cell, meaning that these changes were insignificant to its entry [157].

Tsx has an expected weight of ∼33kDa and functions as a monomer. It forms a flattened cylinder with a cross section of 30 × 15–20 angstroms and the keyhole being 3-5 angstroms in diameter. It is a narrow pore because strands 1-6 are bent inwards at the center to flatten and restrict it further. The pore is lined with aromatic residues which form the narrowest part of the pore. Tsx has at least three distinct nucleoside binding sites in the channel, contacting the aromatic residues on both sides of the channel. It then moves through contacting ionizable residues and is released by the weak binding sites moving with the concentration gradient. Tsx uses alternative binding for different nucleosides due to spatial arrangements between purine and pyrimidines and it also has to accommodate different sugars such as ribose and deoxyribose. This outer membrane protein is not constricted by any extra cellular loops that fold inward like the other two classes of receptors, it instead has the extracellular loops form a lid to the barrel [155].

Tsx was also found to be a CDI receptor based on sequence alignments and transposon mutagenesis. Alignments were done on CdiA from EC 93 and EC 536 showing that there was sequence homology among major parts of CdiA except for two areas in particular. This alignment was important to determine the regions of CdiA and question whether this long protein is modular. One area of misalignment is the C-terminus which is the toxin and toxins can have various effects. The second area was in the middle of CdiA which protrudes the farthest out of the cell. This region is called the receptor binding region. The *E. coli* STECO31 was aligned as well and it did not have any obvious sequence homology to EC 93 or EC 536 RBD. The average homology between the *E. coli* species isolates was 24 to 27% identity. This indicated that it is a possible new class of receptor. Transposon mutagensis was performed and Tsx was the CDI receptor for STECO31. Resistance in a Δtsx mutation in co-culture experiments confirmed the transposon mutagenesis results [106].

2.2.4 CDI Class IV Receptor

The Class IV CDI receptor is the lipopolysaccharide (LPS) core. The LPS components of many bacteria are toxic and can be divided into three parts: lipid A, core polysaccharides, and the O-antigen repeats. The lipid A represents the hydrophobic component of LPS, responsible for the toxic effects, and functions as the scaffold for assembly of the core polysaccharides and O-antigen. The lipid A layer is made of a glucosamine dimer bound to lipid acyl chains and varies from one bacterium to another with the variation impacting the virulence [158, 159]. The core polysaccharides are covalently linked to the lipid A layer [158]. The core polysaccharides consist of an inner core and outer core. The inner core is connected to the lipid A layer. The inner core usually contains 2-keto-3-deoxyoctulosonate (Kdo) and l-glycero-d-manno-heptose (Hep). The Kdo is the most conserved component of the LPS [160].

The outer core is composed of glucose and galactose. The O-antigen is connected to the outer core and made with a repeating saccharide in linear or branched structures. The O-antigen is made of mannose, glucose, N-acetyl-d-galactosamine, and N-acetyl-d-glucosamine [159]. The core layer is generated with three operons: *gmhD*, *waaQ* and *kdtA*. The *gmhD* operon contains the genes for *gmhD*, *waaF*, *waaC*, and *waaL* to make the inner core. The *waaQ* operon contains the other genes to generate the outer core. the *kdtA* operon contains genes to add the Kdo residues to lipid IV [158]. In the discovery of the LPS as a CDI receptor using *E. coli* STECO31-STEC4, mutants that were resistant in co-culture assays were those that were unable to synthesize the full LPS core. These were also found through transposon mutagenesis with insertions in *waaF*, *waaP*, *waaA*, and *waaQ*. WaaA is essential and transfers Kdo to the lipid IV which is a precursor to lipid A. WaaP is needed to phosphorylate HepII. WaaF transfers the Hep residue to the inner core [101]. WaaQ facilitates the transfer of HepIII to HepII [161].

In co-culture assays with STECO31-STEC4 CdiA against the target cells that have different *waa* gene deletions, the mutations that corresponded to resistant target cells were *waaF*, *waaP*, and *waaC*. WaaC is the HepI transferase that attaches Hep to the Kdo that precedes all other sugar attachment. Cells with these mutations were unable to make the full LPS core, thus interrupting binding to the inner core indicating that STECO31-STEC4 CdiA binds to the inner core region. The STECO31-STEC4 inhibitor was also pitted against known classes of CDI receptors. It showed inhibition for each species was inhibited to the same extent as the wild-type target cells indicating that the known receptors are not correct for STECO31-STEC4 [101]. The impact of the LPS as a receptor for this isolate is that it can target a wider variety of bacteria and have more of an impact in its environment.

2.3 Results

2.3.1 *K. aerogenes* CDI Systems

Previously, the lab has shown that CdiA from various species have homologous regions and some of these regions can be interchanged such as the toxins and the receptor binding domains [107, 105]. To identify if *K. aerogenes* has a CDI system, sequence analysis was performed and two CDI systems were discovered. *K. aerogenes* locus 1 and *K. aerogenes* locus 2 both have the canonical *cdiBAI* and homologous regions in regard to CdiA structure (Fig. 2.3). The loci vary in length with the most notable variation in the FHA-1 domain where *K. aerogenes* locus 1 is almost 33% longer than FHA-1 in locus 2 (Fig. 2.3). The FHA-1 length is directly related to the extension of CdiA outside the cell which is a possible explanation of why locus 1 is effective in a laboratory setting while locus 2 is not. This could have an impact on the effectiveness of locus 2 inhibition if it is

unable to physically reach and contact other target cells. To determine the functionality of each system, we generated a knock out of each system. The lab generated *K. aerogenes* Δlocus 1 CdiA and *K. aerogenes* Δlocus 2 CdiA. To test these in co-culture experiments, we added a plasmid with a unique resistance marker. These CdiA knock outs were tested against a wild-type *K. aerogenes* with a different resistance marker. Results show that the wild-type showed inhibition against both ΔcdiA mutants but showed more inhibition against the knock out of loci 1 (Fig.2.3). To confer immunity function, the immunity gene was cloned into a plasmid and transformed into its respective ΔcdiA mutant. These strains were tested against the wild-type inhibitor. The Δcdi-1 strain complemented with the cdiI-1 immunity gene protected Δcdi-1 mutants from inhibition by wild-type KAE cells while the Δcdi-2 strain complemented with the cdiI-2 immunity did not protect compared to the empty vector control (Fig. 2.3).

2.3.2 *K. aerogenes* CDI Receptor

The Δcdi-1 strain complemented with the cdiI-1 immunity gene protected Δcdi-1 mutants from inhibition by wild-type KAE cells while Δcdi-2 mutants were ineffective in the laboratory setting, we decided to focus on the *K. aerogenes* locus 1 CDI system moving forward. To provide an insight into its CDI receptor, sequence analysis was done on the RBD to compare known classes of receptors. *K. aerogenes* in comparison to the four classes of receptors, did not share notable sequence identity (Fig. 2.4). The sequence identity of the RBDs ranged from 16% to 34%. To identify the outer membrane receptor for *K. aerogenes*, we mutagenized the Δcdi-1 strain to make it susceptible to CdiA1-mediated intoxication with *mariner* transposon mutagenesis on *K. aerogenes* to generate mutant libraries. These libraries were tested in co-culture assays against a chimeric inhibitor. The inhibitor consists of the STECO31 CdiBA with the RBD, CT,

and the immunity gene from *K. aerogenes* cloned onto a plasmid and transformed into *E. coli* MC 1061 to inhibit the mutagenized *K. aerogenes* cells with their native toxin.

In iterative cycles of co-culture assays, the libraries were fully resistant to the inhibitor. This indicates that the transposon insertion is in a gene critical to providing resistance to the inhibitor. Single colonies were isolated and genomic DNA was prepared for sequence analysis. The insertions of the transposon occurred in *ompC* at T14, A15, and A74 (Fig. 2.5). OmpC is part of the Class II receptors and usually forms a heterotrimer with OmpF [150]. To test both porins, we cloned OmpC and OmpF from *K. aerogenes* separately onto plasmids and transformed into *E. coli* JCM 158 ΔompC ΔompF to ensure that the only OmpC or OmpF produced by the cell would be plasmid-borne. These strains would only make OmpC or OmpF or both in combination. The inhibitor used is STECO31 CdiBAI with the RBD from *K. aerogenes* cloned on a plasmid and transformed into *E. coli* JCM 158 ΔompC ΔompF Δwzb. We moved the RBD sequence of interest into the *E. coli* CDI STECO31 system because when placed in *E. coli* experiments are facilitated by rapid growth under laboratory conditions. We also placed the plasmid-borne *K. aerogenes* OmpC and OmpF in *E. coli* for the same reason. In co-culture assays, strains with only OmpC and those with OmpC and OmpF showed inhibition which refer to the second and fourth bars in Fig. 2.5. This shows that OmpC is necessary and OmpF is optional but not a necessity to have wild-type levels of inhibition (Fig. 2.5).

2.3.3 *K. aerogenes* OmpC Loop 3 Variations

In previous work we showed that polymorphisms between the surface-exposed loops of OmpC were important for recognition. Specifically, loops 4 and 5 were the most important for recognition [154]. In other literature about OmpC, clinical isolates with

mutations in loop 3 were studied. Structural changes made in AlphaFold2 suggests that residues in the OmpC lumen could be important in terms of volume inside the barrel and the electrostatic charge differences. This internal loop was found to be highly conserved even between different species by Beck et al., but mutations in this loop can affect the interactions inside the pore as seen by conductance changes in experiments by Lou et al. [162]. It is possible that all class II RBD interactions are anchored by conserved interactions in pore.

We next used variations in loop 3 to determine if the structure of the *K. aerogenes* RBD reaches into the barrel of OmpC to trigger translocation of the toxin into target cells (Fig. 2.6). This loop forms a salt bridge between the loop and the barrel and mutations in this loop have been shown to affect pore size and selectivity [163]. Previous mutations in the literature were made near the base of the loop in an area where the α-helix is close to the barrel wall. In their electrophysiology experiments, this resulted in flexibility of this channel meaning that the gate opened and closed more often resulting in differential membrane permeability [164]. OmpC also has a transverse electric field made of the conserved basic amino acids on the barrel wall facing inward and the acidic residues on loop 3. It has been found to dictate ion selectivity and the channel permeability to polar molecules. Zwitterionic antibiotics which are antibiotics that have positive and negatively charged groups bind at the pore to interact with the charged residues. Alterations to the hydrogen bonding in the loop will disrupt the translocation of antibiotics across the cell membrane [162]. The *K. aerogenes* RBD is modeled in AlphaFold and its distal tip is made of two β-strands and two α-helices (Fig. 2.6). The two β-strands are predicted to reach into the barrel of OmpC and the two α-helices are predicted to contact the other exterior loops on OmpC (Fig. 2.6). In the wild-type OmpC, the channel shows a positive wall and a slightly negative loop 3 (Fig. 2.9).

We investigated mutations that would affect the binding surface area of the loop in

co-culture experiments. The inhibitor used in the following co-culture experiments uses STECO31 CdiBAI with the RBD from *K. aerogenes* cloned on a plasmid and transformed into *E. coli* JCM 158 Δ*ompC* Δ*ompF* Δ*slyD*. The OmpC mutations were made to probe the loop 3 interaction in the barrel were cloned into a plasmid and transformed into *E. coli* JCM 158 Δ*ompC* Δ*ompF* Δ*wzb*. Mutations were made at positions 127, 133, and 139 in loop 3 of *K. aerogenes* OmpC. At position 127, aspartic acid is a negatively charged and mutated to a glycine which is lacking a side chain. The D127G mutation provided partial protection against the inhibitor meaning that it did not provide full resistance similar to the empty vector control (Fig. 2.7). The model of this mutation shows a decrease in hydrogen bonds within loop 3 and a rotation of the available binding area to a more horizontal surface instead of a vertical surface inside the barrel (Fig. 2.8). This could have an effect on the RBD where it may block contact and it additionally changes the electrostatics in the barrel to a less positive binding surface (Fig. 2.9).

The wild-type amino acid at 133 is glycine in *K. aerogenes* OmpC. The mutation to aspartic acid at this position is known for causing a decrease of 70% in single channel conductance meaning the permeability of the outer membrane was decreased and the loop stays locked in position [165]. We mutated amino acid 133 to aspartic acid and to a few different amino acids to test its binding abilities. The mutations with glutamic acid and arginine show full resistance. Aspartic acid, histidine, isoleucine, methionine, serine, and valine all show partial resistance to varying degrees (Fig. 2.10). All of these mutations take up more surface area in the barrel and do not change the electrostatics dramatically (Fig. 2.11, Fig. 2.12). The barrel wall remains strongly positive except for G133I, G133R, and G133H which show slight decreases in positive charge on the inside of the barrel (Fig. 2.12). Interruptions that change the bonding to the barrel, the loop itself, electrostatics, hydrophobicity, or that take up more space in the barrel, such as glutamic acid, will alter the binding efficiency of the receptor binding domain (Fig.

2.10). Glutamic acid and arginine take up the most volume in the barrel resulting in their competitive indices showing resistance to the inhibitor with previous mutations to arginine in a different location also show resistance to the inhibitor (Fig. 2.12).

The mutations at position 139, show resistance in S139Q and S139R and partial resistance in S139N (Fig. 2.7). Mutation at 139 changes the serine residue to asparagine and glutamine which are also polar with uncharged side chains but longer chain length (Fig. 2.7). A separate mutation changes the serine to an arginine which is positively charged. The intention of these mutations is to take up more volume inside the barrel of OmpC, therefore occluding the RBD from binding. The mutations at S139 cause the electrostatic charges in the barrel to remain slightly negative with a slight change to become more negative in S139R (Fig. 2.9). A deletion was also made in loop 3 to shorten the loop by 6 residues. This decreased the total number of hydrogen bonds formed between the loop and the barrel leading to a more flexible gate, but may have deleted critical contact points (Fig. 2.9). This mutation changed the electrostatic charges to a more negative charge in loop 3 and provided full resistance in the co-culture experiment. These mutations caused deficiencies in toxin delivery and may also cause expression deficiencies. The point mutations and deletions have affected the binding capacity differently and it could be due to the expression levels of OmpC. To ensure that the protein levels are constant even with the mutation, protein from the *ompC* mutated strains were subjected to immunoblot analysis using polyclonal antisera against OmpC/OmpF from *E. coli* K-12. The immunoblot shows the mutations in OmpC were produced in all strains, indicating that the resistance or partial resistance is not due to the lack of *ompC* expression (Fig. 2.13). The OmpC produced is not equivalent in all strains and lower expression cannot account for CDI-resistance in some instances. In G133E, it is completely resistant and makes lots of protein. In D127G and Δ134-139 mutants, resistance is not an artifact of expression level.

2.3.4 *E. coli* F11 Loop 3 Variations

We also wanted to test if these mutations in *K. aerogenes* can be extended to another class II receptor with an RBD from *E. coli* especially when the sequence identity from EC 536 and *K. aerogenes* is low. We then realized the importance of loop 3 in regards to antibiotic effectiveness in *E. coli* F11 through preivous literature. The F11 strain is an enterotoxigenic *E. coli* strain (ETEC) which can cause diarrhea. It is also associated with urinary tract infections (UTI) and septicemia [166]. A UTI is commonly associated with women and although they are treatable, 30% of women will have a recurrence and 20% will have multiple recurrences. UTIs are treatable with antibiotics, resulting in an increase in prescriptions that account for 15% of nearly all prescribed antibiotics. *E. coli* is one of the most common pathogens in UTIs and has developed resistance over time. UTIs cause over 12,000 deaths per year and if the patient has bacteremia, the chances are more likely [167].

F11 loop 3 in OmpC acts as a gate that controls ion selectivity and channel permeability and the small changes made to amino acids on the loop will change electrostatics inside the barrel, altering the cell's permeability which is the same function as loop 3 in *K. aerogenes* OmpC. F11 RBD has a homologous structure where it also reaches into the barrel of OmpC for contact (Fig. 2.14). We made point mutations in F11 OmpC at position 132 where the wild-type amino acid is glycine. This position corresponds to *K. aerogenes* OmpC G133. The point mutations were tested in co-culture assays to determine their functionality by their ability to bind to the inhibitor strain. The inhibitor used in the following co-culture experiments uses STECO31 CdiBAI with the RBD from *E. coli* F11 cloned on a plasmid and transformed into *E. coli* JCM 158 $\Delta ompC$ $\Delta ompF$ $\Delta slyD$. The F11 OmpC mutations were cloned into a plasmid and transformed into *E. coli* JCM 158 $\Delta ompC$ $\Delta ompF$ Δwzb. Mutations to threonine, alanine, and leucine showed partial

resistance, while asparagine, arginine, isoleucine, and valine show full resistance (Fig. 2.15). The arginine and asparagine take up more space in the thin channel, preventing the RBD for F11 from making contact (Fig. 2.16). The native amino acid is glycine, making the channel electrostatically positive while the arginine and valine change the charge to slightly less positive (Fig. 2.17). To ensure that the protein levels are constant even with the mutation present, protein from the F11 *ompC* mutated strains were subjected to immunoblot analysis using polyclonal antisera against OmpC/OmpF from *E. coli* K-12. The levels of protein were constant throughout. The immunoblot shows that the mutations in F11 OmpC were produced in all strains, indicating that the resistance or partial resistance is not due to the lack of *ompC* expression (Fig. 2.18).

2.3.5 *E. coli* STECO31 Class III Tsx Mutants

This bacteria is important because *E. coli* STECO31 stands for Shiga toxin-producing *E. coli*. STEC infections occur when people eat or come into contact with infected items such as lettuce, alfalfa sprouts, salami, or other meat. The incubation time for these infections ranges from one to ten days. STEC infections can induce symptoms such as severe diarrhea, stomach cramps, vomiting, and associated with hemolytic uremic syndrome (HUS) [168]. According to the CDC, *E. coli* STEC is estimated to cause more than 265,000 illnesses each year with roughly 30 deaths [169]. This number may be under reported due to many people that do not seek medical care during their infection. These STEC isolates have a locus of enterocyte effacement (LEE) and one or more of the *stx* genes [170]. The STECO31 isolate encodes an EndoU nuclease that cleaves tRNA as its toxic effector and uses Tsx which is a Class III receptor as its CDI receptor [107].

STECO31 receptor binding domain forms a similar structure to *K. aerogenes* and *E. coli* F11 where the contact point is a point formed by two β-strands that reach out

to contact the receptor. The STECO31 point consists of the same amino acids of the F11 point, just in a slightly different order where the threonine and alanine are reversed (Fig. 2.19). Tsx is a smaller barrel made with 12 strands and does not have an internal loop. The RBD contacts the extracellular loops, but does not reach deeply into the barrel (Fig. 2.19). Mutations in Tsx were made in the lumen of the barrel and on two different extracellular loops. These mutations were tested in both liquid and on solid agar in co-culture assays. The inhibitor used in the following co-culture experiments uses STECO31 CdiBAI cloned on a plasmid and transformed into *E. coli* MG 1655 Δwzb Δtsx. The STECO31 Tsx mutations were cloned into a plasmid and transformed into *E. coli* MG 1655 Δwzb Δtsx. In solid agar co-culture experiments, all Tsx mutants were shown to be inhibited (Fig. 2.20). On solid agar, the inhibitor has a stable surface to connect to the receptor and it can overcome any mutations that have changed the binding surface area. On a solid surface, the inhibitor also has a finite amount of bacteria that it can come in contact with, thus it is able to possibly target the same bacteria multiple times to exaggerate inhibition.

In comparison to liquid media co-culture experiments, only the mutation in the barrel, G50R, and Tsx from *K. aerogenes* provided full protections against the STECO31 inhibitor (Fig. 2.20). The loop 2 HA tag added to Tsx provides partial protection against the inhibitor which interferes with toxin delivery by partially occluding the barrel in some conformations (Fig. 2.21). This placement of the HA tag in liquid co-culture experiments is interfering with its function as shown in (Fig. 2.21) where the loop is brought out extending past the barrel. These mutations have also caused a shift in the electrostatic pattern of Tsx (Fig. 2.22). G50R and *K. aergoenes* Tsx have changed the adjacent loop to a more negative charge (Fig. 2.22). The mutations at 269 and 271 have created a more negative charge reaching into the extracellular space. The added HA tag in Tsx has pulled the loop to the side of the barrel creating a positively-charged loop that

could affect its binding ability (Fig. 2.22). In liquid media, the Brownian motion, the tumbling rate, and the shear rate cause bacteria to swim at 24 μm/s [171]. This rate of movement for the inhibitors and targets is not enough to overcome a mutation clogging up the barrel of Tsx and for a homologous Tsx with 87% sequence identity for inhibition (Fig. 2.23).

2.4 Discussion

Functional CDI systems have been discovered and studied in a number of Enterobacter species, *Burkholderiaceae*, and the *Bordetella* family which uses a filamentous hemagglutinin adhesin [172, 92, 173]. CDI systems are part of the secretion systems that deliver toxic effectors to target cells directly. These effectors have activity that range from DNases, RNases, and pore-formers [105, 174]. Many emerging nosocomial infections are becoming multidrug-resistant and investigation into their effector delivery systems is imperative to find an alternative answer to the antibiotic resistance war. We took a deeper look into one of the virulence mechanisms of *K.aerogenes*. We have determined that *K. aerogenes* has two CDI systems through sequence analysis and that the system on locus 1 is functional for this study. The system on locus 1 has an extended FHA-1 region in comparison to locus 2. This extended reach of locus 1 may allow it to contact target cells and sister cells more effectively in binding to attach non-kin and bind to sister cells to form biofilms. The Δcdi-1 strain complemented with the cdiI-1 immunity gene protected Δcdi-1 mutants from inhibition by wild-type KAE cells while Δcdi-2 mutants were ineffective in the laboratory setting (Fig. 2.3).

Using the *K. aerogenes* locus 1 CDI system, we discovered the CDI receptor. The sequence analysis of the *K. aerogenes* RBD in comparison to known RBDs with identifiable CDI classes of receptors had low sequence identities. Due to this, we found the receptor

through transposon mutagenesis and iterative cycles of co-culture experiments for complete resistance against the chimeric inhibitor, where the RBD and CT from *K. aerogenes* were cloned into the STECO31 CDI system. The CDI receptor is OmpC meaning that *K. aerogenes* is a Class II receptor which typically uses an OmpC/OmpF heterotrimer as its receptor. We then concluded that OmpF is not a critical factor in binding to the RBD (Fig. 2.5). We decided to investigate loop 3 in OmpC as a gate that selects for ions and other small molecules and as a potential binding contact for the RBD. Previous research has been done investigating the barrel and the base of the loop where mutations found from clinical isolates have led to less cell permeability [165]. These isolates were collected from patients and have spontaneous mutations in OmpC.

Through our site-directed investigation, we have found that changes to the loop interfere with its ability to deliver the toxin to target cells (Fig. 2.7, Fig. 2.10). These experiments can detect whether the RBD of *K. aerogenes* can bind, but cannot detect whether the lateral gate fluctuates in an open or closed conformation making it more or less permeable. The mutation at position 127 provided partial resistance and was due to its structure taking up less space in the barrel (Fig. 2.7). The point mutations in OmpC position 139 were more critical in that two of these mutations caused full resistance in competition due to the side chains occluding more of the barrel and creating a slight increase in negativity in the channel (Fig. 2.9). The mutations at position 133 have shown full or partial resistance with G133S having the highest competitive index, meaning that it is able to bind to the RBD of *K. aerogenes*. G133R was the most resistant in the co-culture experiments due to its structure impeding the RBD from reaching into the barrel and locking loop 3 in place (Fig. 2.10).

We made a corresponding mutation in *E. coli* F11 which is associated with UTI infections and septicemia [166]. Mutations made in F11 OmpC have shown partial or full resistance similar to the mutations in *K. aerogenes*. OmpC *K. aerogenes* at 133 and F11

at 132 are corresponding positions. They have identical mutations, each having a mutation from glycine to isoleucine, arginine, and valine (Fig. 2.11, Fig. 2.16). The mutations at isoleucine and arginine both show full resistance indicating that these mutations cause similar effects in co-culture experiments (Fig. 2.10, Fig. 2.15). The arginine structure obstructs the barrel in both species and causes a slightly more negative channel. The isoleucine in both species alters the electrostatic charges in the barrel thus, altering the binding to the RBD for the respective species. Mutations in Tsx were tested in co-culture experiments on solid agar and in liquid media (Fig. 2.20). On solid agar, the time for inhibitors to contact target cells is more stable due to the solid surface and can overcome the mutational effect on binding. In liquid media, the mutations have a larger effect on the binding ability to the RBD of STECO31 (Fig. 2.20). The G50R mutation inside the barrel shows complete resistance in the liquid co-culture experiment which can be attributed to the change in electrostatic charges causing a more negative charge in the barrel (Fig. 2.22). The mutations on loop 2 and on loop 6 have little to no effect on the binding ability in liquid co-culture assays. The addition of the HA tag on loop 2 has caused the loop to open the barrel, thus causing an increase in inhibition on solid agar and in liquid media. The loop movement may cause partial protection between open and closed conformations (Fig. 2.21). The grafting of *K. aerogenes* loop 6 onto STECO31 Tsx caused the loop to become more negatively charged, thus affecting the binding.

The site directed mutations are important for elucidating the mechanisms of resistance. We present evidence that these small changes can have an effect on the delivery of the toxin to its target receptor. Our analysis shows that these changes can have an effect in the channel for OmpC in either species and change the electrostatic charges in the channel. Although STECO31 Tsx does not have an internal loop that can obstruct the passage of small molecules and antibiotics, it has extracellular loops that can prevent bonding by either opening or closing the loop or electrostatically by increasing negative

charges on the loops forming a "lid". This study is important for expanding on the roles of mutations in the barrel of OmpC leading to a better understanding of the contact points by attacking bacteria. These binding points in the receptor for nosocomial and pathogenic bacteria are important for understanding the effect of permeability of these pathogens. Some of the mutations can lead to a more permeable membrane leading to an uptake of antibiotics contributing to an increase in their effectiveness. An increase of effectiveness may win the war on antibiotic resistance by decreasing the amount of antibiotics needed for treatment or the necessity of antibiotic cocktails.

2.5 Methods

Growth conditions and competition co-cultures. All strains were grown at 37°C in lysogeny broth (LB) or on LB agar unless otherwise noted. Media were supplemented when appropriate with antibiotics at the following concentrations: ampicillin (Amp) 150 μg mL^{-1}; kanamycin (Kan) 50 μg mL^{-1}; chloramphenicol (Cm) 33 μg mL^{-1}; gentamycin (Gm) 15 μg mL^{-1}; and tetracycline (Tet) 25 μg mL^{-1}. For all competition co-cultures, both strains were grown to an optical density at 600nm (OD_{600}) of 0.3 - 0.9 and mixed at an equal ratio of OD_{600} (3.0:3.0), plated in a 20 μL volume on LB agar or LB with Amp when appropriate. For competitions using target cells with *K. aerogenes* or *E. coli* F11, the solid agar was incubated for 5 hours at 37°C. For solid agar competitions using target cells with *E. coli* STECO31, the solid agar was incubated for 3 hours at 37°C. For liquid media competitions using target cells with *E. coli* STECO31, the media was incubated in shaking broth for 3 hours at 37°C. Cells were harvested with a sterile swab into 1 x M9 salts and ten-fold serial dilutions were plated on the appropriate antibiotics to enumerate inhibitor and target cell colony forming units (CFU/mL) for solid agar co-culture experiments. Competitive indices were calculated as the ratio of inhibitor to

target cells at 3 or 5 hours relative to their starting ratios. Each co-culture experiment was repeated at least three times.

Plasmid and strain construction. To generate a wild-type *K. aerogenes* strain with a resistance marker, pUC1r8R6k-miniTn7T-Gmr to generate a mobilizable plasmid with gentamycin resistance linked to P^{BAD} and a gentamycin resistance cassette that could be integrated at the attTn7 site at glmS [175]. Using these constructs, integration of the cassette was accomplished bi-parentally with the MFDpir+ mating strain. Equal ratios of the two donors (CH14478 and CH14480) and CH7838, *K. aerogenes* ATCC 13048, were mixed from overnight cultures in 50 μL, plated on solid agar and incubated at 37°C for 4 hours. The resulting integrants were selected on Gm15 and the insertion site verified by colony PCR with primer pairs CH4672/CH4616. This strain was used in co-culture assays against the CDI locus knockouts.

To generate the CDI system knock outs in *K. aerogenes*, primers CH5248 and CH5249 were used to amplify a region upstream from the locus 1 *cdiA-CT*. Primers CH5250 and CH5251 were used to amplify a region downstream from locus 1 *cdiI*. These two pieces were cloned by the lab into pCAT-KAN-pheS* and used homologous recombination to remove the *cdiA* gene thus, the resulting strain was *K. aerogenes* ATCC 13048 ΔcdiA1-CT-cdiI1-CTo1::kan. To generate the locus 2 knock out, primers 5322 and 5497 were used to amplify a region upstream from the locus 2 *cdiA*. Primers CH5265 and CH5266 were used to amplify a region downstream from locus 2 *cdiI*. These two pieces were cloned by the lab fffinto pCAT-KAN-pheS* and used homologous recombination to remove the *cdiA* gene thus, the resulting strain was *K. aerogenes* ATCC 13048 ΔcdiA2-cdiI2::kan. These strains were used in the CDI locus co-culture experiments. To generate the immunity genes for these experiments, CH5301 and CH5302 were used to amplify the immunity gene from *K. aerogenes* ATCC 13048 locus 1 and ligated into pCH405Δ using KpnI and XhoI. The immunity gene for *K. aerogenes* ATCC 13048 locus 2 is amplified using

CH5549 and CH5550 and ligated into pCH405Δ using KpnI and XhoI. These plasmids were transformed into their respective knock out strains.

The RBD from *K. aerogenes* was amplified using oligonucleotides CH4766 and CH4767, digested with EcoRI/BamHI, and ligated into pET21b::cdiBAI(STEC3) ΔRBD (EcoRI/BamHI) (1726C) to generate pET21b::cdiBAI(STEC3)-RBD(KAE) (1726C). This plasmid was transformed into JCM 158 ΔompC ΔompF ΔslyD::cat to use as an inhibitor for transposon mutagenesis and subsequent competitions with *K. aerogenes*. To confirm the CDI receptor, *ompC* was amplified from *K. aerogenes* ATCC 13048 using primers CH3326 and CH2388 and ligated into pTrc99aKX with NcoI and XhoI. This was then transformed into JCM 158 ΔompC ΔompF. To test whether the CDI receptor also need OmpF, *ompF* was amplified with primers CH5942 and CH5943 and ligated into pZS21 using KpnI and XhoI. This plasmid was transformed into JCM 158 ΔompC ΔompF with empty vector pTrc99a or with pTrc99aKX::ompC from *K. aerogenes*.

The *K. aerogenes* OmpC point mutations were amplified from *K. aerogenes* ATCC 13048 and ligated into pTrc99aKX and transformed into JCM 158 Δwzb ΔompC ΔompF::kan. The point mutation D127G was amplified using primers CH3326 and CH6042 and ligated in with NcoI and EcoRI. In G133D and G133E mutations, these were made was made using primer CH6015 or CH6016 and CH2388 and ligated in with EcoRI and XhoI. S139R was made using primer CH6017 and CH2388 and ligated in with EcoRI and XhoI. The deletion from 134 to 139 in OmC was made using CH3326 and CH6041 and ligated in using NcoI and EcoRI. The remaining mutations at position 133 and 139 were made using CH6093 or CH6094 and CH2388 and ligated in with EcoRI and XhoI. These mutations were made using a randomized primer. The *E. coli* F11 OmpC point mutations at position 132 were made using a randomized primer, CH6093 and CH2388. These were crafted in the same way as the mutations made in *K. aerogenes*. These mutations are in a homologous site where the primers will bind, therefore producing the same randomized

mutations in a different species.

Mutations in Tsx are made from *E. coli* STECO31. These were also cloned into pTrc99a and transformed into MG1655 Δwzb Δtsx::kan. Tsx from *K. aerogenes* was amplified using primers CH6045 and CH6046 and ligated into pTrc99a using EcoRI and XbaI. The G50R Tsx mutation in the barrel was amplified with primers CH6085 and CH6086. The mutation in the outer loop, S239R, was made using primers CH6087 and CH6088. The double mutation on the longest loop, E269K and N271K, was made using primers CH6089 and CH6090. Tsx with the added HA tag onto loop 2 was made using primers CH6083 and CH6084. The grafting of loop 6 from *K. aerogenes* onto the STECO31 Tsx was amplified using primers CH6091 and CH6092.

Transposon mutagenesis to identify CDI-resistant mutants. The *mariner* transposon was introduced into CH7243 by conjugation with MFDpir cells carrying pSC189. Donors were supplemented with 30 μM diaminopimelic acid in shaking liquid LB and grown to mid-log at 37°C. Donors and recipients were mixed in a 1:1 ratio and plated on LB agar at 37°C for 5 hours. Cell mixtures were harvested with a sterile swab, collected in 1xM9 media, and plated on Kan-supplemented LB agar. Each of the five mutant pools were harvested for selection and subjected to selection by co-culture with MG 1655 carrying pET21b::*cdiBAI*(STECO31) with the RBD from *K. aerogenes*. The surviving colonies of each pool were collected again into 1mL 1xM9 media and subjected to two more rounds of co-culture selection. After three rounds, presumptive CDI-resistant clones were randomly selected from each independent transposon mutant pool. Transposon insertion sites were determined by rescue cloning. Chromosomal DNA from each resistant mutant was digested overnight with NspI at 37°C followed by a 20 min inactivation step at 65°C. Each reaction was supplemented with ATP and T4 Ligase and incubated overnight at 16°C. The reactions were electroporated into E. coli DH5 pir+ cells. Plasmids from the resulting kanamycin-resistant colonies were isolated and

transposon insertion junctions identified by sequencing using primer CH2260.

Protein purification and immunoblotting. All strains were grown at 37°C in lysogeny broth (LB) or on LB agar unless otherwise noted. Media were supplemented when appropriate with antibiotics. All cultures were induced with IPTG 30 minutes after the back dilution from the overnight culture and then grown for 2 hours at 37°C with aeration. The cultures were grown to an optical density at 600nm (OD_{600}) of 0.3 - 0.9 and resuspended to OD 1.0. After, pellets were collected and resuspended in denaturing buffer then frozen overnight at -80°C. Lysates were prepared by quick thawing the cultures and pelleting the insoluble material by centrifugation at 15,000 rpm for 15 minutes. Total protein concentration was calculated for the soluble lysates by Bradford reagent and the same amount of protein was loaded for all samples on 10% SDS-PAGE gels for separation at 100V for 90 minutes. The protein was then transferred to polyvinlyidene difluoride (PVDF) membranes for 1 hour at 17V and analyzed with anti-OmpC antisera. The 800CW secondary antibody was visualized with a LI-COR Odyssey infrared imager.

2.6 Tables and Figures

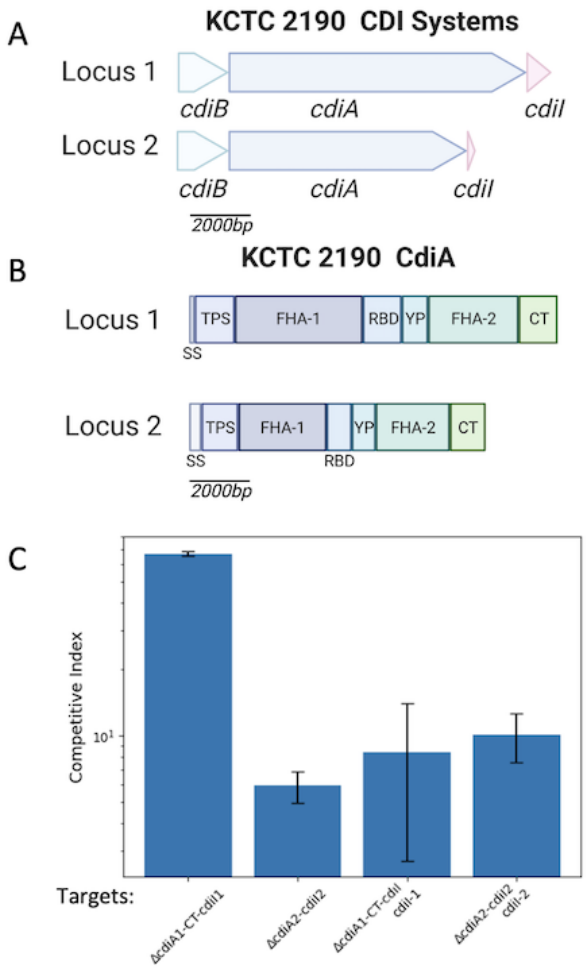

Figure 2.3: ***K. aerogenes* CDI systems and functionaliy**. (A) KCTC 2190 CDI systems to scale with a scale bar denoting 2000bp. (B) *K. aerogenes* CdiA domain map made to scale. (C) Co-culture assay between inhibitor and target strains. Target cells lacking CDI locus 1 or 2 and complemented with immunity. Competitive Index (CI) is the ratio of viable colony-forming units per milliliter (CFU/mL) of inhibitors to targets at 5 hours relative to their starting ratios. CI values are represented as the average of at least 3 independent experiments ±SEM.

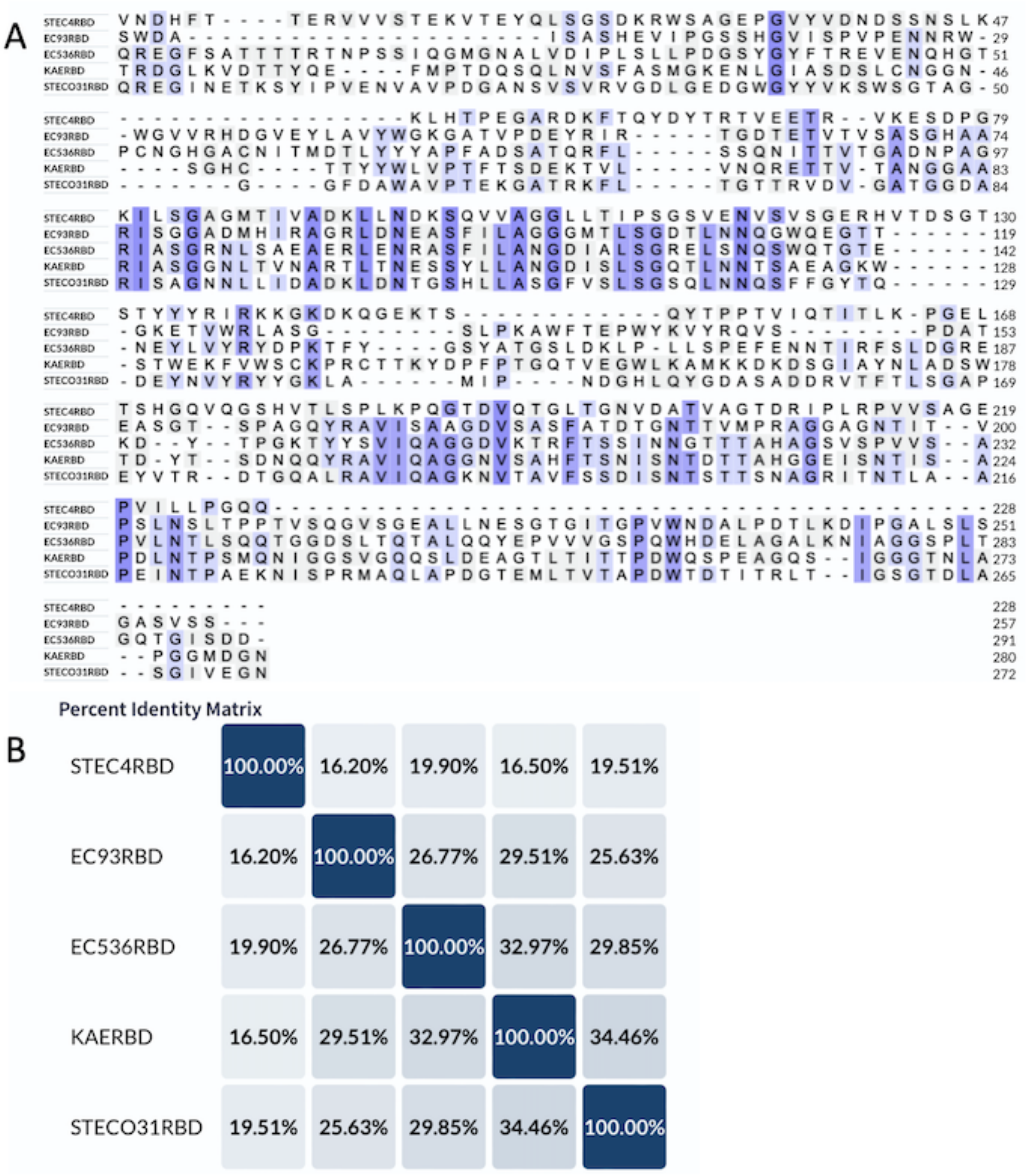

Figure 2.4: **RBD alignment of the different receptor classes and *K. aerogenes*.** (A) Clustal Omega alignment of the different receptor classes with conserved residues highlighted in blue. (B) Percent identity matrix denoting the similarity.

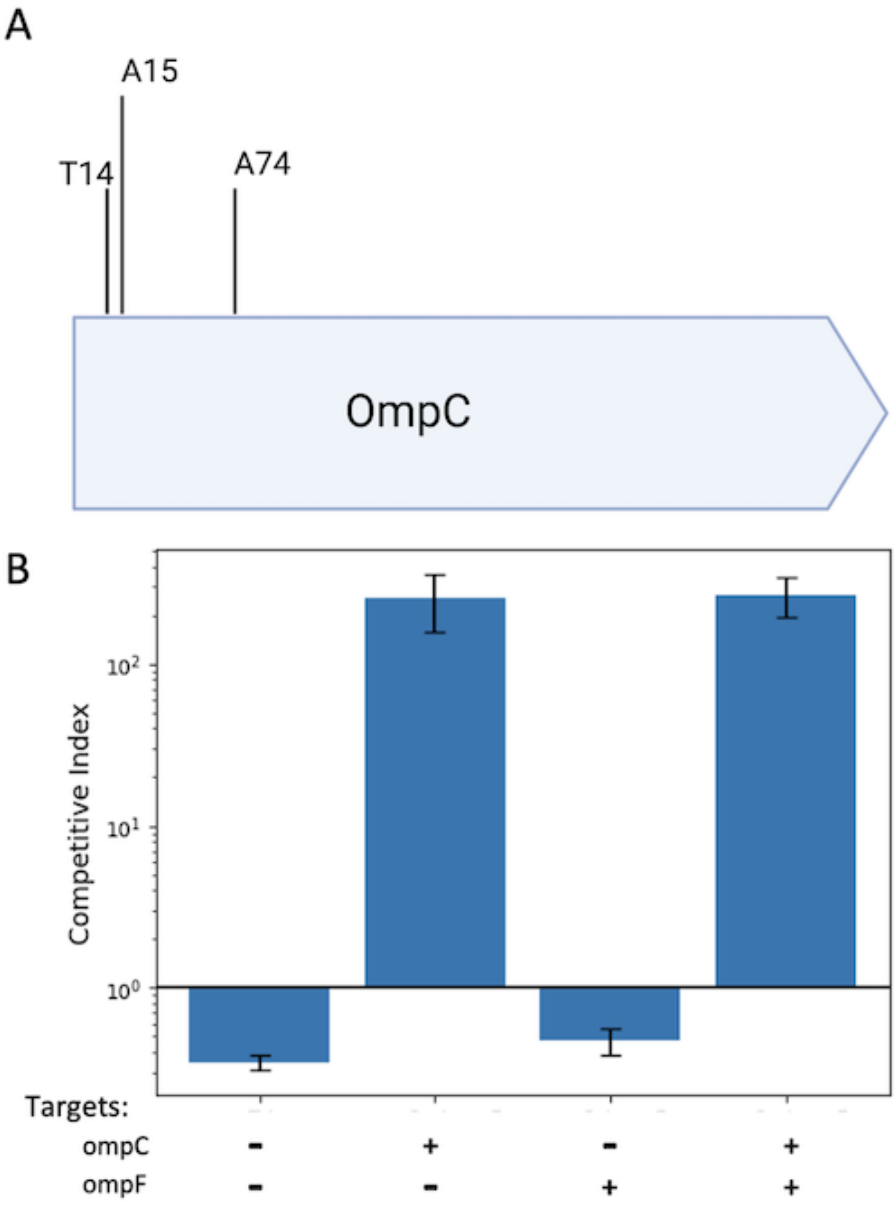

Figure 2.5: ***K. aerogenes* transposon mutagenesis insertions and co-culture assay**. (A) Transposon mutagenesis revealed gene insertions at T14, A15, and A74. (B) Co-culture experiment reveal the necessity of OmpC. Competitive Index (CI) is the ratio of viable colony-forming units per milliliter (CFU/mL) of inhibitors to targets at 5 hours relative to their starting ratios. CI values are represented as the average of at least 3 independent experiments ±SEM.

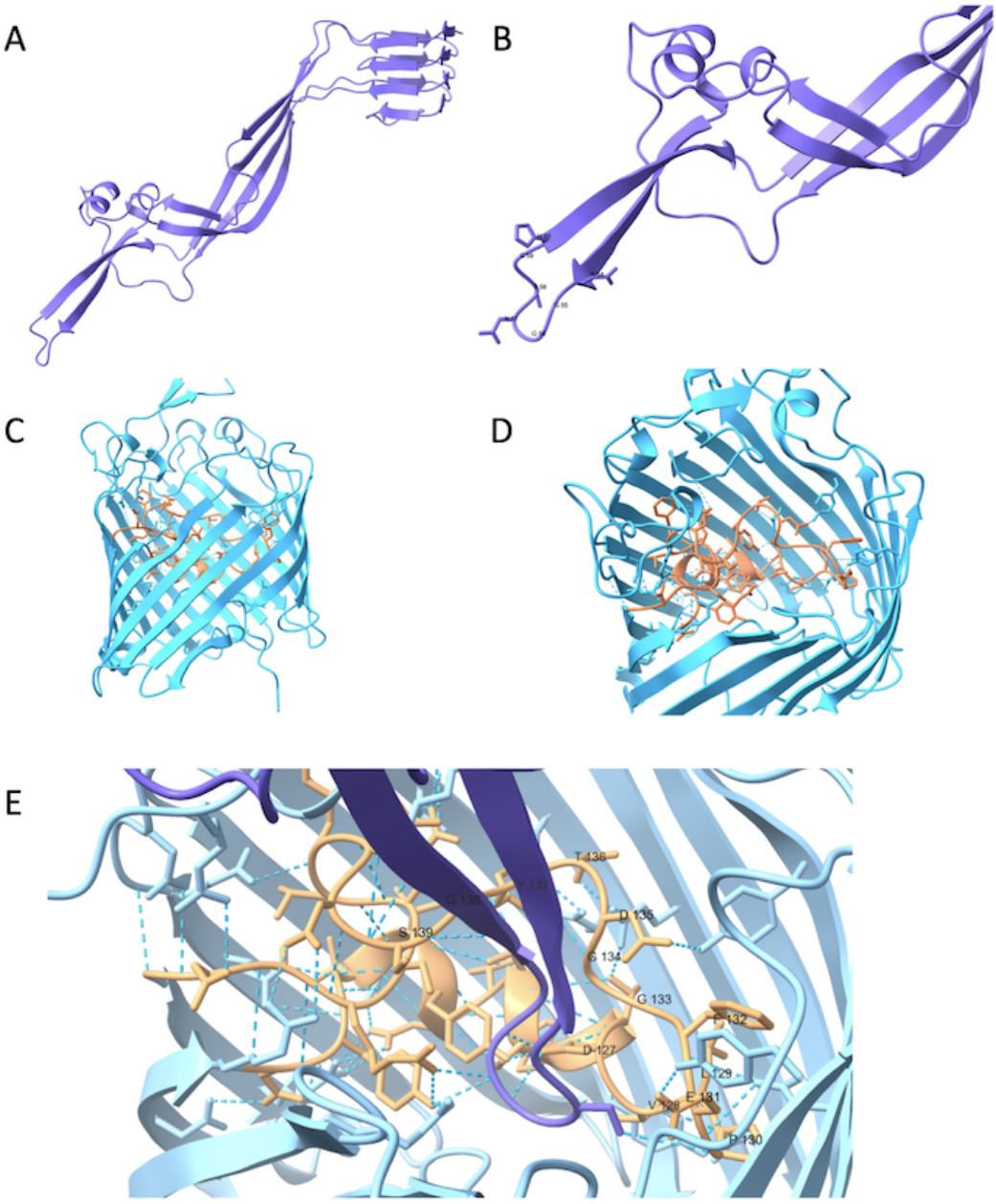

Figure 2.6: ***K. aerogenes* receptor binding domain and *K. aerogenes* OmpC**. (A) Receptor binding domain in purple. (B) Receptor binding domain with the point labeled. (C) OmpC with loop 3 in orange. (D) OmpC top view of loop 3. (E) Docking of RBD into OmpC with select amino acids labeled.

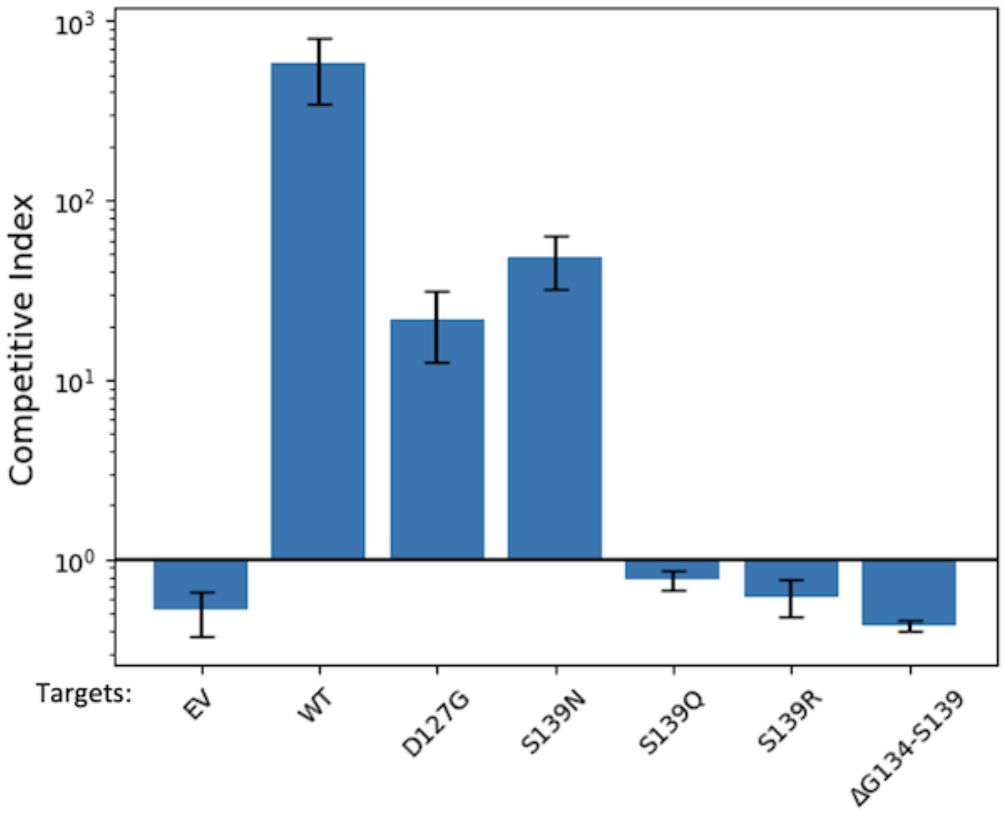

Figure 2.7: ***K. aerogenes* co-culture assay with loop 3 mutations**. Co-culture experiment reveal mutations that disrupt binding in S139Q, S139R, and Δ134-139. Competitive Index (CI) is the ratio of viable colony-forming units per milliliter (CFU/mL) of inhibitors to targets at 5 hours relative to their starting ratios. CI values are represented as the average of at least 3 independent experiments ±SEM.

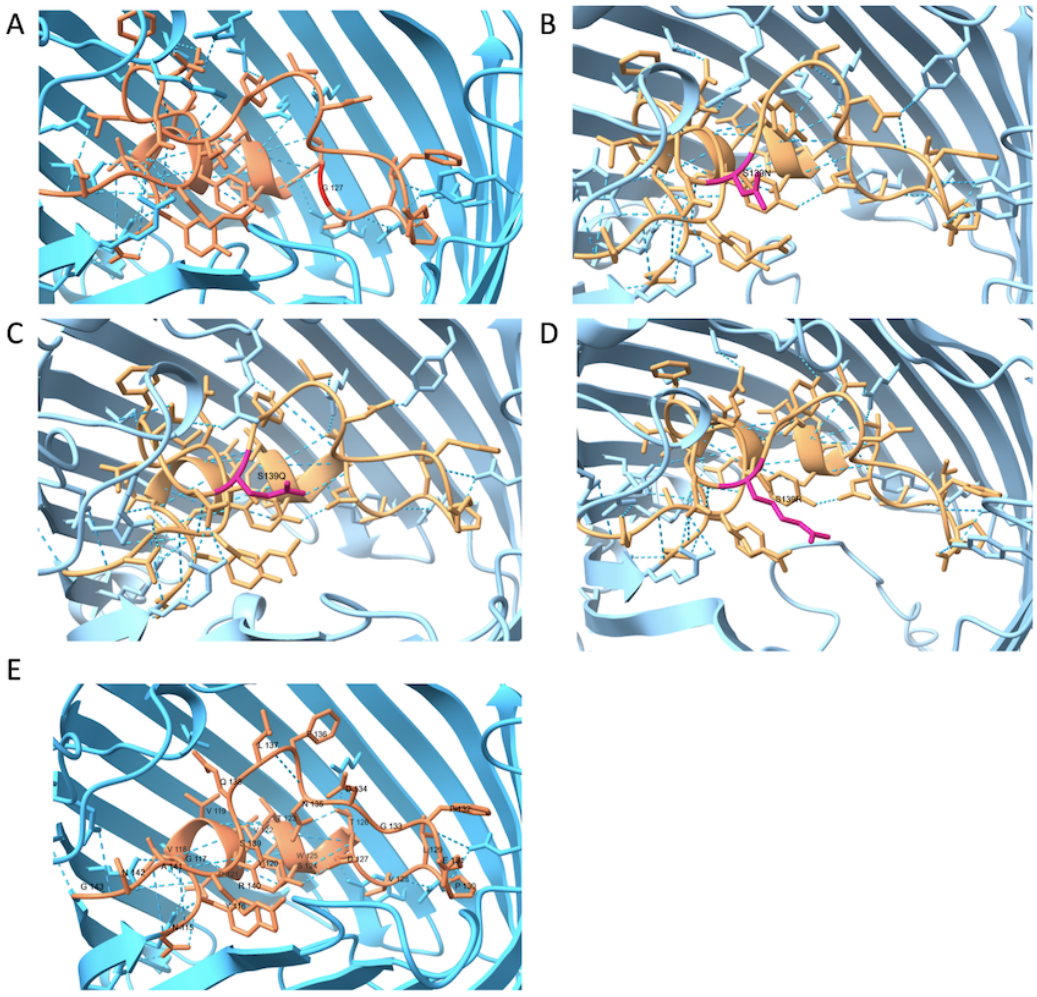

Figure 2.8: ***K. aerogenes* structural changes in loop 3 mutations**. OmpC is shown in blue, loop 3 in orange, and mutations in pink. (A) D127G. (B) S139N. (C) S139Q. (D) S13R. (E) Δ134-139.

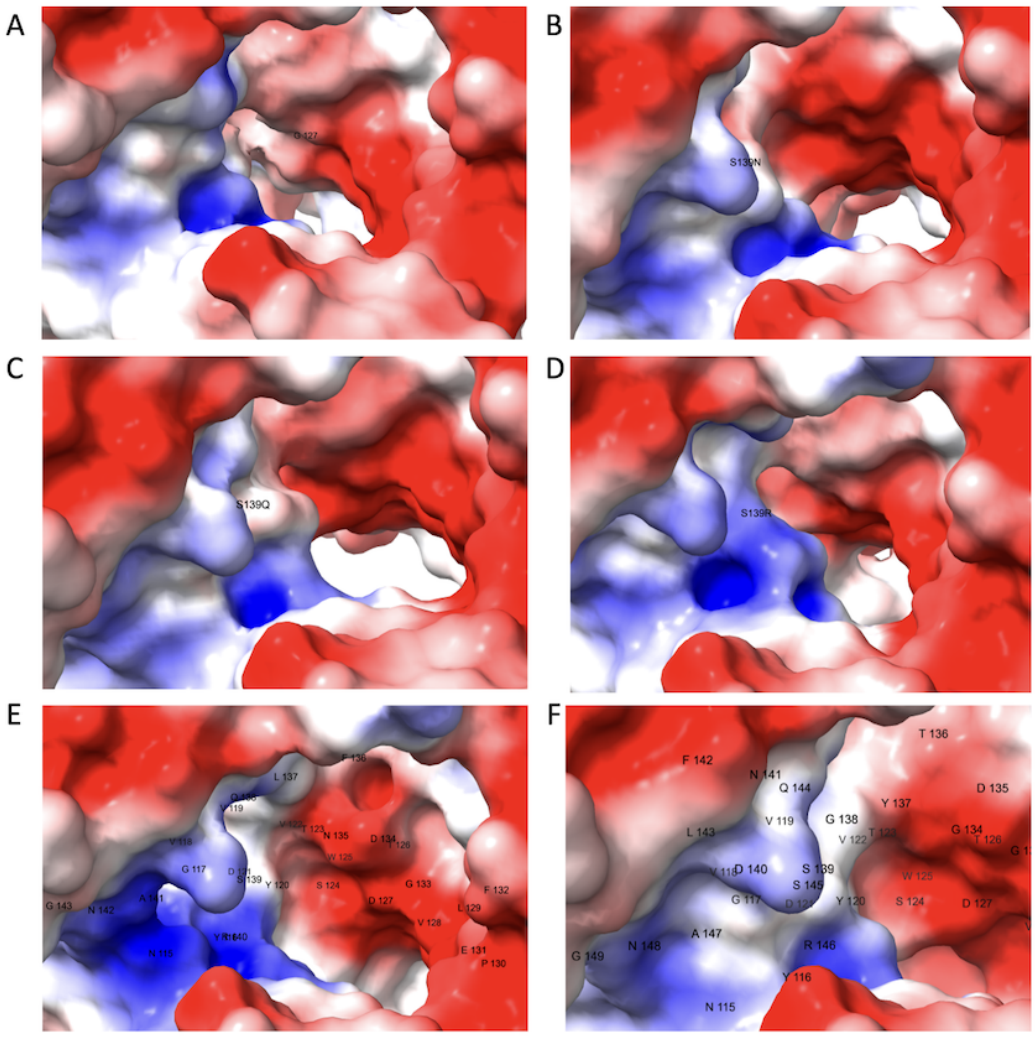

Figure 2.9: ***K. aerogenes* electrostatic changes in loop 3 mutations**. Positive areas are red, negative areas are blue, and neutral zones are white. (A) D127G. (B) S139N. (C) S139Q. (D) S13R. (E) Δ134-139. (F) Wild-type OmpC.

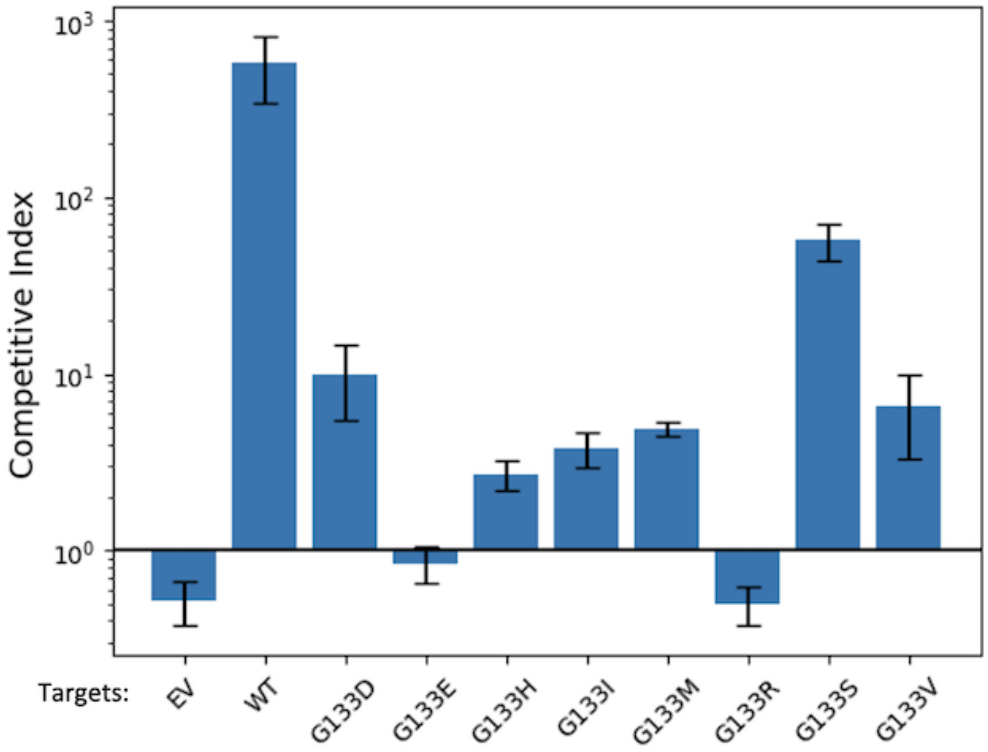

Figure 2.10: ***K. aerogenes* co-culture assay with loop 3 mutations at position 133**. Co-culture experiment reveal mutations that disrupt binding at G133E and G133R. Competitive Index (CI) is the ratio of viable colony-forming units per milliliter (CFU/mL) of inhibitors to targets at 5 hours relative to their starting ratios. CI values are represented as the average of at least 3 independent experiments ±SEM.

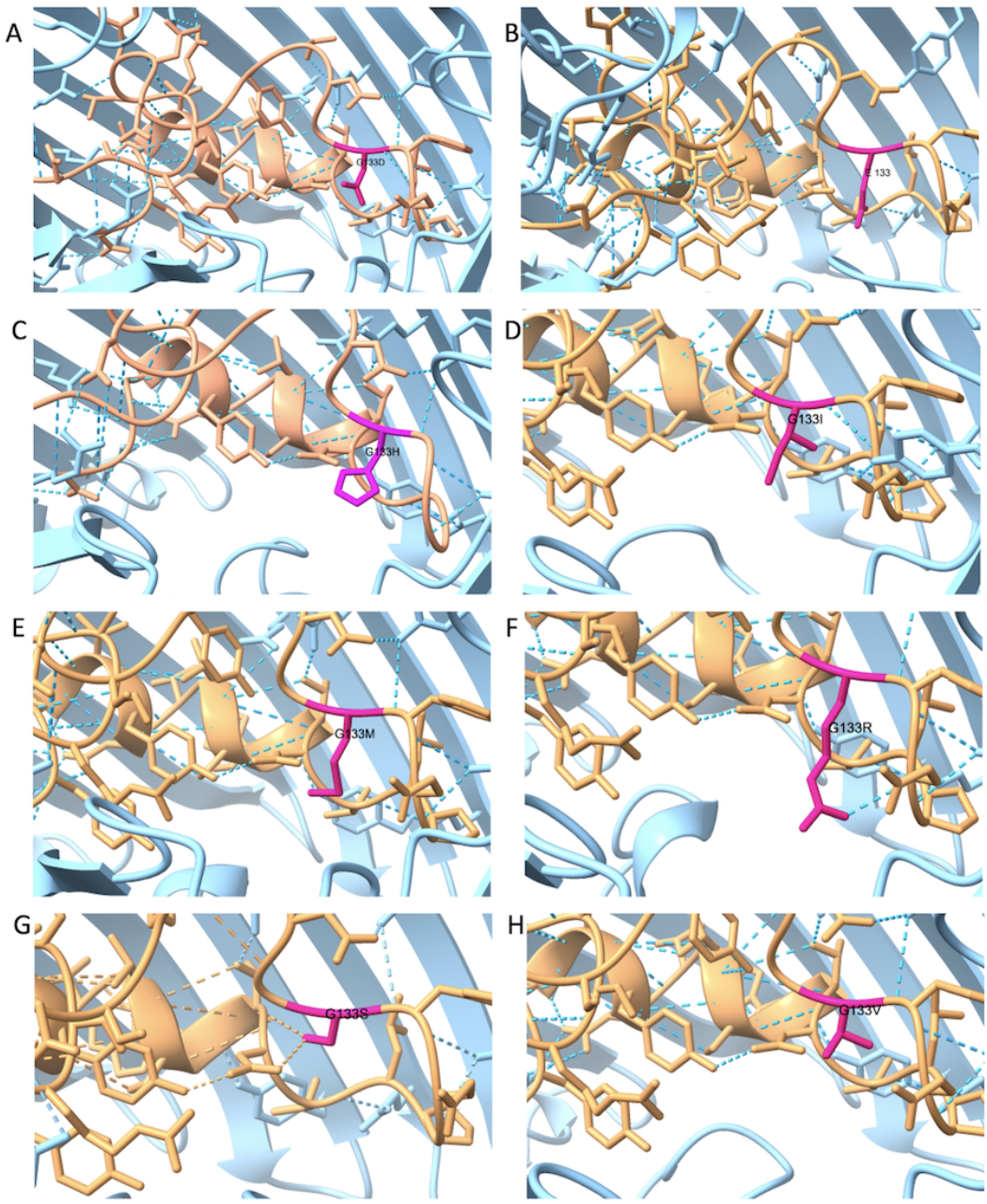

Figure 2.11: ***K. aerogenes* structural changes in loop 3 mutations at position 133**. OmpC is shown in blue, loop 3 in orange, and mutations in pink. (A) G133D. (B) G133E. (C) G133H. (D) G133I. (E) G133M. (F) G133R. (G) G133S. (H) G133V.

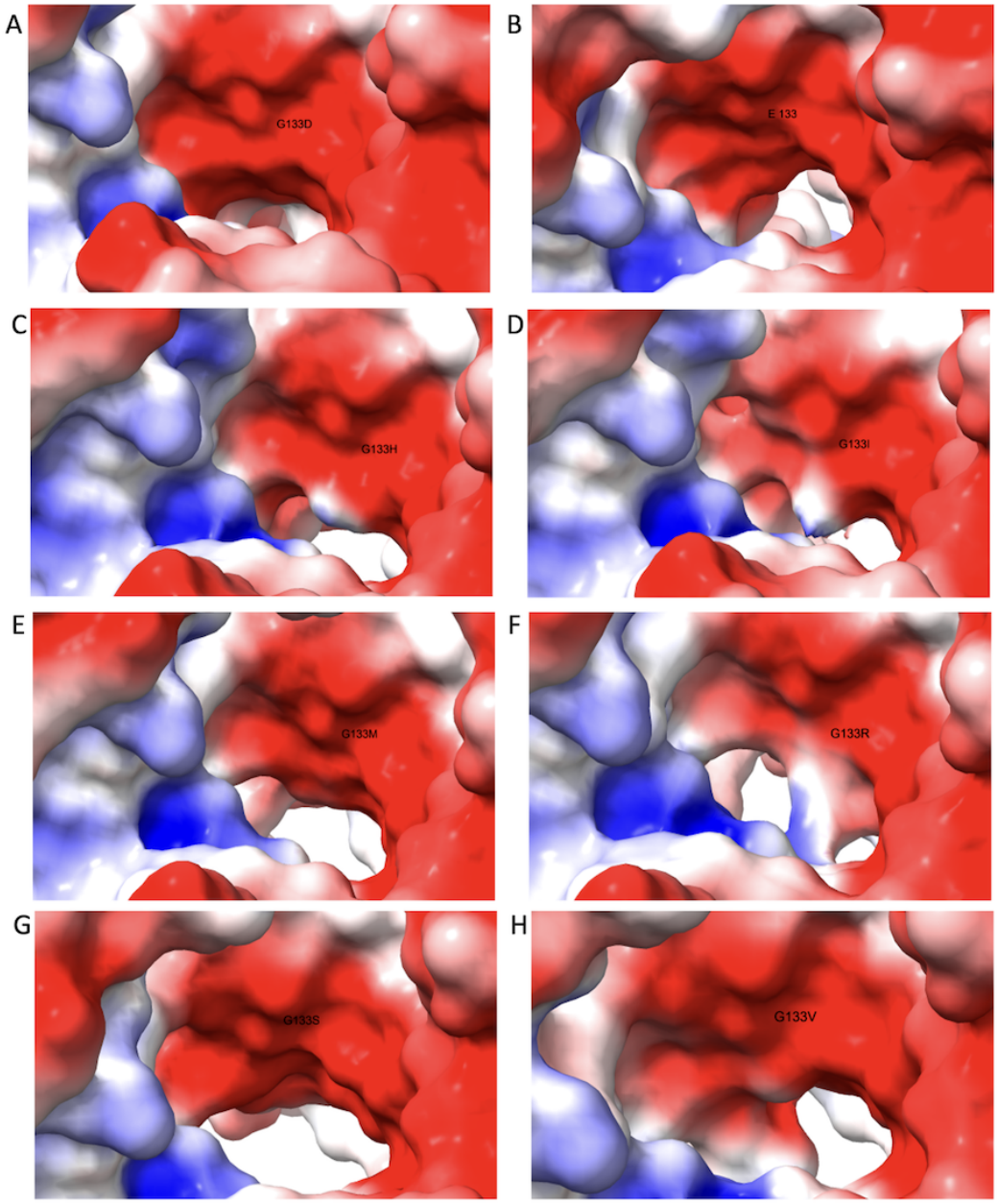

Figure 2.12: ***K. aerogenes* electrostatic changes in loop 3 mutations at position 133**. Positive areas are red, negative areas are blue, and neutral zones are white. (A) G133D. (B) G133E. (C) G133H. (D) G133I. (E) G133M. (F) G133R. (G) G133S. (H) G133V.

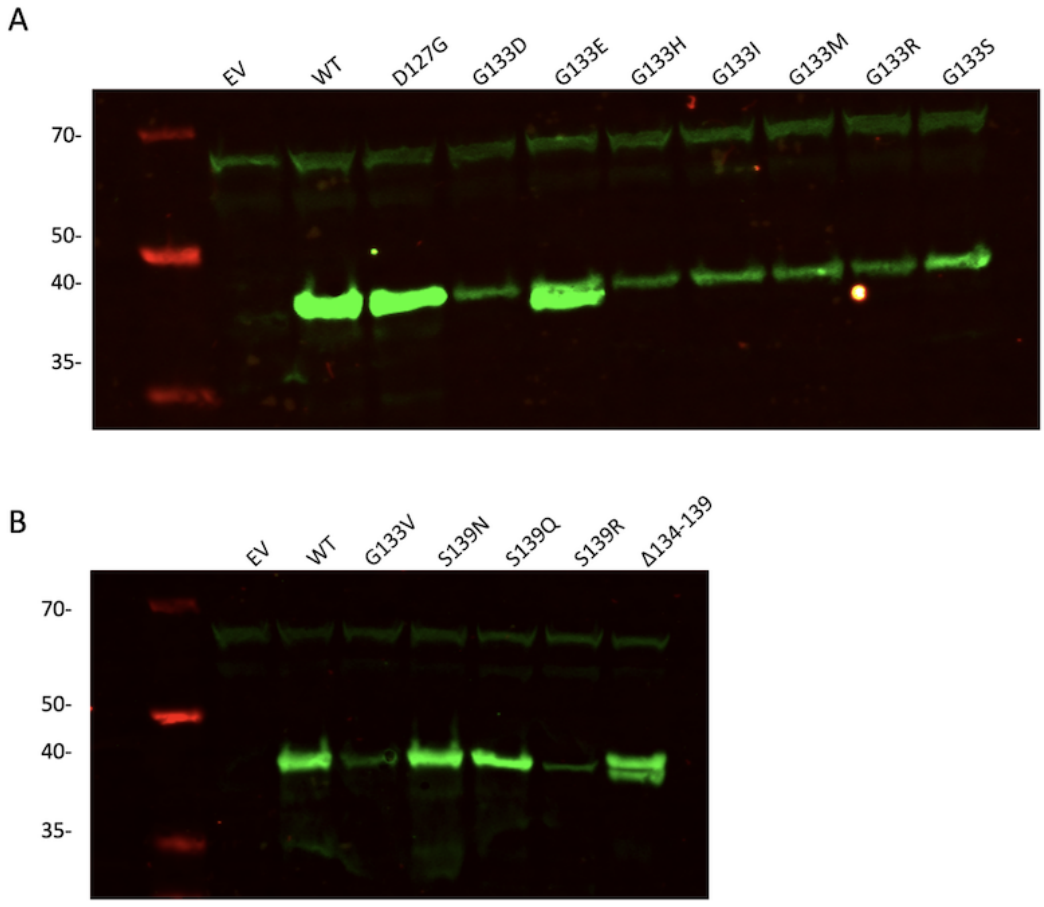

Figure 2.13: ***K. aerogenes* Western blot in kDa**. (A) Anti-OmpC immunoblot of *K. aerogenes* loop 3 mutations. (B) Anti-OmpC immunoblot of *K. aerogenes* loop 3 mutations.

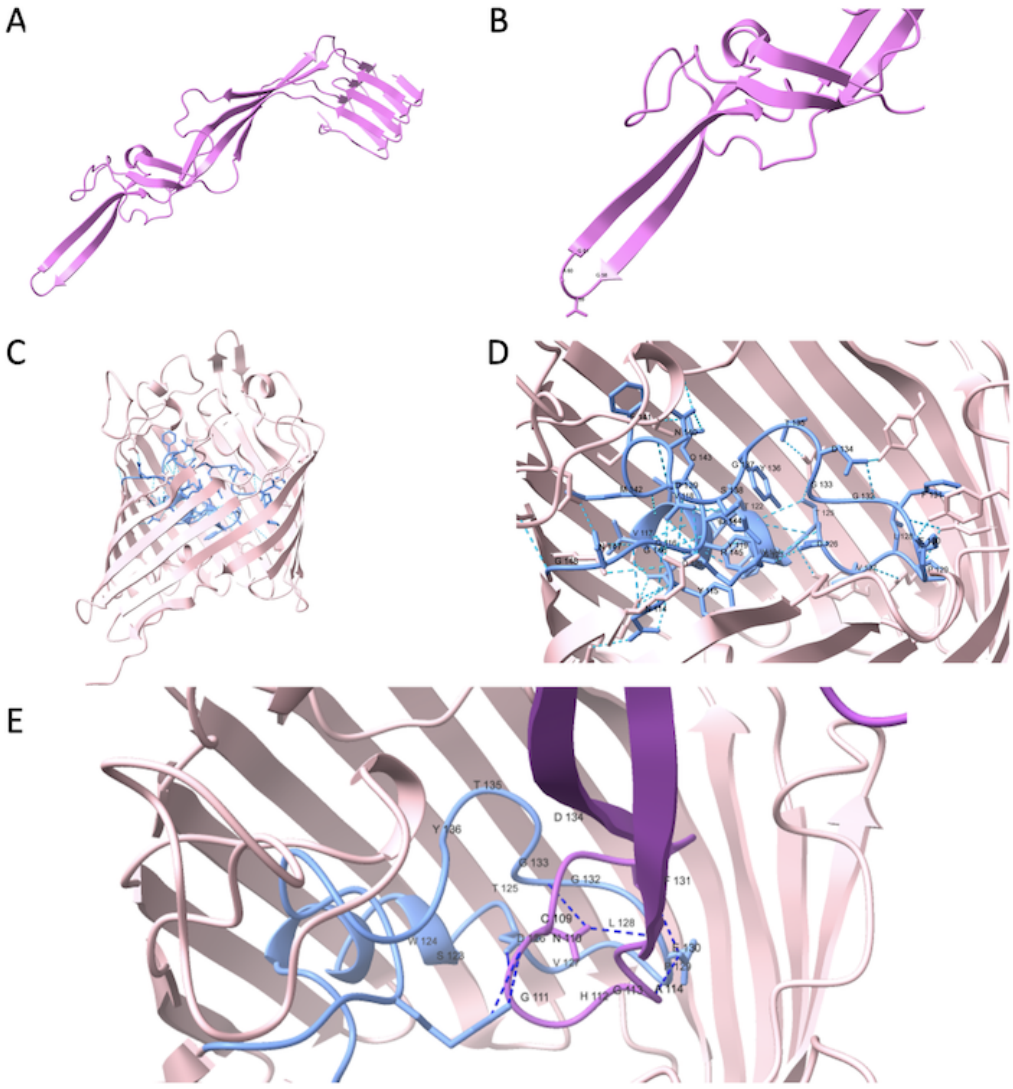

Figure 2.14: ***E. coli* F11 receptor binding domain and *E. coli* F11 OmpC**. (A) Receptor binding domain in magenta. (B) Receptor binding domain with the point labeled. (C) OmpC with loop 3 in blue. (D) OmpC with loop 3 labeled with amino acid and position. (E) Docking of RBD into OmpC.

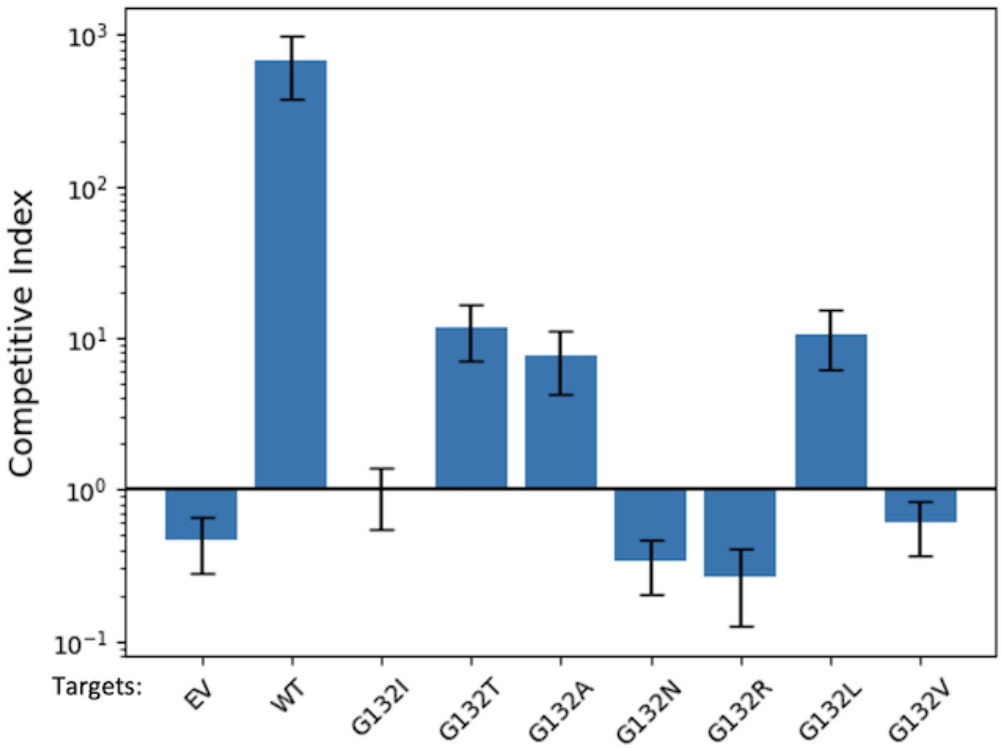

Figure 2.15: ***E. coli* F11 co-culture assay with loop 3 mutations at position 132**. Co-culture experiment reveal mutations that disrupt binding at G132I, G132N, G132R, and G132V. Competitive Index (CI) is the ratio of viable colony-forming units per milliliter (CFU/mL) of inhibitors to targets at 5 hours relative to their starting ratios. CI values are represented as the average of at least 3 independent experiments ±SEM.

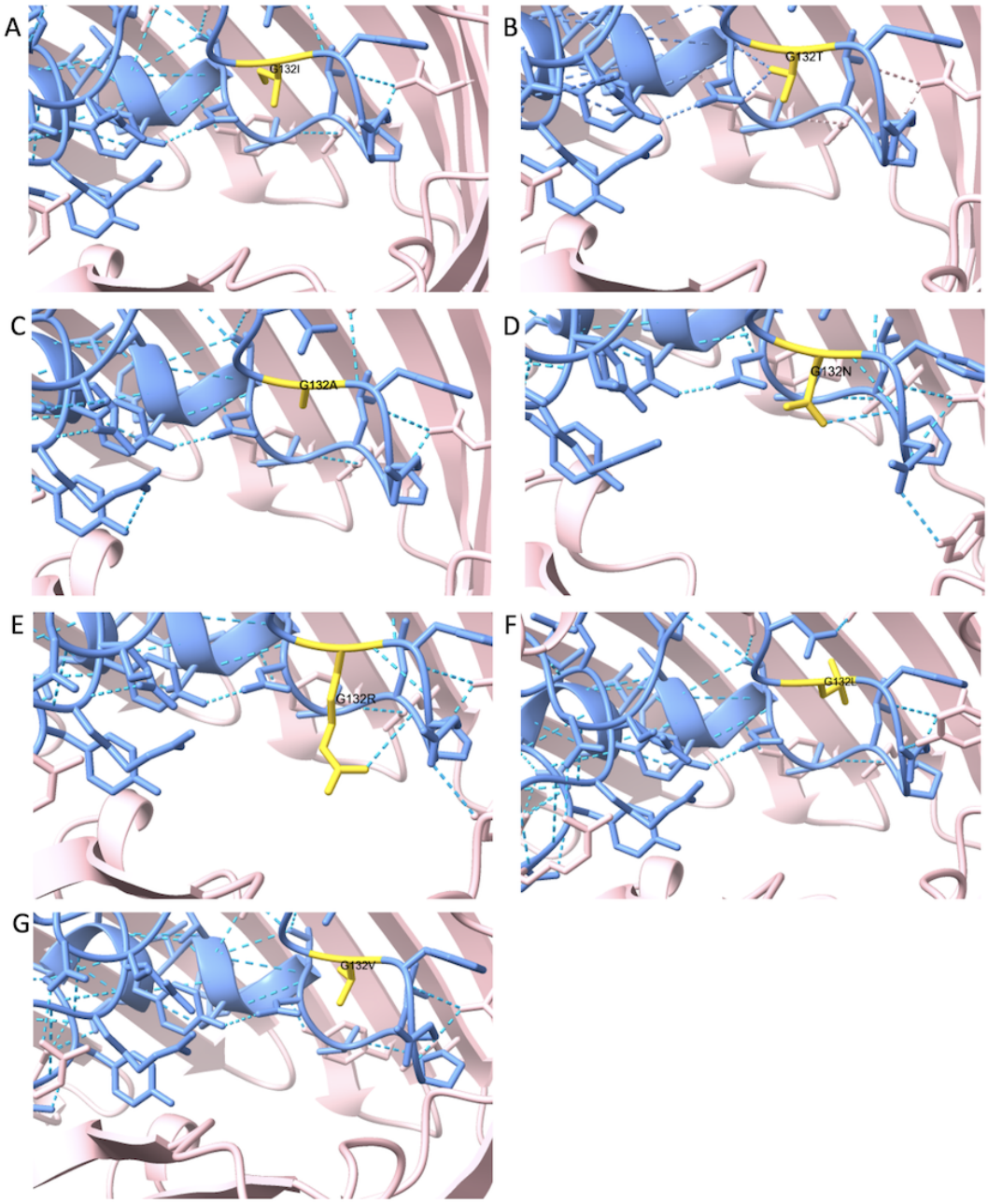

Figure 2.16: ***E. coli* F11 structural changes in loop 3 mutations at position 132**. F11 OmpC is pink, loop 3 is blue, and the mutaion is yellow. (A) G132I. (B) G132T. (C) G132A. (D) G132N. (E) G132R. (F) G132L (G) G132V.

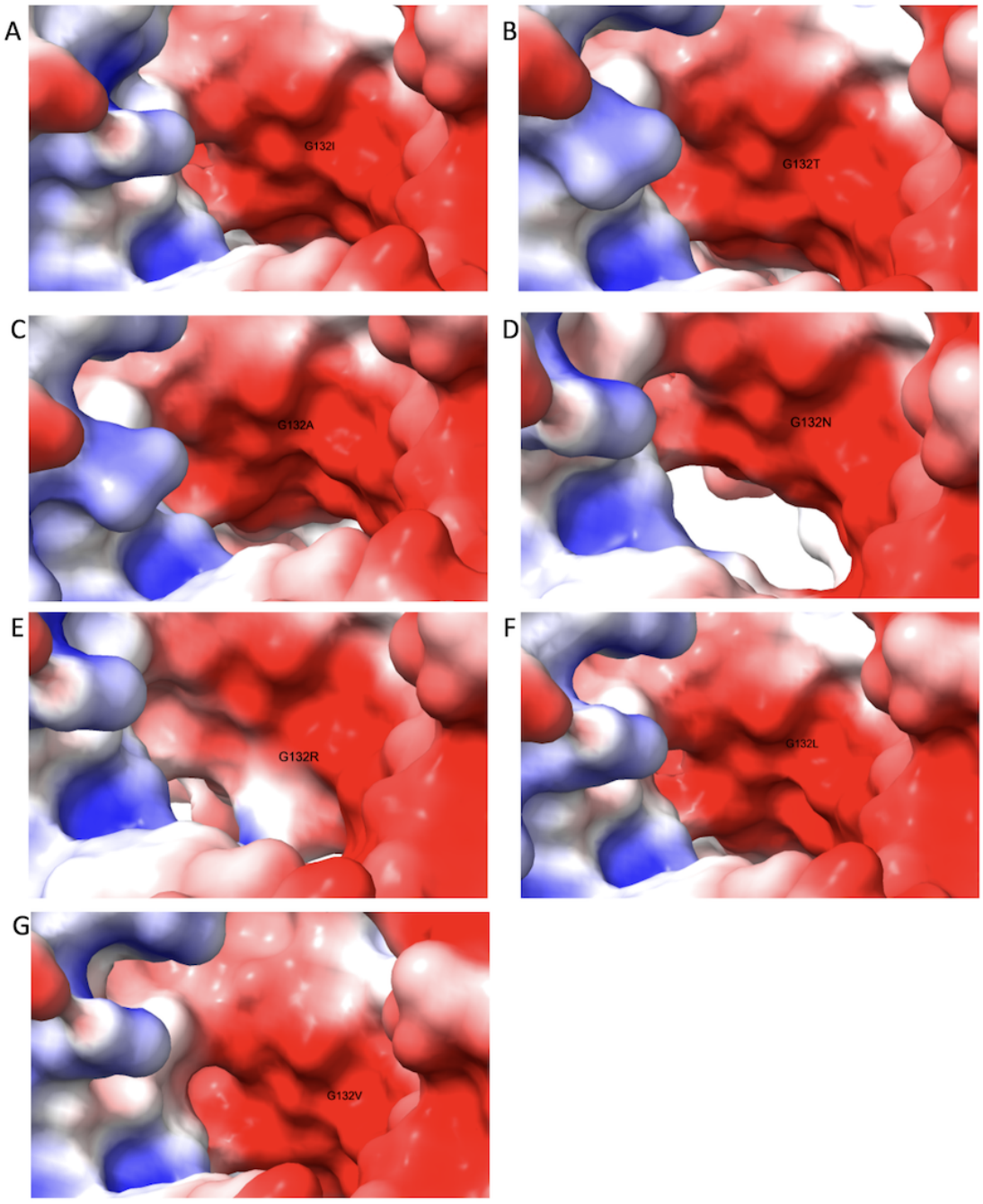

Figure 2.17: ***E. coli* F11 electrostatic changes in loop 3 mutations at position 132**. Positive areas are red, negative areas are blue, and neutral zones are white. A) G132I. (B) G132T. (C) G132A. (D) G132N. (E) G132R. (F) G132L (G) G132V.

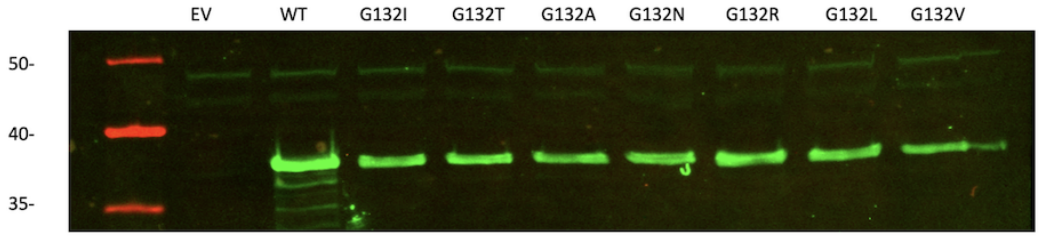

Figure 2.18: ***E. coli* F11 Western blot in kDa**. Anti-OmpC immunoblot of *E. coli* F11 loop 3 mutations at position 132.

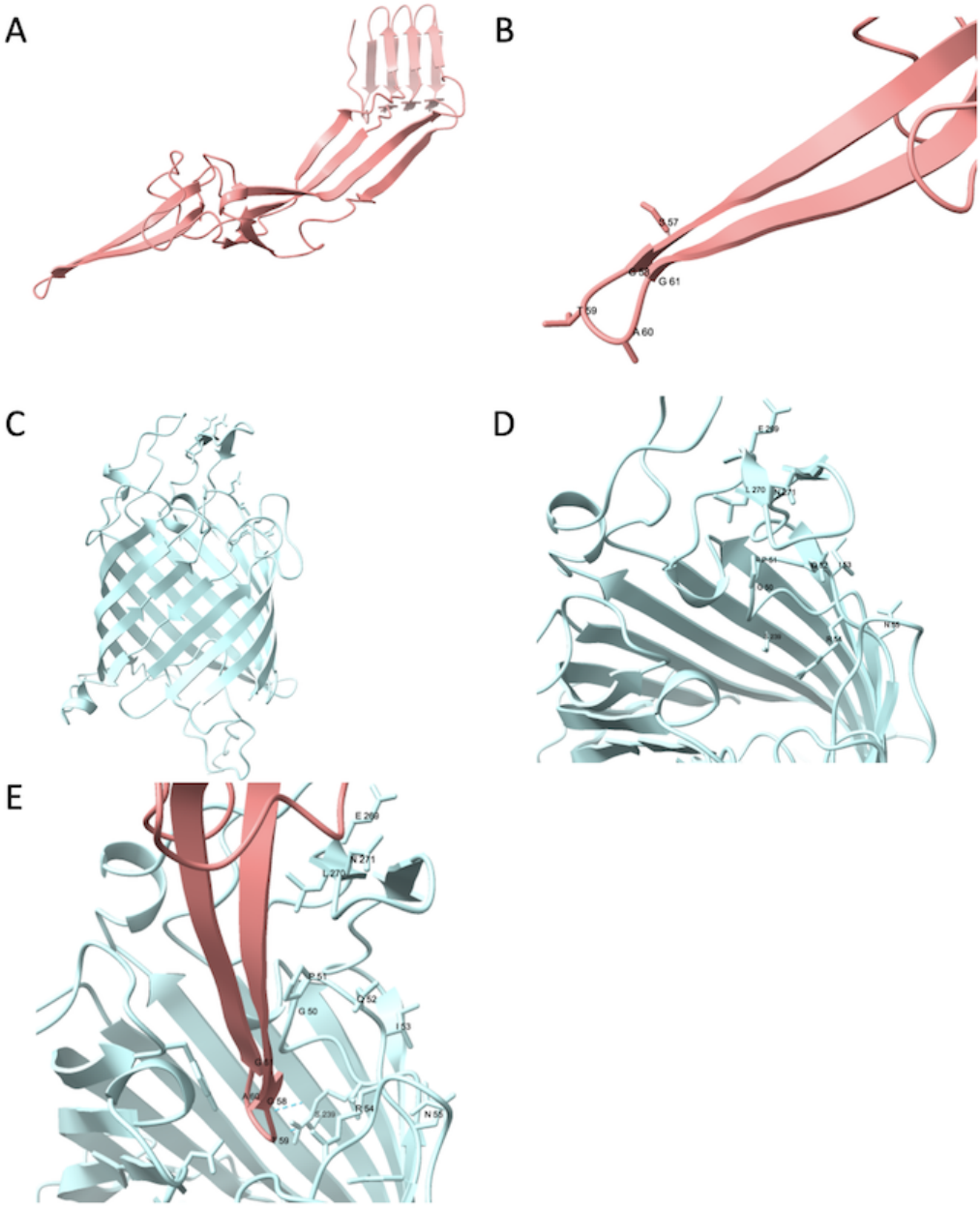

Figure 2.19: ***E. coli* STECO31 receptor binding domain and *E. coli* STECO31 Tsx**. (A) Receptor binding domain. (B) Receptor binding domain with the point labeled. (C) Tsx full view. (D) Tsx with select loops labeled with amino acid and position. (E) Docking of RBD into Tsx.

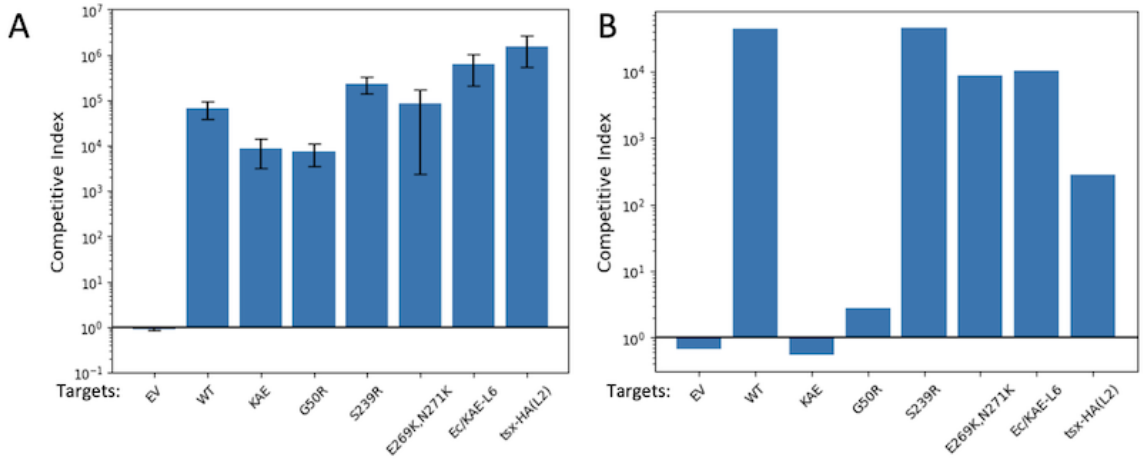

Figure 2.20: ***E. coli* STECO31 co-culture assay with mutations on Tsx**. (A) Co-cultures on solid agar do not show any resistance to the inhibitor strain. Competitive Index (CI) is the ratio of viable colony-forming units per milliliter (CFU/mL) of inhibitors to targets at 3 hours relative to their starting ratios. CI values are represented as the average of at least 3 independent experiments ±SEM (B) Co-culture in liquid media reveal mutations that disrupt binding at G50R and Tsx from *K. aerogenes*. Competitive Index (CI) is the ratio of viable colony-forming units per milliliter (CFU/mL) of inhibitors to targets at 3 hours relative to their starting ratios.

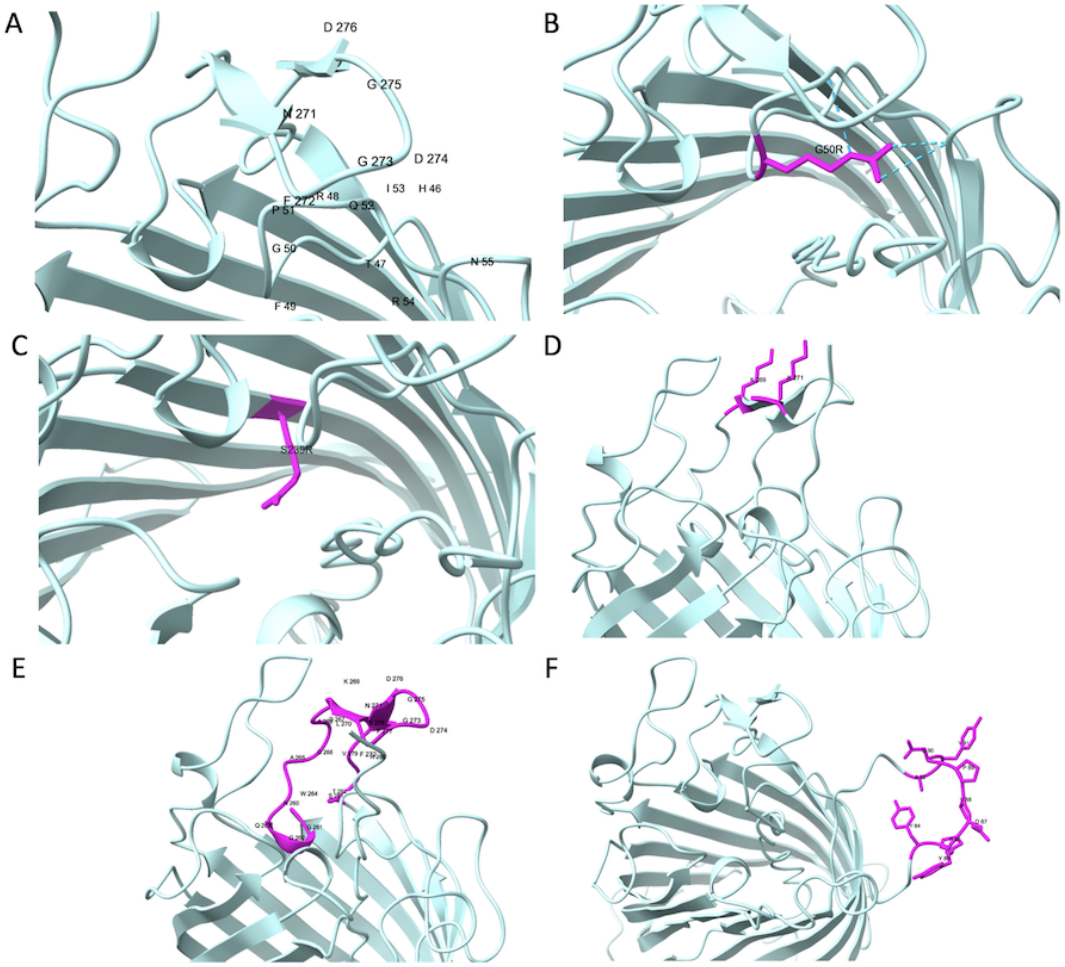

Figure 2.21: ***E. coli* STECO31 structural changes in Tsx**. Tsx is ice blue, mutations are in magenta. (A) *K. aerogenes* Tsx. (B) G50R. (C) S239R. (D) E269K, N271K. (E) Ec/KAE-L6. (F) Tsx-(HA)L2.

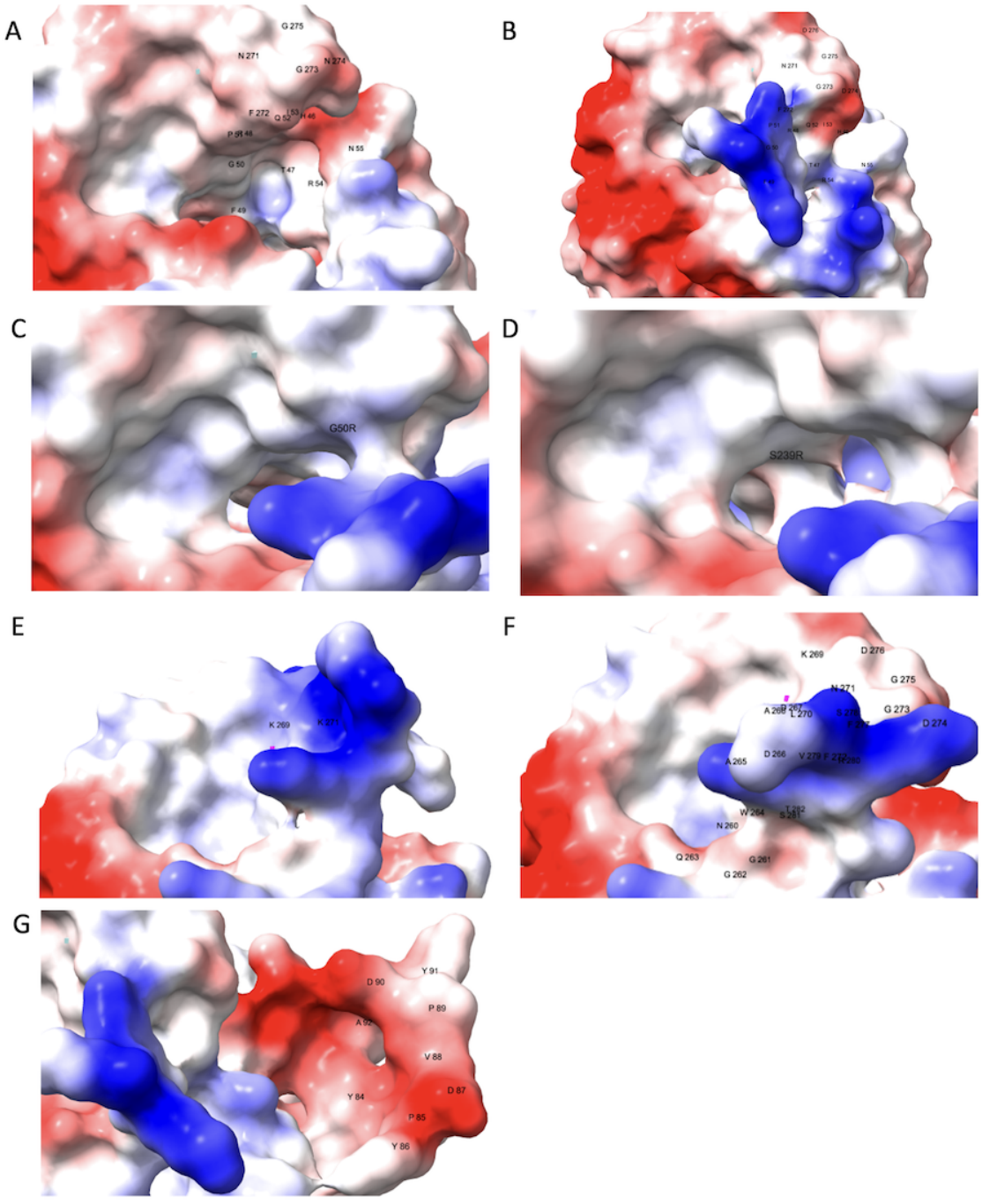

Figure 2.22: ***E. coli* STECO31 electrostatic changes in Tsx**. Positive areas are red, negative areas are blue, and neutral zones are white. (A) STECO31 Tsx. (B) *K. aerogenes* Tsx. (C) G50R. (D) S239R. (E) E269K, N271K. (F) Ec/KAE-L6. (G) Tsx-(HA)L2.

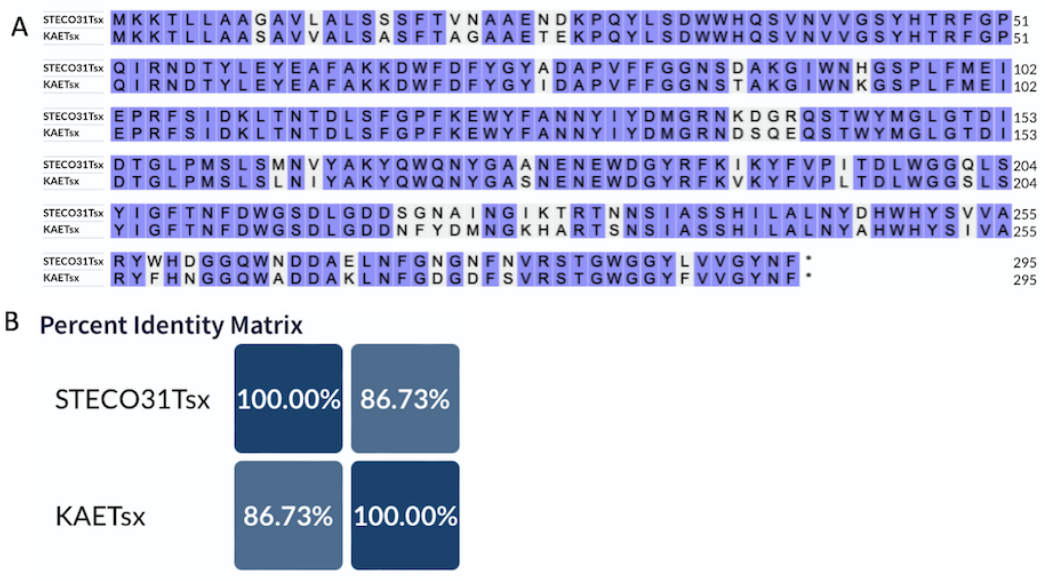

Figure 2.23: **Alignment of Tsx comparing *K. aerogenes* and *E. coli* STECO31**. (A) Clustal Omega alignment of Tsx with conserved residues highlighted in blue. (B) Percent identity matrix denoting the similarity.

Table 2.1: Strains used in Chapter 2.

Strain	**Description**	**Source**
CH7064	E. aerogenes ATCC 13048 attTn7::Gmr	This study
CH14016	MG1655 Δwzb Δtsx	[78]
CH273	K. aerogenes ATCC 13048 ΔcdiA1-CT-cdiI1-CTo1::kan	Hannah Ghasemi
CH282	K. aerogenes ATCC 13048 ΔcdiA2-cdiI2::kan	Christopher Hayes
CH3573	JCM 158 ΔompC ΔompF ΔslyD::cat	This study
CH10136	JCM 158 ΔompC ΔompF	[135]
CH11320	JCM 158 Δwzb ΔompC ΔompF::kan	This study
CH1079	MG1655 Δwzb::cat Δtsx	This study
CH1084	MG1655 Δwzb Δtsx::kan	This study

Table 2.2: Plasmids used in Chapter 2

Plasmid	Description	Source
pSC189-Kan	Mobilizable plasmid with R6K replication origin; carries the mariner transposon containing kanamycin resistance cassette; AmpR, KanR.	[154]
pCH405	Contains multiple cloning sites, and an ssrAgene that encodes ANDH6D peptide tag, TetR.	[107]
pCH405D	pACYC184 derivative with E. coli araBAD promoter for arabinose-inducible expression. TetR.	This study
pTrc99a	IPTG-inducible expression plasmid. AmpR.	Amersham-Pharmacia
pTrc99aKX	IPTG-inducible expression plasmid with added KpnI and XhoI sites. AmpR.	[154]
pUC18R6k-miniTn7T-Gmr	For integration at attTn7 when mated bi parentally with pTNS2. Carries gentamycin resistance cassette between Tn7 homology arms. AmpR, GmR.	[175]
pZS21(MCS)-KAN	pSC101-derived plasmid vector with the multiple cloning site removed. KanR.	[154]
pCH450	pACYC184 derivative with E. coli araBAD promoter for arabinose-inducible expression. TetR.	[154]

pCH450::PtsG	PtsG cloned into pCH450 with primers 3612/3613 and enzymes EcoRI/PstI from CH11840. TetR.	This study
pET21b::cdiBAI(STEC3)-RBD(KAE)	RBD(K. aerogenes) using EcoRI/BamHI and primers 4766/4767 cloned to CdiA(STEC3) from pCH2207. AmpR.	This study
pET21b::cdiBAI(STEC3)-RBD(KAE), CT-I(KAE)	RBD(K. aerogenes) using EcoRI/BamHI and primers 4766/4767 cloned to CdiA(STEC3) from pCH2207. AmpR.	This study
pCH2207	pET21b::cdiBAI(STEC) ΔRBD (EcoRI/BamHI)(1726C). AmpR.	Kiho Song
pCH450K::cdiI-1(EAE)	cdiI-1(KAE) subcloned in to p456 from p527 using Kpn/Xho. TetR.	This study
pCH456	pCH405Δ::cdiI-2(EC93). Plasmid can be used to subclone any KpnI/XhoI fragment for constitutive expression. TetR.	Christopher Hayes
pCH527	pCH450Δ::cdiI-1(EAE). TetR.	This study
pCH405Δ::cdiI-2 (K. aerogenes)	Used primers 5549/5550 to clone immunity gene from K. aerogenes ATCC 13048 cdi-2 locus (EndoU). TetR.	This study
pTrc99aKX::ompC (K. aerogenes)	Gene cloned using primers 3326-Nco/2388-Xho. AmpR.	Christina Beck

pZS21(MCS)-KAN::ompF(KAE)	Used primers 5942Eco/5943Xba to clone in ompF from K. aerogenes ATCC 13048 into pZS21. KanR.	This study
pTrc99aKX::ompC-D127G(KAE)	D127G mutation cloned in with primers 3326/6042. AmpR.	This study
pTrc99aKX::ompC-G133D(KAE)	G133D mutation cloned in with primers 6015/2388. AmpR.	This study
pTrc99aKX::ompC-G133E(KAE)	G133E mutation cloned in with primers 6016/2388. AmpR.	This study
pTrc99aKX::ompC-G133H(KAE)	G133H isolated from random 133 library. AmpR.	Christopher Hayes
pTrc99aKX::ompC-G133I(KAE)	G133I isolated from random 133 library. AmpR.	Christopher Hayes
pTrc99aKX::ompC-G133M(KAE)	G133M isolated from random 133 library. AmpR.	Christopher Hayes
pTrc99aKX::ompC-G133R(KAE)	G133R isolated from random 133 library. AmpR.	Christopher Hayes
pTrc99aKX::ompC-G133S(KAE)	G133S isolated from random 133 library. AmpR.	Christopher Hayes
pTrc99aKX::ompC-G133V(KAE)	G133V isolated from random 133 library. AmpR.	Christopher Hayes
pTrc99aKX::ompC-S139N(KAE)	S139N isolated from random 139 library. AmpR.	Christopher Hayes

pTrc99aKX::ompC-S139Q(KAE)	S139Q isolated from random 139 library. AmpR.	Christopher Hayes
pTrc99aKX::ompC-S139R(KAE)	S139R mutation cloned in with primers 6017/2388. AmpR.	This study
pTrc99aKX::ompC-ΔG134-S139(KAE)	ΔG134-S139 mutation cloned in with primers 6041/2388. AmpR.	This study
pET21b::cdiBAI(STEC3)-RBD(EC536)	RBD(EC536) using EcoRI/BamHI and primers 4787/4788 cloned to CdiA(STEC3) from pCH2207. AmpR.	This study
pTrc99KX::ompC(F11)	Wild-type ompC gene from E. coli F11. AmpR.	This study
pTrc99KX::ompC-G132I(F11)	G132I isolated from random G132 codon library of ompC(F11). AmpR.	Christopher Hayes
pTrc99KX::ompC-G132T(F11)	G132T isolated from random G132 codon library of ompC(F11). AmpR.	Christopher Hayes
pTrc99KX::ompC-G132A(F11)	G232A isolated from random G132 codon library of ompC(F11). AmpR.	Christopher Hayes
pTrc99KX::ompC-G132N(F11)	G132N isolated from random G132 codon library of ompC(F11). AmpR.	Christopher Hayes
pTrc99KX::ompC-G132R(F11)	G132R isolated from random G132 codon library of ompC(F11). AmpR.	Christopher Hayes
pTrc99KX::ompC-G132L(F11)	G132L isolated from random G132 codon library of ompC(F11). AmpR.	Christopher Hayes

pTrc99KX::ompC-G132V(F11)	G132V isolated from random G132 codon library of ompC(F11). AmpR.	Christopher Hayes
pET21(MCS-)::STEC3(RBD-Eco/Bam)-NoCys	RBD(STECO31) using EcoRI/BamHI and primers 4858/4859 cloned to CdiA(STEC3) from pCH2207. AmpR.	This study
pTrc99A::tsx	Nucleoside transport from STECO31. AmpR.	Christopher Hayes
pTrc99A::tsx(KAE)	Nucleoside transport from K. aerogenes. AmpR.	Christopher Hayes
pTrc99A::tsx(G50R)	Nucleoside transport mutation. AmpR.	Christopher Hayes
pTrc99A::tsx(S239R)	Nucleoside transport mutation. AmpR.	Christopher Hayes
pTrc99A::tsx(E269K, N271K)	Phage T6 resistance mutation. AmpR.	Christopher Hayes
pTrc99A::tsx(Ec/KAE-L6)	Chimera with loop 6 from KAE grafted onto E. coli tsx. AmpR.	Christopher Hayes
pTrc99A::tsx-HA(L2)	HA epitope introduced into unresolved loop 2 of E. coli Tsx. AmpR.	Christopher Hayes

Table 2.3: Primers used in Chapter 2

Primer	**Description**	**Sequence**	**Source**
2388	ompC-Xho-rev	5' - TCA CTC GAG ATT AGA ACT GGT AAA CCA GAC - 3'	This study

3326	ompC-Nco-for	5' - TTT CCA TGG TAG TTA AAG TAC TGT CCC - 3'	This study
4766	EAE-N1386-Eco-for	5' - GCT GAA TTC CCG CGA CGG AC - 3'	This study
4767	EAE-P1670-Bam-rev	5' - ATT GGA TCC AGG CAG TGG GTA GT - 3'	This study
4787	EC536-R1378(RBD)-Eco-for	5' - TCT GAA TTC GCG GGA GGG ATT TTC TGC - 3'	This study
4788	EC536-P1671(RBD)-Bam-rev	5' - GTT GGA TCC AGG CAG TGG CCA GTC ATC - 3'	This study
4858	STEC3-N1384(RBD)-Eco-for	5' - ACT GAA TTC GCG GGA GGG CAT AAA TGA G	This study
4859	STEC3-P1660(RBD)-Bam-rev	5' - GTT GGA TCC AGG CAG GGG ATA GTT CCC	This study
5248	EAE09030-CT(KO)-Sac	5' - CCT GAG CTC CGA CAC CAA ACA YG - 3'	This study
5249	EAE09030-CT(KO)-Bam	5' - ACC GGA TCC GGC ACC CGT CG - 3'	This study
5250	EAE09025-cdiI(KO)-Eco	5' - TTT GAA TTC ATA TTG AAA CAG TTG AAT AGG - 3'	This study
5251	EAE09025-cdiI(KO)-Kpn	5' - CGG GGT ACC GAT AAA GAT ACG GAT GAT G - 3'	This study

5263	EAE-cdiI2(KO)-Sac-for	5' - TTT GAG CTC GCC CAT TGC CGG GGA TAT C - 3'	This study
5264	EAE-cdiI2(KO)-Bam-rev	5' - TTT GGA TCC GCA CGA TTA GCC TGA GTC TGA TTT G - 3'	This study
5265	EAE-cdiI2(KO)-Eco-for	5' - TAA GAA TTC AAA ATC TCA ACC TCA AAA TGG TTC -3'	This study
5266	EAE-cdiI2(KO)-Kpn-rev	5' - TTT GGT ACC CAC CTG GTG TAT CTG GTG G - 3'	This study
5301	EAE-cdiI1-Kpn-for	5' - GAA GGT ACC ATG AAG CTG ATG AAA CCA CTA A - 3'	This study
5302	EAE-cdiI1-Xho-rev	5' - GTT CTC GAG TTA TTT ATC CGC TTA TTT TTT GTT TTT GT -3'	This study
5311	EAE-cdiA1(KO)-Sac	5' - CGT GAG CTC TGA TAA CAG CGG TC	This study
5312	EAE-cdiA1(KO)-Bam	5' - CAA GGA TCC TTT AAA ACG CAA CGG CAA	This study
5313	EAE-cdiA1(KO)-Eco	5' - GCT GAA TTC CTA GCG AGG CTG TTG G	This study
5314	EAE-cdiA1(KO)-Kpn	5' - TCC GGT ACC GCT GAC CAG GTT TC	This study

5549	KAE-cdiI2-Kpn-for	5' - GAC GGT ACC ATG AAC GAA TAT ATT TTT GAG AAC ATA G	This study
5550	KAE-cdiI2-Xho-rev	5' - CTA CTC GAG ATC TTT ACT CAG GCT GG	This study
5942	KAE-ompF-Bam-for	5' - TTT GGA TCC ATG ATG AAG CGC AAT ATT CTG GCA GTG G - 3'	This study
5943	KAE-ompF-Xba-rev	5' - TTT TCT AGA TTA GAA CTG GTA AAC GAT ACC AAC CGC - 3'	This study
6015	KAE-ompC-G133D-Eco-for	5'- CCG GAA TTC GAC GGC GAC ACC - 3'	This study
6016	KAE-ompC-G133E-Eco-for	5'- CCG GAA TTC GAA GGC GAC ACC- 3'	This study
6017	KAE-ompC-S139R-Eco-for	5'- CCG GGA TTC GGC GGC GAC ACC TAC GGT CGC GAC ACC TTC - 3'	This study
6041	KAE-ompC-delG134-S139-Eco-for	5' - TTT GAA TTC GGC GAC AAC TTC CTG CAG TCC CG - 3'	This study
6042	KAE-ompC-D127G-Eco-rev	5' - GCC GAA TTC CGG CAG AAC GCC GGT CCA GGA AGT T - 3'	This study

6043	KAE-ompF-Eco-for	5' - AAA GAA TTC TAA TGA GGG TAA TAA ATA ATG ATG AAG CGC - 3'	This study
6044	KAE-ompF-Xho-rev	5' - TTT CTC GAG TTA GAA CTG GTA AAC GAT ACC AAC CG - 3'	This study
6045	KAE-tsx-Eco-for	5' - GCT GAA TTC AAA CAA TGG CAT CAA CAT GAA AAA AAC	This study
6046	KAE-tsx-Xba-rev	5' - CTG TCT AGA TGT ATC AGC AAT TAG AAG TTG	This study
6083	tsx-L2-HA-for	5' - CAT ACG ATG TTC CCG ATT ACG CTG GTA ACT CCG ATG CTA AAG G	This study
6084	tsx-L2-HA-rev	5' - GTA ATC GGG AAC ATC GTA TGG ATA GCC GAA GAA TAC CGG C	This study
6085	tsx-G50R-for	5' - TAT CAC ACC CGT TTC CGA CCG CAG ATC CGC	This study
6086	tsx-G50R-rev	5' - GCG GAT CTG CGG TCG GAA ACG GGT GTG ATA	This study
6087	tsx-S239R-for	5' - ACT CTA TCG CTT CCA GAC ATA TTC TGG CTC	This study

6088	tsx-S239R-rev	5' - GAG CCA GAA TAT GTC TGG AAG CGA TAG AGT	This study
6089	tsx-N271K-for	5' - CGA TGC AGA ACT GAA GTT CGG CAA CGG C	This study
6090	tsx-N271K-rev	5' - GCC GTT GCC GAA CTT CAG TTC TGC ATC G	This study
6091	Ec/KAE-tsx-L6-for	5' - CTG TCG TAG CTC GTT ACT GGC ACA ACG GCG GCC AGT GGG C	This study
6092	Ec/KAE-tsx-L6-rev	5' - GCC CAC TGG CCG CCG TTG TGC CAG TAA CGA GCT ACG ACA G	This study
6093	KAE-ompC(133)-random-Eco-for	5' - CCG GAA TTC VNN GGC GAC ACC TAC GGT TC	This study
6094	KAE-ompC(139)-random-Eco-for	5' - CCG GAA TTC GGC GGC GAC ACC TAC GGT VNN GAC AAC TTC	This study

Chapter 3

CDI interactions between CdiB and CdiA of *Escherichia coli* STEC_O31

3.1 Abstract

E. coli STEC_O31 is uses a type Vb secretion system and releases toxic effectors in a contact-dependent manner. This release is multipurpose in that it poisons nonkin and neighboring cells and it contacts kin to promote adhesion, intracellular survival, biofilm formation, and other virulence factors. The exportation of CdiA by CdiB and the mechanism of association of the two proteins is not well understood. Using the existing crystal structure of CdiB, we hypothesized interactions between the extracellular loops of CdiB and CdiA. Disruption of these contact points may disturb the presentation of CdiA on the cell surface. We also looked for a protein-protein interaction by crosslinking CdiA and CdiB and could see indications of the interaction and will need more investigation to confirm the interaction.

3.2 Introduction

Bacteria live in communities and can communicate with each other through quorum sensing, chemical gradients, and contact-dependent inhibition (CDI). Canonical CDI gene organization consists of *cdiB*, *cdiA*, and *cdiI*. The *cdiB* and *cdiA* genes encode a two-partner secretion (TPS) system that exports CdiA through the central lumen of the CdiB β-barrel. CdiA is also known as TpsA or exoprotein cargos, which can form long β-helical filaments that extend several hundred angstroms from the cell surface [14]. This specialized TpsB/TpsA pair is used to bind and inhibit the growth of neighboring target cells in a contact-dependent manner. CdiA has seven domains and the domain furthest from the cell surface is the receptor binding domain (RBD) [106]. CdiA is secreted through the lumen of CdiB and enters a programmed secretion arrest where the C-terminal half is sequestered in the periplasm. When this domain binds to the receptor, secretion resumes for CdiA by delivering the toxin into the target cell [96].

CdiA effectors show significant variation in sequence and size depending on bacterial species and strain. The smallest known CdiA protein is MhaB1 from *Moraxella catarrhalis* O35E, with a size of around 182 kDa, and the largest is approximately 636 kDa encoded by the PSPTO_3229 locus of *Pseudomonas syringae* DC3000 [176, 98]. Despite this diversity, most CdiA proteins have a similar structure to the filamentous hemagglutinin (FHA/FhaB) adhesins of *Bordetella* species [98]. The N-terminal elements of these proteins are used to move them from the cytoplasm to the periplasm by using the Sec machinery [177]. The N-terminal region of CdiA also contains the TPS transport domain required for export across the outer membrane. CdiB recognizes the TPS transport domain and transports CdiA through the central pore in its β-barrel domain using the hairpin model to move the protein to the exterior of the cell. CdiA proteins also have FHA-1 and FHA-2 peptide repeats with FHA-1 building the "stick"

that extends outward from the cell surface. FHA-2 remains in the periplasm until it is in contact with a target cell receptor where secretion will resume. The "stick" or FHA-1 repeats are predicted to form right-handed parallel β-helices. CdiA proteins could then extend 40–140 nm from the surface of CDI+ bacteria [98].

The C-terminal region of CdiA effectors has a more variable domain composition. This end contains the toxin which can have DNase, RNase, or pore-forming activities [104]. CdiA proteins from *Pseudomonadaceae* and *Moraxellaceae* often contain the predicted α-helical DUF637, a domain of unknown function, while those from *Enterobacteriaceae*, *Moraxellaceae*, *Pasteurellaceae*, and *Neisseria meningitidis* strains usually contain the pretoxin-VENN domain, which identifies the variable CdiA-CT toxin region [92, 94]. Although CdiA proteins from other species lack the pretoxin-VENN domain, the CdiA-CT is identifiable as a sequence-variable region at the end of the C-terminus. The CdiA-CT region varies in domain sequence due to its toxic activity [104]. CdiA is modular to a degree where the toxin domain or receptor binding domain can be exchanged between CdiA proteins to generate a chimeric effector [106, 149].

The other part of the two-partner secretion system, CdiB, belongs to the Omp85 superfamily, which includes two types of proteins: BamA/TamA proteins that insert outer membrane proteins into the outer membrane, and TpsB proteins that secrete proteins to the extracellular surface. TpsB and BamA/TamA proteins share a common fold but have distinct features [178]. They both use a 16-stranded β-barrel to span the outer membrane and have periplasmic interaction modules called POTRA domains. The polypeptide-transport-associated (POTRA) domains are hypothesized to mediate protein-protein interactions and have chaperone-like activity [179]. The extracellular loop 6 (L6) is essential for activity in both the TpsB and BamA/TamA proteins and forms a "lid-lock" in the β-barrel lumen. TpsB proteins also have an N-terminal α-helix (H1) inserted into the barrel pore. The barrel pore is essential for secretion, therefore

this H1 insert must be removed for secretion to occur. [85]. CdiB exports CdiA through the lumen of the β-barrel sending out FHA-1, RBD, and the YP region. Secretion arrest occurs after the partial secretion of CdiA where FHA-2, pre-toxin domain, and the toxin domain remain in the periplasm. The interactions of CdiB and CdiA are essential for learning more about the secretion process and secretion arrest.

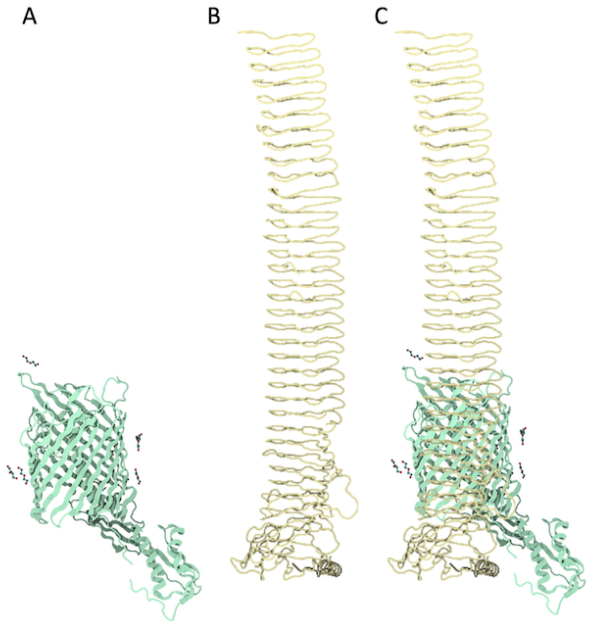

Figure 3.1: **CdiB and CdiA from *E. coli* STEC_O31.** (A) STEC_O31 CdiB. (B) STEC_O31 signal sequence, transport domain, and part of FHA-1. (C) STEC_O31 CdiB with CdiA in the lumen of the β-barrel. All figures created with Biorender.

3.3 Results

3.3.1 CdiB cysteine scan for topology and interaction with CdiA

We introduced cysteine residues in select areas of *E. coli* STEC_O31 CdiB to map the exterior residues and the interaction between CdiA and CdiB for points of contact. CdiB is a β-barrel that two native cysteines in the signal sequence and in the first POTRA

domain. The cysteines in the signal sequence are cleaved off [85]. Proteins that do have cysteines can form secondary structures that allow proximal cysteines to reduce and form disulfide bonds. These bonds provide extra structural support. Incorrect formation of these bonds can lead to targeted degradation of the protein [180]. Without any native cysteines in the barrel, CdiB is an excellent candidate for a cysteine scan using maleimide dye, which stains unoccluded cysteine residues. The maleimide dye binds to the thiol group in the cysteine to form a thiosuccinimide product [181].

We started our investigation in the 3rd exterior loop and continued down the 6th β-strand because it is a longer strand that may contact CdiA. Mutations N339C, R340C, and G341C are on loop 3 of CdiB (Fig. 3.2). CdiB without the presence of CdiA was produced alone and purified by Nickel purification using the His-tag on S88. The purified CdiB were then treated with maleimide dye to label the cysteine residues. After purification, the maleimide labeled cysteine mutants were run on an SDS-PAGE gel and subject to fluorimetry. Without the presence of CdiA, N339C and G341C are dyed with maleimide indicating that they are on the exterior surface of the cell (Fig. 3.4). Without a wild-type control, the labeling could be due to the two cysteines in the first POTRA domain, but if that were the case R345C with CdiA would also be labeled with the dye. CdiB in the presence of CdiA were produced on the same operon and CdiB was purified using Nickel purification using the His-tag on S88. The purified CdiB were then treated with maleimide dye to label the cysteine residues that are unoccluded by CdiA. After purification, the maleimide labeled cysteine mutants were run on an SDS-PAGE gel and subject to fluorimetry. In the presence of CdiA, these residues were stained as well, meaning that CdiA does not occlude these residues or make contact with them. R340C did not stain with or without the presence of CdiA when its structure places it on the exterior of the cell. W342C, R343C, and W344 were stained in the presence and absence of CdiA showing that they are on the exterior of the cell and that they are not

blocked by CdiA upon presentation (Fig. 3.4). R345C is stained without the presence of CdiA and unstained in the presence of CdiA. This residue may contact CdiA, but we did not analyse with CdiB antisera at the time. It may be contacted by CdiA or may not have been purified. In co-culture assays, these cysteine mutations were functional and inhibited the target strains to the same effect as wild-type, showing that the mutation in CdiB does not affect the presentation of CdiA on the outside of the cell (Fig. 3.3).

3.3.2 CdiB and CdiA crosslinking

In an effort to show association or interaction of CdiB with CdiA, we crosslinked the proteins together. We used CdiA with the cysteine mutations to encourage association with CdiB. The proteins were treated with formaldehyde or (1-ethyl-3-(3-dimethylaminopropyl) carbodiimide hydrochloride) (EDC) to promote crosslinking. EDC reacts with carboxylic acid groups to form an active O-acylisourea intermediate that is easily displaced by primary amino groups. The primary amine forms an amide bond with the original carboxyl group, and an EDC by-product is released as a soluble urea derivative. The O-acylisourea intermediate is unstable in aqueous solutions and inability to react with an amine results in hydrolysis of the intermediate and a regeneration of the carboxyls. The regeneration disrupts the formation of the crosslink. No association would show the CdiA on an immunoblot at ∼320kDa, its wild-type molecular weight. Association with CdiB and CdiA would show at ∼380kDa on an immunoblot, which is an increase of 60kDa when crosslinked to CdiB. In the immunoblot analyzed with CdiA antisera, the untreated lanes show CdiA at its wild-type molecular weight (Fig. 3.5). In the lanes treated with formaldehyde, there is a faint band above the untreated bands, suggesting a potential interaction of CdiA and CdiB. These faint bands in the formaldehyde treated lanes indicate that something may be crosslinked to CdiA (Fig. 3.5). CdiA

is only known to associate with CdiB and we can surmise that it is crosslinked to CdiB or alternativey analyzed with CdiB antisera. In the lanes treated with EDC, the crosslinking did not occur as the bands appear to be the same molecular weight as the untreated bands (Fig. 3.5). This can be attributed to an unstable O-acylisourea intermediate resulting in no formation of crosslinking between the proteins and future work with EDC could include N-hydroxysulfosuccinimide to improve the efficiency of the reaction.

3.3.3 CdiB loop mutations to identify CdiA contact points

To investigate the external loop contact points between CdiB and CdiA, mutations were made on the loops in an attempt to abrogate the stability of CdiA by changing the hydrophobicity and charge (Fig. 3.6). CdiA is exported by CdiB and may contact the extracellular loops for stability upon exportation. Zach Ruhe and I discussed the extracellular loops and their length and potential to contact CdiA. We investigated strand 6 because it is one of the longer loops on CdiB. We mutated positions at the end of the loop and farther into the barrel. These mutations at 335 and 336 changed the amino acid from a polar residue to a hydrophobic residue and from a positive to negatively charged residue. The second pair of mutations changed a negative charge to a polar uncharged amino acid and negative to a positive charge. If the presentation of CdiA is disrupted, the delivery of the toxin will cease as will the appearance of CdiA in the immunoblot. The mutations did not abrogate the function of CdiA in co-culture experiments where the mutations inhibited target strains to the same degree as wild-type CdiB. These results were also reflected in immunoblot analysis analyzed with anti-CdiA antisera where CdiA was shown to process in the presence and absence of the target strains (Fig. 3.6). These changes were not drastic enough to show a phenotype in the exportation and presentation of CdiA on the exterior of the cell.

With the small mutations on the exterior loops resulting in functional CdiA, we then made a larger mutation in the loop. This mutation was a deletion from Y324 to Q347 (Fig. 3.7). This resulted in a no inhibition by CdiA in co-culture experiments (Fig. 3.7). In order to determine what the cause of the nonfunctional CdiA is, we did an immunoblot analysis, which indicated that the loop mutation caused CdiA exportation to cease (Fig. 3.7). This mutation produced a non-functional CdiB that was largely unable to export CdiA as shown in the immunoblot where the bands at the top of the blot in the loop deletion show a reduction in CdiA and have not delivered the toxin which would leave a second band below the full-length band. In the co-culture assay, the delivery of the toxin to target cells ceased. The crystal structure of CdiB was reported for *Acinetobacter baumannii* and *E. coli* EC93, where it was discovered that loop 6 is conserved and folds into the barrel [85]. Their work has determined which residues are on the exterior, embedded in the membrane, and on the periplasmic side of the cell. They also investigated the secretion of CdiA where CdiB is necessary for the secretion of CdiA. They discovered that the β-strands of the CdiB barrel influence the exportation of CdiA, where β-strand 1 and the DxxG motif facilitate secretion. When β-strand 1 and β-strand 16 are linked by a disulfide bond, the secretion of CdiA is decreased. However, when the bond is reduced, secretion is resumed. The authors also studied the interactions between loop 2 and the internal loop 6 by creating mutations to form a salt bridge. This salt bridge decreased the exportation of CdiA [85].

3.4 Discussion

Type Vb secretion systems are crucial for the survival and pathogenesis of Gram-negative bacteria by releasing large exoproteins on the cell surface that can deliver toxic effectors. TpsA proteins, including CdiA toxins, form a distinct subgroup of hundreds of

proteins with varying sizes and domain organizations, as reported in genome databases. Recent studies have revealed that CdiA proteins have multifunctional roles independent of their toxin activity. For example, CdiA promotes adhesion on epithelial cells in *A. baumannii*, plays a crucial role in intracellular survival and escape in *Neisseria meningitidis*, increases virulence in *Pseudomonas aeruginosa* infection models, and controls biofilm establishment in human pathogens [92, 94]. CdiA has shown association with and exportation through CdiB. Disruptions in flexible regions in CdiB result in decreased secretion of CdiA [85]. In our work, the topology of CdiB was mapped using a maleimide dye to stain available cysteine residues. CdiB does not have any native cysteines to interfere with the stain. From the residues that were scanned, R345 may show a possible interaction with CdiA, where it was stained in the absence of CdiA and unstained in the presence of CdiA (Fig. 3.4). This may indicate that the interaction is blocking the dye from accessing the cysteine residue.

To show interaction between CdiA and CdiB, the cysteine mutations were crosslinked with formaldehyde or EDC. The crosslinks formed with formaldehyde suggest an interaction between the two proteins due to the increase in band size on the immunoblot. We then made site-directed mutations on CdiB loop 3 to abrogate the interaction between it and CdiA. These mutations allowed the presentation of CdiA on the cell surface and inhibitory activities to behave like the wild-type isolate (Fig. 3.6). We then deleted a loop from CdiB and abrogated the function and expression of CdiA. This deletion altered the structure of CdiB to prevent the secretion of CdiA (Fig. 3.7). During this time, the crystal structure of CdiB was reported explaining the exterior, inner membrane, and interior residues of CdiB. The work also included the interaction and exportation of CdiA. The exportation of CdiA is reduced if the flexibility of β-strand 1 is linked in a disulfide bond to β-strand 16, and if loop 2 and loop 6 are mutated to form a salt bridge.

3.5 Methods

Growth conditions and competition co-cultures. All strains were grown at 37°C in lysogeny broth (LB) or on LB agar unless otherwise noted. Media were supplemented when appropriate with antibiotics at the following concentrations: ampicillin (Amp) 150 μg mL^{-1}; kanamycin (Kan) 50 μg mL^{-1}; chloramphenicol (Cm) 33 μg mL^{-1}; and tetracycline (Tet) 25 μg mL^{-1}. For all competition co-cultures, both strains were grown to an optical density at 600nm (OD_{600}) of 0.3 - 0.9 and mixed at an equal ratio of OD_{600} (3.0:3.0), and diluted to OD 0.025 in 2mL of LB shaking for 3 hours. Cells were diluted in ten-fold serial dilutions and then plated on the appropriate antibiotics to enumerate inhibitor and target cell colony forming units (CFU/mL). Competitive indices were calculated as the ratio of inhibitor to target cells at 3 hours relative to their starting ratios.

Plasmid and strain construction. To generate the cysteine mutations with the His-tag, *cdiB* was amplified from STECO31 using primers ZR447 and ZR448. The His-tag was made by overlapping the histidine residues in Gibson Assembly to join fragments of amplified genes in a single reaction. The strains made with CdiB-His6 were used in the proposed cysteine scan and the crosslinking experiments. Gibson assembly was then used to generate the cysteine mutations using CH5333 as the forward primer of the first segment and CH5334 as the reverse primer for the second segment to clone into CdiB at the appropriate location. To generate N339C, CH5333 and ZR449 amplified the area before the cysteine mutation. The first segment will be used in Gibson assembly for each of the following mutations. ZR450 and CH5334 amplified the mutation to form the second segment that will overlap with the first segment. To generate the subsequent mutations, ZR451, ZR452, ZR453, ZR454, ZR455, and ZR456 were used to create the second segment to overlap with the first. The segments were cloned in using NotI and

KnpI. The Gibson assembly generated R340C, G341C, W342C, R343C, W344C, and R345C.

The loop mutations were generated in the same fashion with two different PCR segments that are amplified. N339V and R340D were generated using ZR260/ZR332 and ZR333/ZR343 to amplify CdiB from STECO31. These mutations were then cloned into pET21b using EcoRI/SalI and SalI/XhoI. The second loop mutation of D385S and D386R were made using the same technique of having an overlapping restriction enzyme site. The primers used were ZR260/ZR334 and ZR335/ZR343 to amplify the segments from STECO31 CdiB. These mutations were cloned into pET21b with EcoRI/XbaI and XbaI/XhoI. These plasmids were generated in a two-step process where one mutation is generated first and the second follows. The loop deletion was made by using primers CH5333/CH5212 and CH5213/CH5334 to amplify CdiB from STECO31. These segments generated an overlapping sequence, allowing assembly through the Gibson method. These segments were cloned into pET21b using NotI and KpnI.

The inhibitor strains were made by amplifying *cdiBAI* from STECO31 and cloned into pET21b. In the deletion, primers CH4241 and CH4240 were used to remove amino acids D900-A999 and replaced with an XhoI site. These inhibitors were used in co-culture and cross-linking experiments.

Protein purification and cross-linking. All strains were grown at 37°C in lysogeny broth (LB) or on LB agar unless otherwise noted. Media were supplemented when appropriate with antibiotics. The cultures were grown to an optical density at 600nm (OD_{600}) of 0.3 - 0.9 and resuspended to OD 1.0. Lysates were washed with 1xPBS with 1mM $MgSO_4$ pH 7.0. The lysate was spun down at 5000g for 30 seconds and resuspended in 1mL 1xPBS. The lysates treated with formaldehyde are incubated in a 1% formaldehyde solution for 30 minutes. After 30 minutes, the reaction is quenched with 150 μL of 1.25M glycine for 15 minutes, washed with 1xPBS and spun down at 5000g for 30 seconds then

remove the solute and collect the pellet in 50 μL denaturing buffer to freeze overnight at -80°C. Lysates are then prepared by quick thawing the cultures and pelleting the insoluble material by centrifugation at 15,000 rpm for 15 minutes. Lysates that are cross-linked with EDC are washed with 1xPBS with 1mM $MgSO_4$ pH 5.0. The lysate was spun down at 5000g for 30 seconds and resuspended in 1mL 1xPBS. 1mg/mL solution of EDC in 1xPBS pH 5.0 with 1mM $MgSO_4$ was prepared. 100 μL of the freshly prepared EDC solution was added to the lysate, which was then incubated at room temperature for 15 minutes. The reaction was quenched with 150 μL of 1.25M glycine for 15 minutes. The pellet was spun down at 5000g for 30 seconds and resuspended in 50 μL to freeze overnight at -80°C. Lysates were prepared by quick thawing the cultures and pelleting the insoluble material by centrifugation at 15,000 rpm for 15 minutes. Total protein concentration was calculated for the soluble lysates by Bradford reagent and the same amount of protein was loaded for all samples on 6% SDS-PAGE gels for separation at 100V for 3 hours and 30 minutes. The protein was then transferred to polyvinlyidene difluoride (PVDF) membranes for 1 hour at 17V and analyzed with anti-CdiA antisera. The 800CW secondary antibody was visualized with a LI-COR Odyssey infrared imager.

Protein purification and immunoblotting. All strains were grown at 37°C in lysogeny broth (LB) or on LB agar unless otherwise noted. Media were supplemented when appropriate with antibiotics. The cultures were grown to an optical density at 600nm (OD_{600}) of 0.3 - 0.9 and resuspended to OD 1.0. After, pellets were collected and resuspended in denaturing buffer then frozen overnight at -80°C. Lysates were prepared by quick thawing the cultures and pelleting the insoluble material by centrifugation at 15,000 rpm for 15 minutes. Total protein concentration was calculated for the soluble lysates by Bradford reagent and the same amount of protein was loaded for all samples on 6% SDS-PAGE gels for separation at 100V for 3 hours and 30 minutes. The protein was then transferred to polyvinlyidene difluoride (PVDF) membranes for 1 hour at 17V

and analyzed with anti-CdiA antisera. The 800CW secondary antibody was visualized with a LI-COR Odyssey infrared imager.

Protein CdiB purification and maleimide staining. All strains were grown at 37°C in lysogeny broth (LB) or on LB agar unless otherwise noted. Media were supplemented when appropriate with antibiotics. The cultures were grown to an optical density at 600nm (OD_{600}) of 0.3 - 0.9 and resuspended to OD 1.0. Lysates were stained by washing the cells with 1mL of 1xPBS pH 7.0 with 1mM $MgSO_4$ and spun down at 5500g for 3 minutes. Cells were resuspended in 50 μL of 1xPBS pH 7.0. 0.5 μL of maleimide dye was added in the dark and then incubated at room temperature in the dark for 20 minutes. This reaction was quenched by adding 6 μM beta-mercaptoethanol in 8M urea lysis buffer for 5 minutes. The cells were spun down and resuspended in 300 μL of 1xPBS pH 7.0 when done. The solution was frozen overnight at -80°C. Lysates were prepared by quick thawing the cultures and pelleting the insoluble material by centrifugation at 15,000 rpm for 15 minutes. The soluble fraction was removed and placed in 20 μL of Profinity IMAC Resin, Ni-charged. It was then incubated at room temperature for at least 60 minutes on a gentle rotator. Afterwards, the lysates were washed 3x with 1mL urea lysis buffer and spun down at 3000g for 10 seconds to remove the wash. After the three washes, liquid was removed as much as possible without removing the beads. The lysates were eluted from the beads using 20 μL of urea lysis buffer made with 25 μM EDTA. This was mixed well and incubated for at least 15 minutes at room temperature. Total protein concentration was calculated for the soluble lysates by Bradford reagent and the same amount of protein was loaded for all samples on 10% SDS-PAGE gels for separation at 100V for 1 hour and 30 minutes. The maleimide dye was visualized with a LI-COR Odyssey infrared imager.

3.6 Tables and Figures

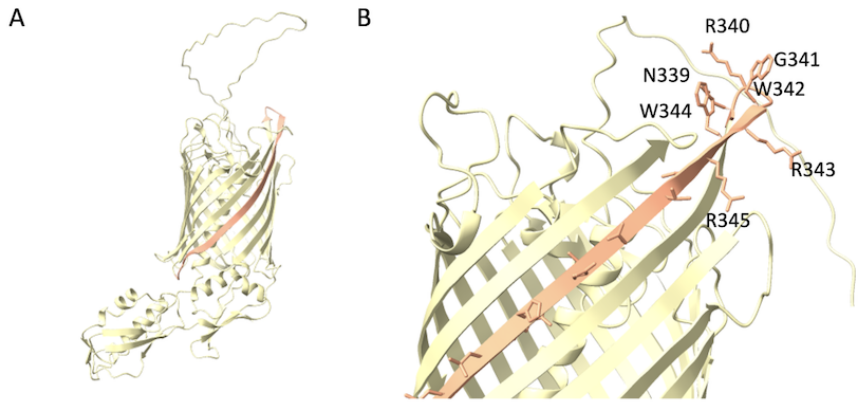

Figure 3.2: ***E. coli* STEC_O31 CdiB β-strand 6 labeled in orange for investigation**. (A) STEC_O31 CdiB whole protein. (B) STEC_O31 CdiB beginning of β-strand 6 labeled with locations of the cysteine mutations.

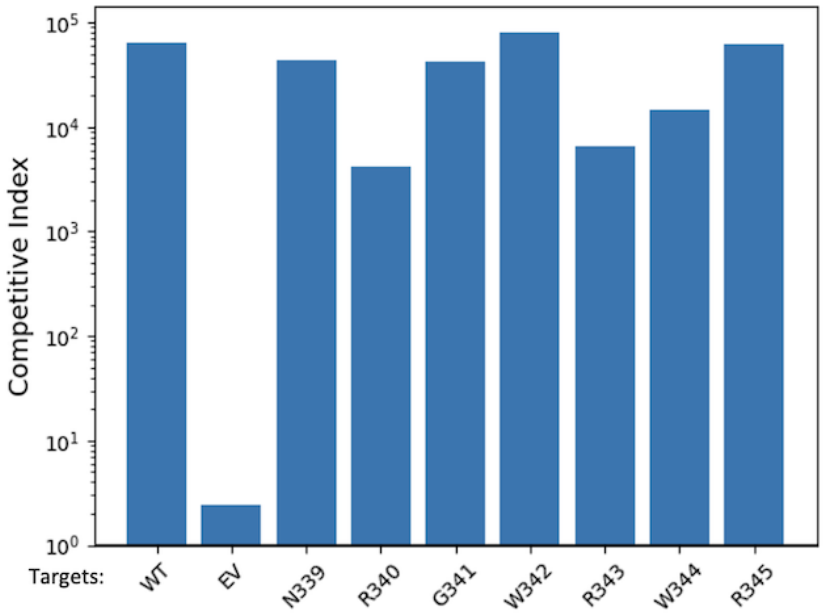

Figure 3.3: ***E. coli* STEC_O31 CdiB β-strand cysteine mutations in co-culture assay**. Co-culture in liquid media reveal mutations that do not disrupt binding to Tsx from STEC_O31. Competitive Index (CI) is the ratio of viable colony-forming units per milliliter (CFU/mL) of inhibitors to targets at 3 hours relative to their starting ratios.

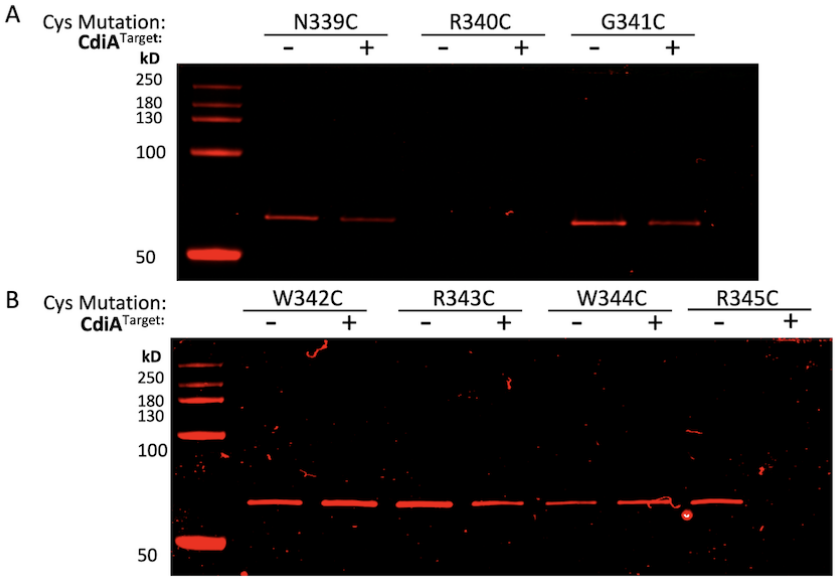

Figure 3.4: ***E. coli* STEC_O31 CdiB maleimide cysteine stain**. (A) N339C, R340C, and G341C stained with maleimide in the presence and absence of CdiA. (B) W342C, R343C, W344C, and R345C stained with maleimide in the presence and absence of CdiA. Note: no wild-type control.

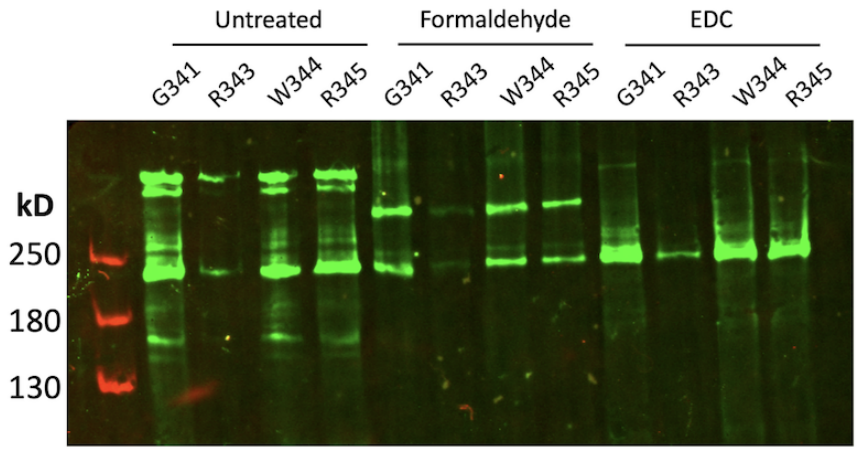

Figure 3.5: ***E. coli* STEC_O31 CdiA and CdiB crosslinked with formaldehyde and EDC**. G341C, R343C, W344C, and R345C untreated, treated with formaldehyde or EDC. The untreated mutations of CdiA are predicted to be ∼320kDa on the immunoblot. The formaldehyde treated mutations show CdiA-CdiB crosslinked form to be ∼380kDa and shown on the immunoblot with bands slightly higher on the gel than the untreated proteins. The formation of the middle band in the formaldehyde treated lanes could be attributed to CdiA digestion. The proteins treated with EDC show the truncated form and full length CdiA may be in the supernatant which was not collected. CdiA crosslinking has not been successfully performed and the full length CdiA with CdiB is not shown, the truncated CdiA shows bands similar to those that are untreated and truncated. Note: no wild-type control.

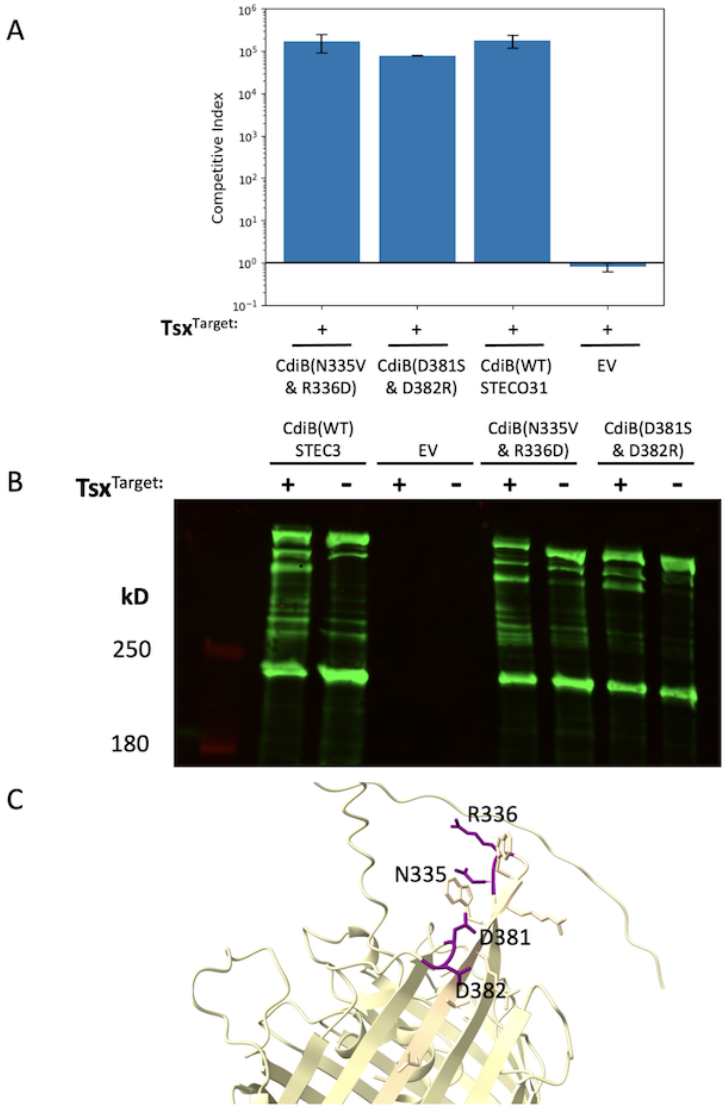

Figure 3.6: ***E. coli* STEC_O31 CdiB β-strand 6 mutations**. (A) Co-culture in liquid media reveal mutations that do not disrupt binding to Tsx from STEC_O31. Competitive Index (CI) is the ratio of viable colony-forming units per milliliter (CFU/mL) of inhibitors to targets at 3 hours relative to their starting ratios. CI values are represented as the average of at least 3 independent experiments ±SEM. (B) Anti-CdiA immunoblot of strand 6 mutations with the presence and absence of Tsx target cells. (C) CdiB labeled mutations in purple.

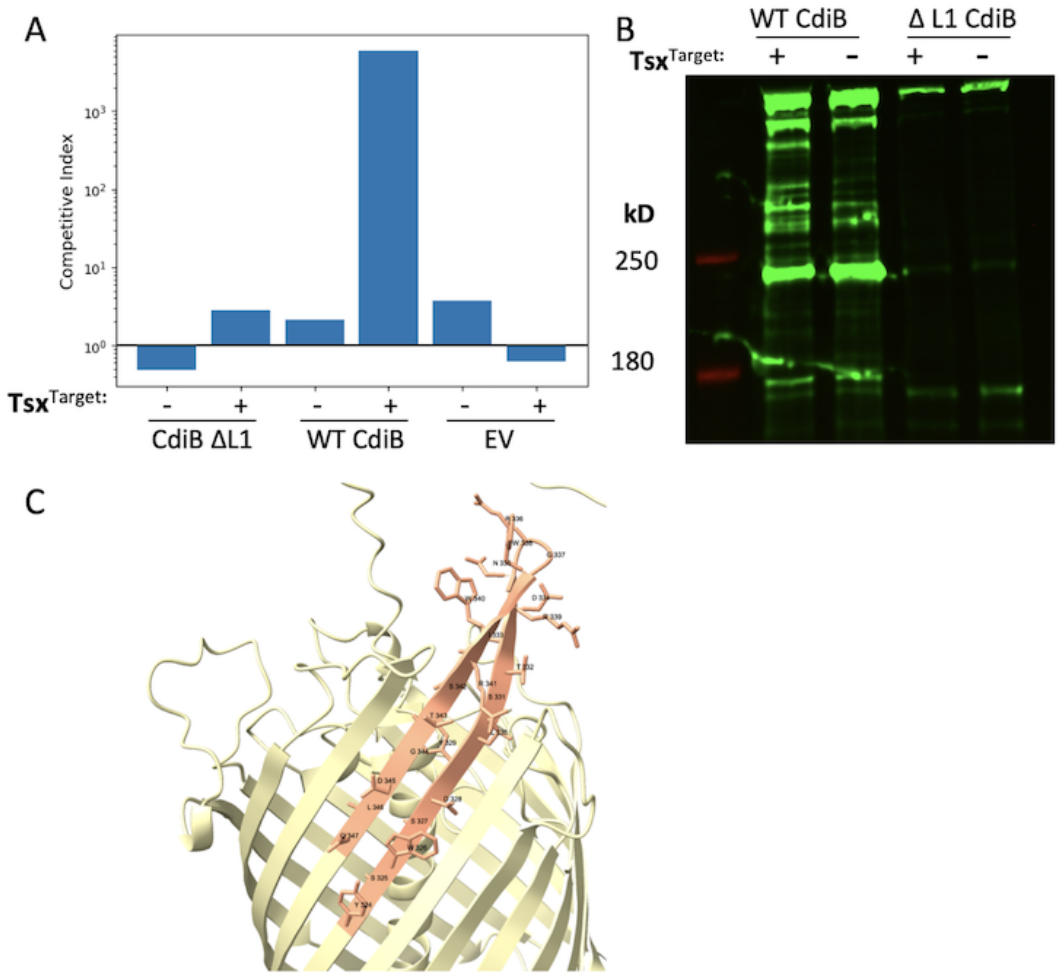

Figure 3.7: ***E. coli* STEC_O31 CdiB loop 1 deletion**. (A) Co-culture in liquid media reveals this mutant does not allow toxin delivery to target cells. Competitive Index (CI) is the ratio of viable colony-forming units per milliliter (CFU/mL) of inhibitors to targets at 3 hours relative to their starting ratios. (B) Anti-CdiA immunoblot of strand 6 mutations with the presence and absence of Tsx target cells. (C) CdiB labeled deletion in orange.

Table 3.1: Strains from Chapter 3

Strain	**Description**	**Source**
CH14016	MG1655 Δwzb Δtsx	[96]
CH14017	MG1655 Δwzb Δtsx ΔompT	[96]

Table 3.2: Plasmids used in Chapter 3.

Plasmid	**Description**	**Source**
pET21b	Same as pET24abcd(+). AmpR.	Novagen Cat69741-3
p14027	cdiBAI from STEC_O31 J2M139 cloned into pET21b. AmpR.	[96]
p14047	pSC101-derived plasmid vector with Tsx from STEC_O31 J2M139 cloned in. KanR.	[96]
pZS21	pSC101-derived plasmid vector with the multiple cloning site removed. KanR.	[182]
p1812	PCR with primers 5333/5334 from CH1798 into pET21b using NotI/Xho. AmpR.	This study
p1815	PCR with primers 5333/5334 from CH1799 into pET21b using NotI/Xho. AmpR.	This study
p1816	PCR with primers 5333/5334 from CH1800 into pET21b using NotI/Xho. AmpR.	This study

p1817	PCR with primers 5333/5334 from CH1807 into pET21b using NotI/Xho. AmpR.	This study
p1818	PCR with primers 5333/5334 from CH1809 into pET21b using NotI/Xho. AmpR.	This study
p6971	Used primers ZR260/ZR332 and ZR333/ZR343 to amplify STEC3 CdiB with N339V and R340D mutations. Cloned into p2208 with NotI/KpnI. AmpR.	This study
p6972	Used primers ZR260/ZR334 and ZR335/ZR343 to amplify STEC3 CdiB with D385S and D386R mutations. Cloned into p2208 with NotI/KpnI. AmpR	This study
p1798	Gibson Assembly of cdiB(S88His6)N339C made with primers 5333/ZR449 and ZR450/5334 into CH14563 using NotI/KpnI. Sequenced. AmpR.	This study
p1799	Gibson Assembly of cdiB(S88His6)R340C made with primers 5333/ZR449 and ZR451/5334 into CH14563 using NotI/KpnI. Sequenced. AmpR.	This study

p1800	Gibson Assembly of cdiB(S88His6) G341C made with primers 5333/ZR449 and ZR452/5334 into CH14563 using NotI/KpnI. Sequenced. AmpR.	This study
p1807	Gibson Assembly of cdiB(S88His6)W342C made with primers 5333/ZR449 and ZR453/5334 into CH14563 using NotI/KpnI. Sequenced. AmpR.	This study
p1809	Gibson Assembly of cdiB(S88His6)R343C made with primers 5333/ZR449 and ZR454/5334 into CH14563 using NotI/KpnI. Sequenced. AmpR.	This study
p1810	Gibson Assembly of cdiB(S88His6)W344C made with primers 5333/ZR449 and ZR455/5334 into CH14563 using NotI/KpnI. Sequenced. AmpR.	This study
p1811	Gibson Assembly of cdiB(S88His6)R345C made with primers 5333/ZR449 and ZR456/5334 into CH14563 using NotI/KpnI. Sequenced. AmpR.	This study
p7151	CdiB ΔY329-Q351 made with Gibson assembly using primers 5333/5212 and 5213/5334. Cloned into p13658 using NotI/KpnI. AmpR.	This study

Table 3.3: Primers used in Chapter 3.

Primer	**Description**	**Sequence**	**Source**
ZR256	tsx-Not-for	5' - TTT GCG GCC GCG AAT TCG GGA TTT TCA AAC AGT GGC ATA C	[96]
ZR257	tsx-Xho-rev	5' - TTT CTC GAG TCT AGA AAA TCC CGG CAT TTT CAT AAT CAG	[96]
ZR260	J2M139 CDI-Not-for	5' - TTT GCG GCC GCA ATG TCT GGT TGT GGC AGG	This study
ZR332	cdiB(N339V)-Sal-rev	5' - TTT GTC GAC ATC AAT GGT GCT GAG GTA GTC	This study
ZR333	cdiB(R340D)-Sal-for	5' - TTT GTC GAC GGC TGG CGG TGG CGT TCC	This study
ZR334	cdiB(D385S)-Xba-rev	5' - TTT TCT AGA CAG ATA ATT GTG AAT AAT GCG GTG C	This study
ZR335	cdiB(D386R)-Xba-for	5' - TTT TCT AGA GTT CTG CTT CAG GGC AGC	This study
ZR343	cdiA(T506)-Kpn-rev	5' - TTT CTC GAG GTA CCG CTG TTG TTT ATC TGC	This study
ZR443	CdiB (STEC)-Eco-for	5' - TTT GAA TTC GAC ATT ACA CAG GCC AGA ATA CG	This study

ZR444	CdiB (STEC)-Xho-rev	5' - TTT CTC GAG GAT CCG TAA TAA TCC CTT AAA ACG CGA CG	This study
ZR447	CdiB (S88His6) (STEC)-rev GA	5' - ATG ATG ATG GTG GTG GTG AGA ACC GTG ATG ACT GCG CTC CAG CGC ATC	This study
ZR448	CdiB (S88His6) (STEC)-for GA	5' - CAC CAC CAC CAT CAT CAT GGT TCT GCG CCG CTG ACT GTC ATA C	This study
ZR449	CdiB (D338) (STEC)-rev GA	5' - ATC AAT GGT GCT GAG GTA G	This study
ZR450	CdiB (N339C) (STEC)-for GA	5' - CTA CCT CAG CAC CAT TGA TTG TCG GGG CTG GCG GTG GCG	This study
ZR451	CdiB (R340C) (STEC)-for GA	5' - CTA CCT CAG CAC CAT TGA TAA CTG TGG CTG GCG GTG GCG TTC	This study
ZR452	CdiB (G341C) (STEC)-for GA	5' - CTA CCT CAG CAC CAT TGA TAA CCG GTG TTG GCG GTG GCG TTC CAC G	This study
ZR453	CdiB (W342C) (STEC)-for GA	5' - CTA CCT CAG CAC CAT TGA TAA CCG GGG CTG TCG GTG GCG TTC CAC GGG AG	This study

ZR454	CdiB (R343C) (STEC)-for GA	5' - CTA CCT CAG CAC CAT TGA TAA CCG GGG CTG GTG TTG GCG TTC CAC GGG AGA C	This study
ZR455	CdiB (W344C) (STEC)-for GA	5' - CTA CCT CAG CAC CAT TGA TAA CCG GGG CTG GCG GTG TCG TTC CAC GGG AGA CCT G	This study
ZR456	CdiB (R345C) (STEC)-for GA	5' - CTA CCT CAG CAC CAT TGA TAA CCG GGG CTG GCG GTG GTG TTC CAC GGG AGA CCT GCA G	This study
CH4240	STEC-L899-Xho-rev	5' - TTT CTC GAG CAG AGT GAT GTT CTG CCC C - 3'	[96]
CH4241	STEC-R1000-Xho-for	5' - AAA CTC GAG AGA GAC ATC AGC AAT AGT GGG C - 3'	[96]
CH5212	STEC3-CdiB(T352)-GA-for	5' - TAC ACG TAT ACT CAC CGG CTG GGA CTG TC - 3'	This study
CH5213	STEC3-CdiB(H377)-GA-rev	5' - CGA CAG AAA AGT GCT GCA GAC CTC CGG T - 3'	This study
CH5333	pET-Not-GA-for	5' -GTC GAC AAG CTT GCG GCC - 3'	This study
CH5334	STEC3-(S504)-Kpn-GA-rev	5' -GTT CCT TTG CCC CGG AGA G - 3'	This study

Chapter 4

Investigation into the Class IV receptor of STECO31 CDI locus 2

4.1 Abstract

CDI systems facilitate the exchange of protein toxins between competing Gram-negative bacteria via direct contact. CDI+ strains use CdiA effector proteins on their cell surface to bind to specific receptors on neighboring bacteria, initiating toxin transfer. Three known classes of CdiA effectors in *Escherichia coli* recognize different outer membrane protein receptors, and we describe a fourth class that uses the lipopolysaccharide (LPS) core as a receptor to target bacteria. CDI-resistant target cells were selected and found to have mutations in genes required for the synthesis of the full LPS core. The presence of phosphorylated inner-core heptose residues is crucial for CdiA recognition. Class IV CDI loci also encode lysyl acyltransferases (CdiC) that are similar to enzymes involved in lipidating repeats-in-toxin (RTX) cytolysins. Our research shows acyltransferase CdiC as necessary for full target cell killing activity, and it adds 3-hydroxydecanoate to a specific lysine residue within the CdiA receptor-binding domain.

4.2 Introduction

Bacteria in densely populated communities compete for limited resources and growth niches. They use various specialized export pathways to deploy toxic effectors, and can use either Type I, Type IV, Type V, and Type VI secretion systems of Gram-negative bacteria [14, 13, 59, 60]. Some use outer membrane exchange to deliver lipoprotein toxins and *Vibrio cholerae* deliver their virulent proteins in a contact-dependent manner, targeting eukaryotic cells and other bacteria [183, 184]. Direct interbacterial toxin delivery was first observed as contact-dependent growth inhibition (CDI) in *E. coli* EC 93, which uses CdiB and CdiA two-partner secretion (TPS) proteins to kill K-12 and other strains of *E. coli*. Several other bacteria, including *Dickeya dadantii*, *Burkholderiaceae*, *Neisseria meningitidis*, *Pseudomonas aeruginosa*, and *Acinetobacter baumannii*, have also exhibited CDI activity [79, 80, 84, 77]. This competitive advantage helps bacteria compete with other strains for environmental resources, recognizing kin, and communicating with kin. The connection of kin with CdiA helps to form cooperative group activities by promoting cellular autoaggregation and biofilm formation [85].

CdiA proteins are diverse: they vary in size and sequence between bacterial species, but all CdiA proteins share a common architecture with domains arranged from the N to C terminus in the order they function during toxin delivery. All CdiA proteins have the seven regions of signal sequence, two partner secretion, FHA-1 repeats, receptor binding domain, YP region, FHA-2, and the CT. Initial secretion of CdiA forms the β-helical structure that protrudes out into the extra cellular matrix. After export, the receptor-binding domain (RBD) of CdiA interacts with neighboring cells. Once the RBD contacts its target receptor, secretion resumes and CdiA is able to deposit the FHA-2 domain onto the target cell, where it becomes embedded within the outer membrane. FHA-2 forms a translocation conduit to transfer the toxin-containing CdiA-CT region into the target

cell periplasm. Once inside the periplasm, the CdiA-CT is cleaved from the effector, and the released fragment enters the target cell cytoplasm by hijacking integral membrane proteins [96]. So far three classes of receptors have been discovered. Class I receptors use BamA, class II receptors form the OmpC/OmpF heterotrimer, and class III receptors use Tsx as their CDI receptor. This CDI system in STECO31 is the second CDI locus and it has an additional CDI gene, CdiC that is required for its toxic activity. CdiC is located between CdiB and CdiA. CdiC is homologous to lysyl acyltransferases, which activates pore-forming cytolysins of the repeats-in-toxin (RTX) family. The second CDI locus also targets a new receptor. The CDI receptor for this system targets the core oligosaccharide of lipopolysaccharide (LPS). [101].

4.3 Results

The *E. coli* STEC4 CDI system shows CdiC between CdiB and CdiA in a four gene operon (Fig. 4.1). To determine the activity of the STEC4 CDI system, co-culture assays were performed on solid and liquid media. These experiments were also performed with the target cells containing a plasmid-borne immunity gene to rescue the inhibitory effect. The inhibitor cells were mock, with the STEC4 CDI system, and with the STEC4 CDI system without the promoter. These inhibitors should show no inhibition, inhibition, and no inhibition respectively. The mock inhibitors on solid and liquid media did not have inhibition of the target cells as expected (Fig. 4.1). The STEC4 CDI system showed inhibition on solid agar and less inhibition in liquid media. With the presence of the immunity gene in the target cells, the amount of inhibition was reduced to the wild-type level of inhibition. The STEC4 CDI system without the promoter in co-culture assays, showed no inhibition on solid agar or liquid media (Fig. 4.1). This suggests that this gene cluster is expressed under native regulatory elements.

Through transposon mutagenesis, the core oligosaccharide of lipopolysaccharide (LPS) was discovered as the CDI receptor. The LPS is made up of the lipid A, inner core, outer core, and O-antigen. The different sections are added in a sequence of operons to add the sugars to form the inner an outer core in a specific order. The enzymes used are able to facilitate the transfer of sugars onto the LPS. Strains were made with different *waa* mutations that affected the addition of sugars to the LPS. Co-culture experiments were performed in liquid media with the target cells having different *waa* mutations. WaaG, WaaQ, and WaaY were inhibited while WaaC, WaaF, and WaaP were not inhibited (Fig. 4.2). WaaC facilitates the addition of HepI to the inner core, thus preventing the binding of STEC4 RBD to deliver the toxin. WaaF facilitates the addition of HepII to HepI also in the inner core. These defects in the early inner core prevent binding of the RBD. WaaP phosphorylates HepI and also prevents binding. WaaG, WaaQ, and WaaY facilitate the formation of the second half of the inner core (Fig. 4.2). These bridge the gap between the formation of the inner core and outer core, WaaQ adds HepII to HepIII, WaaY phosphorylates HepII. These mutations are not at the base of the inner core and therefore, allow binding of the STEC4 RBD and toxin delivery into target cells.

The effect of CdiC was studied in co-culture assays on liquid and solid media. In liquid media, the deletion of CdiC caused an increase in inhibition compared to the STEC4 CDI system with CdiC. On solid media, the STEC4 CDI system with CdiC showed more inhibition than the system without CdiC (Fig. 4.3). CdiC is required for toxic activity and on solid media, the requirement is shown with the STEC4 CDI system inhibiting the target cells more than the system with the deletion. In *Citrobacter rodentium* and under induction, the CdiC deletion strain inhibited, as well as the wild-type. Under induction, the amount of STEC4 CdiA can be effective in toxin delivery to the target cells. *C. rodentium* with *fimA* under induction did not show any inhibition. *C. rodentium* with the full CdiBCAI showed inhibition under arabinose induction and a

rescue of the target cells when provided with plasmid-borne immunity (Fig. 4.3). The induction of this CDI system is important in its effectiveness.

4.4 Discussion

Many Gram-negative bacteria use and exploit CDI receptors to their evolutionary advantage. The specificity of the receptor is a way to mitigate the use by other nonkin bacteria. In this study, the LPS was found to be a new class of receptors. The LPS is a commonality between Gram-negative bacteria and therefore, the second CDI system from STECO31 can be deadly. This receptor allows STECO31 to target nonkin cells anywhere on the bacteria surface and target a wider variety of bacteria. The critical point for this receptor is the ability to reach the inner core. The WaaC and WaaP mutations do not allow binding and prevent HepI and the phosphorylation of HepI from developing the inner core. Mutations that allow binding are those that form the second half of the inner core. These mutations are WaaY, WaaQ, and WaaG. The RBD binds to GlcI, HepIII, and phosphorylated regions on the inner core. Investigation was also done on CdiC which is required for full toxic activity and adds a 3-hydroxydecanoate to a specific Lys residue within the CdiA receptor-binding domain[101]. Without the native promoter, STEC4 CDI system does not inhibit target cells. With an inducible promoter, the STEC4 CDI system can inhibit target cells and STEC4 without CdiC can also inhibit target cells.

Through sequence analysis, other species of bacteria may also target this new class of receptors. Some *Pseudomonadales*, *Burkholderiales*, and *Enterobacterales* have homologous receptor binding domains to STEC4 [79, 80, 84, 77]. We can sumise that these bacteria with CdiA will also bind to the inner core and provide an anchor for interactions with the core oligosaccharide. The LPS-binding CDI systems have adapted an acyltransferase that activates RTX toxins to increase the affinity of CdiA effectors for the outer

membrane of the target cell. These connections may provide a stronger bond to increase proximity and communicate with sister cells. The CDI phenotype confers a competitive advantage in densely populated living spaces in antagonistic or commensal ways.

4.5 Methods

Growth conditions and competition co-cultures. All strains were grown at 37°C in lysogeny broth (LB) or on LB agar unless otherwise noted. Media were supplemented when appropriate with antibiotics at the following concentrations: ampicillin (Amp) 150 μg mL^{-1}; kanamycin (Kan) 50 μg mL^{-1}; chloramphenicol (Cm) 33 μg mL^{-1}; and tetracycline (Tet) 25 μg mL^{-1}. For liquid co-culture assays, strains were grown to an optical density at 600nm (OD_{600}) of 0.3 - 0.9. Cells were mixed in an equal ratio of OD_{600} (0.3:0.3) with a total volume of 10mL in shaking baffled flasks for 3 hours. Cells were diluted in ten-fold serial dilutions, then subsequently plated on the appropriate antibiotics to enumerate inhibitor and target cell colony forming units (CFU/mL). Competitive indices were calculated as the ratio of inhibitor to target cells at 3 hours relative to their starting ratios. For solid agar co-culture assays, both strains were grown to an optical density at 600nm (OD_{600}) of 0.3 - 0.9 and mixed at an equal ratio of OD_{600} (3.0:3.0) and plated in a 15 μL spot on LB or LB supplemented with 0.2% arabinose when appropriate. The spots were incubated for 3 hours and then transferred for cell harvest with a sterile swab into 600 μ 1 x M9 salts for the first dilution; ten-fold serial dilution folllowed for every other dilution. The dilutions were plated on the appropriate antibiotics to enumerate inhibitor and target cell colony forming units (CFU/mL). Competitive indices were calculated as the ratio of inhibitor to target cells at 3 hours relative to their starting ratios. Each co-culture experiment was repeated at least three times.

4.6 Tables and Figures

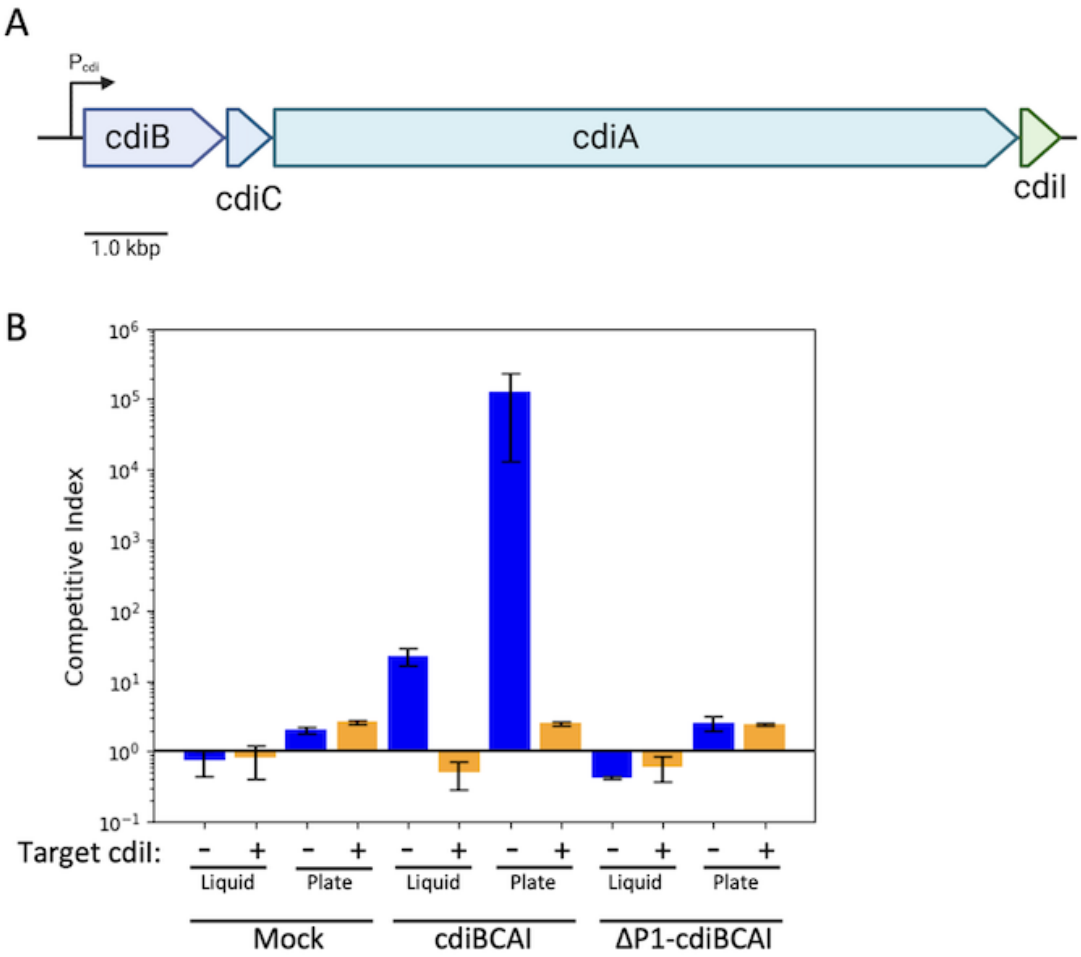

Figure 4.1: ***E. coli* STEC4 CDI genes**. (A) STEC4 CDI genes *cdiBCAI* shown to scale with the native promoter. (B) Co-culture assay in liquid and on solid media with and without the immunity gene. The inhibitors used are mock, *cdiBCAI*, and *cdiBCAI* without the native promoter. Competitive Index (CI) is the ratio of viable colony-forming units per milliliter (CFU/mL) of inhibitors to targets at 3 hours relative to their starting ratios. CI values are represented as the average of at least 3 independent experiments ±SEM.

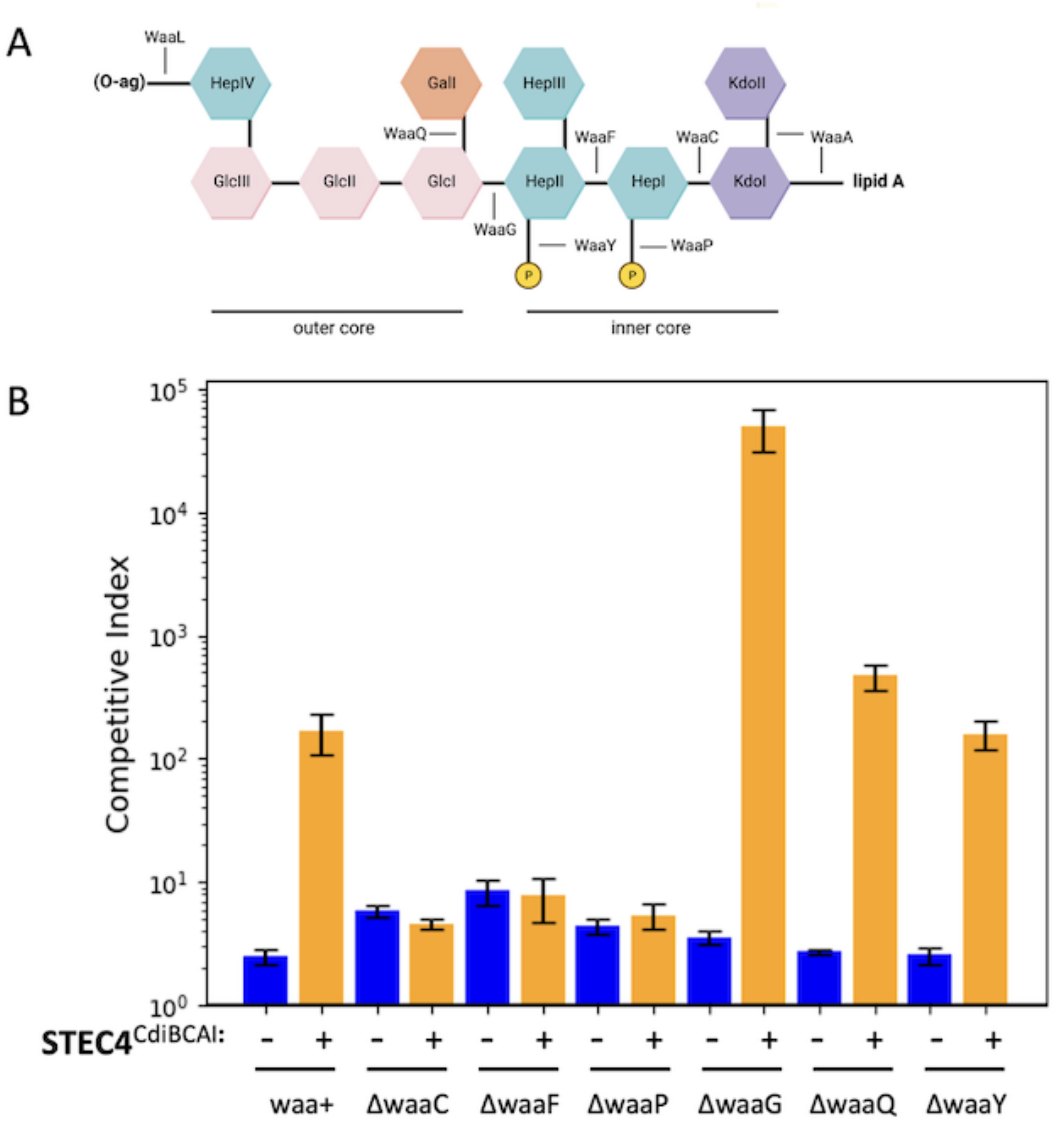

Figure 4.2: ***E. coli* STEC4 co-culture assay against *waa* mutants**. Co-culture in liquid media reveal mutations that WaaC, WaaP, and WaaF have an impact on binding efficiency. Competitive Index (CI) is the ratio of viable colony-forming units per milliliter (CFU/mL) of inhibitors to targets at 3 hours relative to their starting ratios. CI values are represented as the average of at least 3 independent experiments ±SEM.

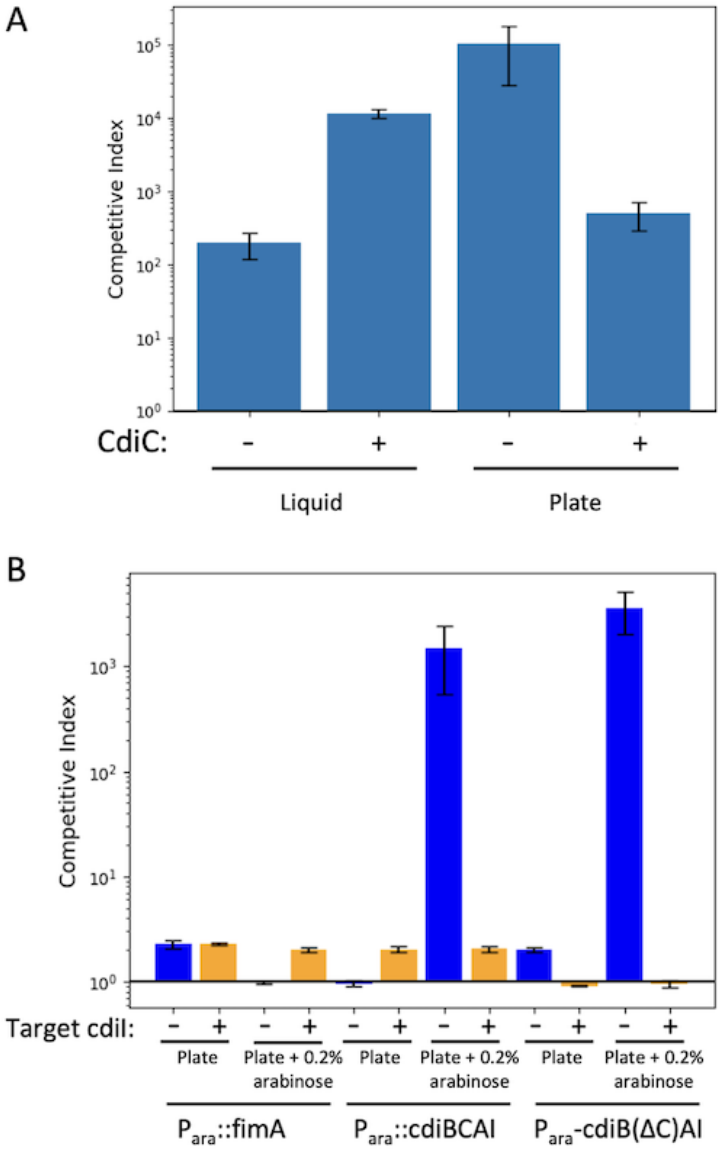

Figure 4.3: ***E. coli* STE4 co-cultures assays with ΔcdiC**. (A) Co-culture assay in liquid and on solid media against *waa*+ target cells. (B) Co-culture assay with the STEC4 CDI system with or without CdiC against *waa*+ target cells. Competitive Index (CI) is the ratio of viable colony-forming units per milliliter (CFU/mL) of inhibitors to targets at 3 hours relative to their starting ratios. CI values are represented as the average of at least 3 independent experiments ±SEM.

Table 4.1: Strains used in Chapter 4.

Strain	Description	Source
178	MC1061	[185]
7176	EPI100 Dwzb::kan	This study
13815	EPI100 Δwzb ΔwaaC::kan	This study
13816	EPI100 Δwzb ΔwaaF::kan	This study
13817	EPI100 Δwzb ΔwaaP::kan	This study
5806	EPI100 Δwzb ΔwaaG::kan	This study
5807	EPI100 Δwzb ΔwaaQ::kan	This study
13818	EPI100 Δwzb ΔwaaY::kan	This study
5948	C. rodentium DBS100 P_ara::fimA	This study
5808	C. rodentium P_ara::cdiBCAI	This study
5829	C. rodentium P_ara-cdiB(ΔC)AI	This study
330	C. rodentium ΔcdiCAI	This study

Table 4.2: Plasmids used in Chapter 4

Plasmid	**Description**	**Source**
pET21b	Derivative of pET21b lacking XbaI-NheI-BamHI-EcoRI to facilitate cloning. AmpR.	[101]
pCH405Δ	pACYC184 empty vector derivative. TetR.	[101]
pET21(MCS-)::cdiBCAI (STEC4)	cdiBCAI (class 4) locus from E. coli STECO31 on pET21b, with expression driven by native promoter. AmpR.	[101]

pET21(MCS-)::cdiBCAI (STEC4) ΔcdiC	An internal 442 bp of cdiC was removed from the WT locus on pET21b, leaving the first 26 bp and the last 55 bp of cdiC intact. AmpR.	[101]
pET21(MCS-)::ΔP1-cdiBCAI (STEC4)	STEC4 promoter region deleted by PCR and ligated to pCH1055 using HindIII/NcoI. AmpR.	[101]
pCH405Δ::cdiI(STEC4)	CdiI from STEC4 cloned into pCH405Δ. TetR.	[101]
pCH405Δ::cdiI-4(DBS100)	CdiI from DBS100 cloned into pCH405Δ. TetR.	[101]

Table 4.3: Primers used in Chapter 4.

Primer	**Description**	**Sequence**	**Source**
CH4195	waaC-KO-Sac-for	5′ - TTT GAG CTC GCT TTC ATC AGA ACG TCC GAT G	[101]
CH4196	waaC-KO-Bam-rev	5′ - TTT GGA TCC GTAA CAA TAG CGC GTT GAG TTC TTC C	[101]
CH4197	waaC-KO-Eco-for	5′ - TTT GAA TTC AGG TAA AAC ATG CTA ACA TCC TTT AAA C	[101]
CH4198	waaC-KO-Kpn-rev	5′ - TTT GGT ACC AAC GCC ACT AAC TAT CCC TAT TAG C	[101]

CH4199	waaP-KO-Sac-for	5′ - TTT GAG CTC GCT TTG GCA TCG TTA CCG G	[101]
CH4200	waaP-KO-Bam-rev	5′ - TTT GGA TCC CCA AAG TGT GGC AAG CGG	[101]
CH4201	waaP-KO-Eco-for	5′ - TTT GAA TTC GAG CGA ACA CAA CGC AAA GG	[101]
CH4202	waaP-KO-Kpn-rev	5′ - TTT GGT ACC GGA AAA AAC ATA TTG GCT GGC TG	[101]
CH4203	waaP-KO-Sac-for	5′ - TTT GAG CTC GAA AGG GAT GAC ATT ATT TTT GCC TCG	[101]
CH4204	waaP-KO-Bam-rev	5′ - TTT GGA TCC CCA GTT AAA TGT TAT TTA CGG TAA TAT TTT C	[101]
CH4205	waaP-KO-Eco-for	5′ - TTT GAA TTC CCA CAA TTA CAT GTC TTC ACC AGG	[101]
CH4206	waaP-KO-Kpn-rev	5′ - TTT GGT ACC CCC GAC GGT AAA AGG ACC G	[101]
CH4207	waaF-Not-for	5′ - TTT GCG GCC GCA ATC GCG ACG CAT AAG AGC	[101]
CH4208	waaF-Xho-rev	5′ - TTT CTC GAG TCC GTC AGC TTC CTC TTG	[101]
CH4209	waaP-Not-for	5′ - TTT GCG GCC GCG GAT ATC ATT ACA GGT GG	[101]

CH4210	waaP-Xho-rev	5′ - TTT CTC GAG TTA TAA TCC TTT GAG TTG TGT TCG	[101]
CH4299	waaF-Sac-for	5′ - TTT GAG CTC CCT GCC TGA AGC GAA CTC G	[101]
CH4300	waaF-Kpn-rev	5′ - TTT GGT ACC GCG ATA GCA TAA TCG CCC TGG	[101]
CH5507	waaG-KO-Sac-for	5′ - TTC GAG CTC AGT AAA TAG CTG ACT TAT GGA TG	[101]
CH5508	waaG-KO-Kpn-rev	5′ - TCA GGT ACC GTT TGA TAA TGC TTC TGG AAA TC	[101]
CH5509	waaQ-KO-Sac-for	5′ - GAT GAG CTC CAA CAG CGA GGC	[101]
CH5510	waaQ-KO-Kpn-rev	5′ - TTA GGT ACC ATA GTT GCT ACA CGT GCG	[101]
CH4087	cdiC-Kpn-for	5′ - GAA GGT ACC ATG CGT AAC GGG AAA TAT	[101]
CH4088	cdiC-Xho-rev	5′ - AAA CTC GAG TTA TCT CTC CGG CAC ATC	[101]
CH4358	STEC4-V1328-Nco-for	5′ - TTT CCA TGG TCA ATG ACC ATT TCA CCA CGG AGC	[101]
CH4359	STEC4-P1589-Xho-rev	5′ - TTT CTC GAG TTA GTG GTG ATG ATG ATG ATG TGG CAC ATT CAC TGC CGG	[101]

Chapter 5

Discussion

Bacteria are everywhere, from the deep sea vents to possibly life on Mars. They are sturdy beyond belief and will always find a way to survive. They evolve and change at a much faster rate due to their small genome size. Changes can occur very quickly through their mechanisms of gene transfer. Horizontal gene transfer which consists of transformation, transduction, and conjugation are used to transfer genetic information that can have immediate or delayed effects on the host. Additionally, gene transfer agents, nanotubes, and membrane vesicles, also known as extracellular vesicles or exosomes, are other mechanisms involved in horizontal gene transfer. Through direct transformation of DNA or RNA from a donor and subsequent integration into the recipient cell's genome, foreign genetic material can be integrated, resulting in the production of recombinant DNA. This phenomenon is widespread among bacteria and facilitates the transfer of mobile genetic elements, including transposons, integrons, and/or gene cassettes between bacterial species [186]. With immediate or delayed effects, this transfer of genetic information can directly impact infections and antibiotic resistance in hospitals leading to multidrug-resistant species that are persistent in an environment where there are immunocompromised, elderly, and infants leading to disastrous outcomes.

One of the challenges of combating these infections is the large community that bacteria live in. When multiple species coexist in the same community, they compete with each other for available resources through a process called exploitation. One species may prevent the other from accessing resources by consuming or sequestering them. In these communities with multiple species, they adopt "high risk, high reward" strategies that reflect their specific metabolic adaptations. This concept is based on models of bacterial growth, where bacteria that constantly grow without being dependent on the environment will outcompete those whose growth rate relies on external conditions [187]. However, constant growth patterns are not typically observed in bacteria. No bacterial species has a growth rate that remains constant under all types of changing conditions. Cells that better exploit their environment have a greater potential to produce more kin or sister cells [188]. Nevertheless, resources in the environment may fluctuate frequently. Nutrient-sensitive growth strategies are vulnerable to the environment and cells that encounter suboptimal conditions relative to their metabolic adaptations will be outcompeted. Overall, the growth and occupancy of any community depends on the flexibility of metabolic strategies that adapt to changes in the external environment.

The competition for resources also employs the collaborative nature of bacteria or at least between sister cells. Bacterial biofilms and quorum sensing are increase the survivorship of the bacterial colony or community. Biofilms are collections of kin or multi-species cells that secrete polymers, which act as an adhesive to bind cells together with the idea that "We are stronger together than apart". The resilient biofilm structures have species stratification to optimize productivity and channel formation to increase nutrient and oxygen flow between the layers [189]. Similarly, quorum sensing is a process where bacteria secrete and detect molecular signals to express traits in a context-dependent manner, usually among members of the same species. The detection of these signals in cell groups allows bacteria to perform functions that would only be advantageous

when a critical mass has been reached, such as the release of virulence compounds in animal pathogens or plant-cell-degrading compounds by bacterial phytopathogens [190]. The assumption is that quorum sensing ensures that pathogenic characteristics are only expressed when the bacterial population size is sufficient to overcome host defenses. Therefore, in both biofilms and quorum sensing, cooperation is seen as an evolutionary strategy that enhances the greater good of the community. This contradicts the argument that natural selection favors selfish behavior and group-level adaptations should be used only when necessary [191]. Quorum sensing can be modeled on the basis of individual cell action alone where a single cell can monitor levels of diffused products selfishly rather than coordinating with other cells [192]. A challenge in predicting cooperation in bacterial communities has been the absence of models that can mimic to microbe-microbe interactions due to their complex signals for competition and cooperation.

We are able to exploit the modularity of the CDI system as previously studied by the lab. In previous work, receptor binding domains differ among CdiA proteins upon sequence analysis and there are at least four different receptor classes of CDI receptors [106, 101]. The lab has demonstrated that the receptor binding domain and toxin domains can be swapped which highlights the modularity of this system. This thesis explores the *K. aerogenes* CDI system and investigates an outer membrane receptor that has been previously identified as important in the uptake of antibiotics. Through sequence analysis, we have identified two functional CDI systems in *K. aerogenes*, with locus 1 having an extended FHA-1 region, potentially enabling it to bind to non-kin and sister cells more effectively. Using the *K. aerogenes* locus 1 CDI system, we were able to discover the CDI receptor, OmpC, which is a Class II receptor typically using an OmpC/OmpF heterotrimer for binding. Sequence analysis of the *K. aerogenes* RBD was inconclusive, so the receptor was identified through transposon mutagenesis and co-culture experiments. OmpC was discovered as the only binding partner for the locus 1 CDI system, unlike

the usual Class II receptor where the receptor binding domain binds to both OmpC and OmpF. Further investigation of loop 3 in OmpC was done, as it is known as a nonselective porin for ions and small molecules and because this loop folds down into the barrel acting as a gate. In previous work, clinical isolates were studied and mutations in OmpC were linked to less cell permeability. These mutations did not allow antibiotics into the cell rendering them useless. Mutations from the clinical isolates and from site-directed mutageneis confirmed the locking of the gate in place, preventing binding to the receptor binding domain and possibly entrance of antibiotics into the cell.

The CDI system of *K. aerogenes* is important to study because this system can easily become multidrug-resistant and the treatment alternatives are few. The CDI system mechanism as a whole is important to study because the mechanism of delivery and presentation on the exterior of the cell still have many mysteries to be unraveled. The Type Vb secretion systems are important for Gram-negative bacterial survival and pathogenesis by secreting large exoproteins that can deliver toxic effectors. CdiA toxic effectors are part of a subgroup of TpsA proteins that have multi functional roles in offense where nonkin are injected with a toxin and in defense where CdiA joins attaches the cells to each other. Recent studies have shown that CdiA promotes adhesion, intracellular survival, virulence, and biofilm establishment in human pathogens [149]. CdiA has been associated with and exported through CdiB, and disruptions in flexible regions in CdiB result in decreased secretion of CdiA [85]. The topology of CdiB was mapped by introducing non-native cysteines and stained using a maleimide dye. In the presence and absence of CdiA, a possible interaction between CdiA and CdiB was suggested based on R345 staining. The interaction between CdiA and CdiB was further confirmed with crosslinking data. Mutations in loops of CdiB that may contact CdiA did not change the presentation of CdiA on the exterior of the cell. The deletion of a loop in CdiB altered its structure and prevented the secretion of CdiA with the conclusion that this produced a

nonfunctional CdiB. In other work, the exportation of CdiA is reduced if specific regions in CdiB are mutated to form a salt bridge linking specific β-strands.

I was also fortunate to be able to use a protein modeling system, AlphaFold, to model and hypothesize possible interactions of the receptor binding domain of CdiA and the contact points of the receptor. AlphaFold has been able to predict over 100,000 protein structures and become an instrumental tool in moving science forward at a faster rate [193]. I used ChimeraX developed by UCSF to analyze these structures and various collaborative notebooks to perform docking between proteins. With the increase in computer AI and machine learning, viewing sequences, proteins, and genes that can lead to predictions about activity and function will move research forward. People will be able to hypothesize with more accuracy and people with less research experience will be able to see what is happening instead of struggling to see a mental visual that is difficult to understand. I enjoyed these tools and was able to see the predicted effect of the mutations much easier.

The implication of studying *K. aerogenes* CDI system and its CDI receptor are that it is an opportunistic bacteria, it can win the war against antibiotics, and the receptor can be used in identifying areas that are important for contact for uptake of antibiotics. This bacteria is multidrug-resistant will need a new therapy. The continued use of antibiotics to treat bacterial infections will only increase the list of antibiotics that bacteria are resistant to. Bacteria are hardy, sturdy, and will find a way to survive. Humans will have to target multiple mechanisms of action to make antibiotics more effective. This may be in the form of antibiotic cocktails or multi-step dosing with drugs that target different aspects of bacterial cell survival such as cell wall biogenesis, protein production, or efflux pumps. The identification of different amino acids and their effect on binding to the receptor binding domain and locking the internal loop into place in OmpC will aid in the discovery of a target for efflux pumps. This one factor will have an impact on

the overall treatment when antibiotic cocktails become the norm. The CDI system as a whole could be weaponized to target specific bacteria once the opportunistic bacteria has been identified. This is similar to phage therapy where phages are used to target bacteria to lyse cells. The CDI system can be modulated to target a bacteria with a specific toxin to stop protein production by injecting DNases or RNases or form pores in the target bacteria. The direct application of CDI will require additional studies into the complete understanding of this mechanism from secretion to insertion into the target cells of all CDI systems that can be used as a therapy and specific binding contacts in the receptors to identify a complete list of binding partners that are the most conserved and least likely to mutate.

Bibliography

[1] Y. M. Bar-On, R. Phillips, and R. Milo, *The biomass distribution on earth*, *Proceedings of the National Academy of Sciences* **115** (2018), no. 25 6506–6511.

[2] M.-K. Looi, *The human microbiome: Everything you need to know about the 39 trillion microbes that call our bodies home*, Jul, 2020.

[3] G. Taubes, *The bacteria fight back*, 2008.

[4] R.-Y. G. T. Z. D.-P. X. Yu-Jie Zhang, Sha Li and H.-B. Li, *Impacts of gut bacteria on human health and diseases*, *International Journal of Molecular Sciences* **16** (2015), no. 4 7493–7519, [https://www.ncbi.nlm.nih.gov/pmc/articles/PMC4425030/].

[5] S. S. Grant and D. T. Hung, *Persistent bacterial infections, antibiotic tolerance, and the oxidative stress response*, *Virulence* **4** (2013), no. 4 273–283, [https://www.ncbi.nlm.nih.gov/pmc/articles/PMC3710330/].

[6] A. Bush, *Persistent bacterial bronchitis: Time to venture beyond the umbrella*, *Frontiers in Pediatrics* **5** (2017), no. 264 264, [https://www.ncbi.nlm.nih.gov/pmc/articles/PMC5732151/].

[7] M. G. Blango and M. A. Mulvey, *Bacterial landlines: contact-dependent signaling in bacterial populations*, *Current opinion in microbiology* **12** (2009), no. 2 177–181.

[8] B. L. Bassler, *Small talk: cell-to-cell communication in bacteria*, *Cell* **109** (2002), no. 4 421–424.

[9] T. R. Costa, A. Ilangovan, M. Ukleja, A. Redzej, J. M. Santini, T. K. Smith, E. H. Egelman, and G. Waksman, *Structure of the bacterial sex f pilus reveals an assembly of a stoichiometric protein-phospholipid complex*, *Cell* **166** (2016), no. 6 1436–1444.

[10] U. Baumann, *Structure–function relationships of the repeat domains of rtx toxins*, *Toxins* **11** (2019), no. 11 657.

[11] L. Bumba, J. Masin, P. Macek, T. Wald, L. Motlova, I. Bibova, N. Klimova, L. Bednarova, V. Veverka, M. Kachala, *et. al.*, *Calcium-driven folding of rtx domain β-rolls ratchets translocation of rtx proteins through type i secretion ducts*, *Molecular cell* **62** (2016), no. 1 47–62.

[12] K. J. F. Satchell, *Martx, multifunctional autoprocessing repeats-in-toxin toxins*, *Infection and immunity* **75** (2007), no. 11 5079–5084.

[13] O. Spitz, I. N. Erenburg, T. Beer, K. Kanonenberg, I. B. Holland, and L. Schmitt, *Type i secretion systems—one mechanism for all?*, *Microbiology Spectrum* **7** (2019), no. 2 7–2.

[14] E. R. Green and J. Mecsas, *Bacterial secretion systems: an overview*, *Microbiology spectrum* **4** (2016), no. 1 4–1.

[15] D. C. Rees, E. Johnson, and O. Lewinson, *Abc transporters: the power to change*, *Nature reviews Molecular cell biology* **10** (2009), no. 3 218–227.

[16] J. L. Morgan, J. F. Acheson, and J. Zimmer, *Structure of a type-1 secretion system abc transporter*, *Structure* **25** (2017), no. 3 522–529.

[17] D. Murata, H. Okano, C. Angkawidjaja, M. Akutsu, S.-i. Tanaka, K. Kitahara, T. Yoshizawa, H. Matsumura, Y. Kado, E. Mizohata, *et. al.*, *Structural basis for the serratia marcescens lipase secretion system: crystal structures of the membrane fusion protein and nucleotide-binding domain*, *Biochemistry* **56** (2017), no. 47 6281–6291.

[18] S. Peherstorfer, H. H. Brewitz, A. A. P. George, A. Wißbrock, J. M. Adam, L. Schmitt, and D. Imhof, *Insights into mechanism and functional consequences of heme binding to hemolysin-activating lysine acyltransferase hlyc from escherichia coli*, *Biochimica et Biophysica Acta (BBA)-General Subjects* **1862** (2018), no. 9 1964–1972.

[19] I. N. Erenburg, S. Hänsch, F. M. Chacko, A. Hamacher, S. Wintgens, F. Stuhldreier, G. Poschmann, O. Spitz, K. Stühler, S. Wesselborg, *et. al.*, *Heterologously secreted mbxa from moraxella bovis induces a membrane blebbing response of the human host cell*, *Scientific Reports* **12** (2022), no. 1 17825.

[20] K. V. Korotkov, M. Sandkvist, and W. G. Hol, *The type ii secretion system: biogenesis, molecular architecture and mechanism*, *Nature Reviews Microbiology* **10** (2012), no. 5 336–351.

[21] K. V. Korotkov and M. Sandkvist, *Architecture, function, and substrates of the type ii secretion system*, *EcoSal Plus* **8** (2019), no. 2.

[22] N. P. Greene, A. Crow, C. Hughes, and V. Koronakis, *Structure of a bacterial toxin-activating acyltransferase*, *Proceedings of the National Academy of Sciences* **112** (2015), no. 23 E3058–E3066.

[23] S. Naskar, M. Hohl, M. Tassinari, and H. H. Low, *The structure and mechanism of the bacterial type ii secretion system*, *Molecular Microbiology* **115** (2021), no. 3 412–424.

[24] L. S. McLaughlin, R. J. Haft, and K. T. Forest, *Structural insights into the type ii secretion nanomachine*, *Current opinion in structural biology* **22** (2012), no. 2 208–216.

[25] L. L. Burrows, *Prime time for minor subunits of the type ii secretion and type iv pilus systems*, *Molecular microbiology* **86** (2012), no. 4 765–769.

[26] M. Sandkvist, L. O. Michel, L. P. Hough, V. M. Morales, M. Bagdasarian, M. Koomey, V. J. DiRita, and M. Bagdasarian, *General secretion pathway (eps) genes required for toxin secretion and outer membrane biogenesis in vibrio cholerae*, *Journal of bacteriology* **179** (1997), no. 22 6994–7003.

[27] R. Kulkarni, B. K. Dhakal, E. S. Slechta, Z. Kurtz, M. A. Mulvey, and D. G. Thanassi, *Roles of putative type ii secretion and type iv pilus systems in the virulence of uropathogenic escherichia coli*, *PLoS One* **4** (2009), no. 3 e4752.

[28] W. Swietnicki, A. Czarny, L. Antkowiak, E. Zaczynska, M. Kolodziejczak, J. Sycz, L. Stachowicz, M. Alicka, and K. Marycz, *Identification of a potent inhibitor of type ii secretion system from pseudomonas aeruginosa*, *Biochemical and biophysical research communications* **513** (2019), no. 3 688–693.

[29] D. Ghosal, K. W. Kim, H. Zheng, M. Kaplan, H. K. Truchan, A. E. Lopez, I. E. McIntire, J. P. Vogel, N. P. Cianciotto, and G. J. Jensen, *In vivo structure of the legionella type ii secretion system by electron cryotomography*, *Nature microbiology* **4** (2019), no. 12 2101–2108.

[30] M. Tauschek, R. J. Gorrell, R. A. Strugnell, and R. M. Robins-Browne, *Identification of a protein secretory pathway for the secretion of heat-labile enterotoxin by an enterotoxigenic strain of escherichia coli*, *Proceedings of the National Academy of Sciences* **99** (2002), no. 10 7066–7071.

[31] J. Jyot, V. Balloy, G. Jouvion, A. Verma, L. Touqui, M. Huerre, M. Chignard, and R. Ramphal, *Type ii secretion system of pseudomonas aeruginosa: in vivo evidence of a significant role in death due to lung infection*, *Journal of Infectious Diseases* **203** (2011), no. 10 1369–1377.

[32] O. Rossier, S. R. Starkenburg, and N. P. Cianciotto, *Legionella pneumophila type ii protein secretion promotes virulence in the a/j mouse model of legionnaires' disease pneumonia*, *Infection and immunity* **72** (2004), no. 1 310–321.

[33] W. Deng, N. C. Marshall, J. L. Rowland, J. M. McCoy, L. J. Worrall, A. S. Santos, N. C. Strynadka, and B. B. Finlay, *Assembly, structure, function and regulation of type iii secretion systems*, *Nature Reviews Microbiology* **15** (2017), no. 6 323–337.

[34] P. Abrusci, M. A. McDowell, S. M. Lea, and S. Johnson, *Building a secreting nanomachine: a structural overview of the t3ss*, *Current opinion in structural biology* **25** (2014) 111–117.

[35] B. J. Burkinshaw and N. C. Strynadka, *Assembly and structure of the t3ss*, *Biochimica et Biophysica Acta (BBA)-Molecular Cell Research* **1843** (2014), no. 8 1649–1663.

[36] A. Kawamoto, Y. V. Morimoto, T. Miyata, T. Minamino, K. T. Hughes, T. Kato, and K. Namba, *Common and distinct structural features of salmonella injectisome and flagellar basal body*, *Scientific reports* **3** (2013), no. 1 3369.

[37] J. Van Der Heijden and B. B. Finlay, *Type iii effector-mediated processes in salmonella infection*, *Future microbiology* **7** (2012), no. 6 685–703.

[38] B. Raymond, J. C. Young, M. Pallett, R. G. Endres, A. Clements, and G. Frankel, *Subversion of trafficking, apoptosis, and innate immunity by type iii secretion system effectors*, *Trends in microbiology* **21** (2013), no. 8 430–441.

[39] D. Büttner, *Behind the lines–actions of bacterial type iii effector proteins in plant cells*, *FEMS microbiology reviews* **40** (2016), no. 6 894–937.

[40] C. Staehelin and H. B. Krishnan, *Nodulation outer proteins: double-edged swords of symbiotic rhizobia*, *Biochemical Journal* **470** (2015), no. 3 263–274.

[41] A. S. Santos and B. B. Finlay, *Bringing down the host: enteropathogenic and enterohaemorrhagic e scherichia coli effector-mediated subversion of host innate immune pathways*, *Cellular microbiology* **17** (2015), no. 3 318–332.

[42] J. B. Bliska, X. Wang, G. I. Viboud, and I. E. Brodsky, *Modulation of innate immune responses by y ersinia type iii secretion system translocators and effectors*, *Cellular microbiology* **15** (2013), no. 10 1622–1631.

[43] F. Makino, D. Shen, N. Kajimura, A. Kawamoto, P. Pissaridou, H. Oswin, M. Pain, I. Murillo, K. Namba, and A. J. Blocker, *The architecture of the cytoplasmic region of type iii secretion systems*, *Scientific reports* **6** (2016), no. 1 33341.

[44] B. Hu, D. R. Morado, W. Margolin, J. R. Rohde, O. Arizmendi, W. L. Picking, W. D. Picking, and J. Liu, *Visualization of the type iii secretion sorting platform of shigella flexneri*, *Proceedings of the National Academy of Sciences* **112** (2015), no. 4 1047–1052.

[45] M. Kudryashev, M. Stenta, S. Schmelz, M. Amstutz, U. Wiesand, D. Castaño-Díez, M. T. Degiacomi, S. Münnich, C. K. Bleck, J. Kowal, *et. al.*, *In situ structural analysis of the yersinia enterocolitica injectisome*, *Elife* **2** (2013) e00792.

[46] A. Nans, M. Kudryashev, H. R. Saibil, and R. D. Hayward, *Structure of a bacterial type iii secretion system in contact with a host membrane in situ*, *Nature communications* **6** (2015), no. 1 10114.

[47] T. Izore, V. Job, and A. Dessen, *Biogenesis, regulation, and targeting of the type iii secretion system*, *Structure* **19** (2011), no. 5 603–612.

[48] A. Puhar and P. J. Sansonetti, *Type iii secretion system*, *Current Biology* **24** (2014), no. 17 R784–R791.

[49] C. J. Hueck, *Type iii protein secretion systems in bacterial pathogens of animals and plants*, *Microbiology and molecular biology reviews* **62** (1998), no. 2 379–433.

[50] S. S. Abby and E. P. Rocha, *The non-flagellar type iii secretion system evolved from the bacterial flagellum and diversified into host-cell adapted systems*, .

[51] D. S. A. Beeckman and D. C. Vanrompay, *Bacterial secretion systems with an emphasis on the chlamydial type iii secretion system*, *Current issues in molecular biology* **12** (2010), no. 1 17–42.

[52] M. Muthuramalingam, S. K. Whittier, W. L. Picking, and W. D. Picking, *The shigella type iii secretion system: an overview from top to bottom*, *Microorganisms* **9** (2021), no. 2 451.

[53] Y. Litvak, S. Sharon, M. Hyams, L. Zhang, S. Kobi, N. Katsowich, S. Dishon, G. Nussbaum, N. Dong, F. Shao, *et. al.*, *Epithelial cells detect functional type iii secretion system of enteropathogenic escherichia coli through a novel nf-κb signaling pathway*, *PLoS Pathogens* **13** (2017), no. 7 e1006472.

[54] G. V. Plano and K. Schesser, *The yersinia pestis type iii secretion system: expression, assembly and role in the evasion of host defenses*, *Immunologic research* **57** (2013) 237–245.

[55] H.-J. Yeo and G. Waksman, *Unveiling molecular scaffolds of the type iv secretion system*, *Journal of bacteriology* **186** (2004), no. 7 1919–1926.

[56] D. P. Souza, G. U. Oka, C. E. Alvarez-Martinez, A. W. Bisson-Filho, G. Dunger, L. Hobeika, N. S. Cavalcante, M. C. Alegria, L. R. Barbosa, R. K. Salinas, *et. al.*, *Bacterial killing via a type iv secretion system*, *Nature communications* **6** (2015), no. 1 6453.

[57] P. J. Christie, *Type iv secretion: the agrobacterium virb/d4 and related conjugation systems*, *Biochimica et Biophysica Acta (BBA)-Molecular Cell Research* **1694** (2004), no. 1-3 219–234.

[58] J. M. Chung, M. J. Sheedlo, A. M. Campbell, N. Sawhney, A. E. Frick-Cheng, D. B. Lacy, T. L. Cover, and M. D. Ohi, *Structure of the helicobacter pylori cag type iv secretion system*, *Elife* **8** (2019) e47644.

[59] E. Cascales and P. J. Christie, *The versatile bacterial type iv secretion systems*, *Nature Reviews Microbiology* **1** (2003), no. 2 137–149.

[60] V. Chandran, R. Fronzes, S. Duquerroy, N. Cronin, J. Navaza, and G. Waksman, *Structure of the outer membrane complex of a type iv secretion system*, *Nature* **462** (2009), no. 7276 1011–1015.

[61] K. Atmakuri, E. Cascales, and P. J. Christie, *Energetic components vird4, virb11 and virb4 mediate early dna transfer reactions required for bacterial type iv secretion*, *Molecular microbiology* **54** (2004), no. 5 1199–1211.

[62] P. J. Christie, N. Whitaker, and C. González-Rivera, *Mechanism and structure of the bacterial type iv secretion systems*, *Biochimica et Biophysica Acta (BBA)-Molecular Cell Research* **1843** (2014), no. 8 1578–1591.

[63] H. H. Low, F. Gubellini, A. Rivera-Calzada, N. Braun, S. Connery, A. Dujeancourt, F. Lu, A. Redzej, R. Fronzes, E. V. Orlova, *et. al.*, *Structure of a type iv secretion system*, *Nature* **508** (2014), no. 7497 550–553.

[64] S. T. Miyata, M. Kitaoka, L. Wieteska, C. Frech, N. Chen, and S. Pukatzki, *The vibrio cholerae type vi secretion system: evaluating its role in the human disease cholera*, *Frontiers in microbiology* **1** (2010) 117.

[65] N. R. Salama, M. L. Hartung, and A. Müller, *Life in the human stomach: persistence strategies of the bacterial pathogen helicobacter pylori*, *Nature Reviews Microbiology* **11** (2013), no. 6 385–399.

[66] E. Pachulec, K. Siewering, T. Bender, E.-M. Heller, W. Salgado-Pabon, S. K. Schmoller, K. L. Woodhams, J. P. Dillard, and C. van der Does, *Functional analysis of the gonococcal genetic island of neisseria gonorrhoeae*, *PloS one* **9** (2014), no. 10 e109613.

[67] J. P. Vogel and R. R. Isberg, *Cell biology of legionella pneumophila*, *Current opinion in microbiology* **2** (1999), no. 1 30–34.

[68] I. Meuskens, A. Saragliadis, J. C. Leo, and D. Linke, *Type v secretion systems: an overview of passenger domain functions*, *Frontiers in microbiology* **10** (2019) 1163.

[69] J. C. Leo, I. Grin, and D. Linke, *Type v secretion: mechanism (s) of autotransport through the bacterial outer membrane*, *Philosophical Transactions of the Royal Society B: Biological Sciences* **367** (2012), no. 1592 1088–1101.

[70] P. Van Ulsen, S. ur Rahman, W. S. Jong, M. H. Daleke-Schermerhorn, and J. Luirink, *Type v secretion: from biogenesis to biotechnology*, *Biochimica et Biophysica Acta (BBA)-Molecular Cell Research* **1843** (2014), no. 8 1592–1611.

[71] E. Fan, N. Chauhan, D. G. Udatha, J. C. Leo, and D. Linke, *Type v secretion systems in bacteria*, *Virulence Mechanisms of Bacterial Pathogens* (2016) 305–335.

[72] M. Rojas-Lopez, M. A. Zorgani, L. A. Kelley, X. Bailly, A. V. Kajava, I. R. Henderson, F. Polticelli, M. Pizza, R. Rosini, and M. Desvaux, *Identification of the autochaperone domain in the type va secretion system (t5ass): prevalent feature of autotransporters with a β-helical passenger*, *Frontiers in microbiology* **8** (2018) 2607.

[73] J. Pohlner, R. Halter, K. Beyreuther, and T. F. Meyer, *Gene structure and extracellular secretion of neisseria gonorrhoeae iga protease*, *Nature* **325** (1987), no. 6103 458–462.

[74] R. Albrecht, M. Schütz, P. Oberhettinger, M. Faulstich, I. Bermejo, T. Rudel, K. Diederichs, and K. Zeth, *Structure of bama, an essential factor in outer membrane protein biogenesis*, *Acta Crystallographica Section D: Biological Crystallography* **70** (2014), no. 6 1779–1789.

[75] M. H. Mulks and A. G. Plaut, *Iga protease production as a characteristic distinguishing pathogenic from harmless neisseriaceae*, *New England Journal of Medicine* **299** (1978), no. 18 973–976.

[76] I. Benz and M. A. Schmidt, *Cloning and expression of an adhesin (aida-i) involved in diffuse adherence of enteropathogenic escherichia coli*, *Infection and immunity* **57** (1989), no. 5 1506–1511.

[77] E. Leininger, M. Roberts, J. G. Kenimer, I. G. Charles, N. Fairweather, P. Novotny, and M. J. Brennan, *Pertactin, an arg-gly-asp-containing bordetella pertussis surface protein that promotes adherence of mammalian cells.*, *Proceedings of the National Academy of Sciences* **88** (1991), no. 2 345–349.

[78] M.-È. Charbonneau and M. Mourez, *The escherichia coli aida-i autotransporter undergoes cytoplasmic glycosylation independently of export*, *Research in microbiology* **159** (2008), no. 7-8 537–544.

[79] M. Junker, C. C. Schuster, A. V. McDonnell, K. A. Sorg, M. C. Finn, B. Berger, and P. L. Clark, *Pertactin β-helix folding mechanism suggests common themes for the secretion and folding of autotransporter proteins*, *Proceedings of the National Academy of Sciences* **103** (2006), no. 13 4918–4923.

[80] K. G. Swihart and R. A. Welch, *Cytotoxic activity of the proteus hemolysin hpma*, *Infection and immunity* **58** (1990), no. 6 1861–1869.

[81] J. W. S. Geme and H.-J. Yeo, *A prototype two-partner secretion pathway: the haemophilus influenzae hmw1 and hmw2 adhesin systems*, *Trends in microbiology* **17** (2009), no. 8 355–360.

[82] C. Fournier, A. Smith, and P. Delepelaire, *Haem release from haemopexin by hxua allows haemophilus influenzae to escape host nutritional immunity*, *Molecular microbiology* **80** (2011), no. 1 133–148.

[83] V. Girard, J.-P. Côté, M.-È. Charbonneau, M. Campos, F. Berthiaume, M. A. Hancock, N. Siddiqui, and M. Mourez, *Conformation change in a self-recognizing autotransporter modulates bacterial cell-cell interaction*, *Journal of Biological Chemistry* **285** (2010), no. 14 10616–10626.

[84] P. Klemm, R. M. Vejborg, and O. Sherlock, *Self-associating autotransporters, saats: functional and structural similarities*, *International journal of medical microbiology* **296** (2006), no. 4-5 187–195.

[85] J. Guerin, I. Botos, Z. Zhang, K. Lundquist, J. C. Gumbart, and S. K. Buchanan, *Structural insight into toxin secretion by contact-dependent growth inhibition transporters*, *Elife* **9** (2020) e58100.

[86] J. Mazar and P. A. Cotter, *Topology and maturation of filamentous haemagglutinin suggest a new model for two-partner secretion*, *Molecular microbiology* **62** (2006), no. 3 641–654.

[87] F. Menozzi, P. Boucher, G. Riveau, C. Gantiez, and C. Locht, *Surface-associated filamentous hemagglutinin induces autoagglutination of bordetella pertussis*, *Infection and Immunity* **62** (1994), no. 10 4261–4269.

[88] R. Hertle, M. Hilger, S. Weingardt-Kocher, and I. Walev, *Cytotoxic action of serratia marcescens hemolysin on human epithelial cells*, *Infection and immunity* **67** (1999), no. 2 817–825.

[89] N. A. Kadry, E. A. Porsch, H. Shen, and J. W. St. Geme III, *Immunization with hmw1 and hmw2 adhesins protects against colonization by heterologous strains of nontypeable haemophilus influenzae*, *Proceedings of the National Academy of Sciences* **118** (2021), no. 32 e2019923118.

[90] M. J. Bottery, I. Passaris, C. Dytham, A. J. Wood, and M. W. van der Woude, *Spatial organization of expanding bacterial colonies is affected by contact-dependent growth inhibition*, *Current Biology* **29** (2019), no. 21 3622–3634.

[91] S. K. Aoki, R. Pamma, A. D. Hernday, J. E. Bickham, B. A. Braaten, and D. A. Low, *Contact-dependent inhibition of growth in escherichia coli*, *Science* **309** (2005), no. 5738 1245–1248.

[92] K. Nikolakakis, S. Amber, J. S. Wilbur, E. J. Diner, S. K. Aoki, S. J. Poole, A. Tuanyok, P. S. Keim, S. Peacock, C. S. Hayes, *et. al.*, *The toxin/immunity network of burkholderia pseudomallei contact-dependent growth inhibition (cdi) systems*, *Molecular microbiology* **84** (2012), no. 3 516–529.

[93] R. P. Morse, J. L. Willett, P. M. Johnson, J. Zheng, A. Credali, A. Iniguez, J. S. Nowick, C. S. Hayes, and C. W. Goulding, *Diversification of β-augmentation interactions between cdi toxin/immunity proteins*, *Journal of molecular biology* **427** (2015), no. 23 3766–3784.

[94] M. S. Anderson, E. C. Garcia, and P. A. Cotter, *The burkholderia bcpaiob genes define unique classes of two-partner secretion and contact dependent growth inhibition systems*, .

[95] T. Myers-Morales, A. E. Oates, M. S. Byrd, and E. C. Garcia, *Burkholderia cepacia complex contact-dependent growth inhibition systems mediate interbacterial competition*, *Journal of bacteriology* **201** (2019), no. 12 e00012–19.

[96] Z. C. Ruhe, P. Subramanian, K. Song, J. Y. Nguyen, T. A. Stevens, D. A. Low, G. J. Jensen, and C. S. Hayes, *Programmed secretion arrest and receptor-triggered toxin export during antibacterial contact-dependent growth inhibition*, *Cell* **175** (2018), no. 4 921–933.

[97] R. F. Simmerman, A. M. Dave, and B. D. Bruce, *Structure and function of potra domains of omp85/tps superfamily*, *International Review of Cell and Molecular Biology* **308** (2014) 1–34.

[98] J. L. Willett, Z. C. Ruhe, C. W. Goulding, D. A. Low, and C. S. Hayes, *Contact-dependent growth inhibition (cdi) and cdib/cdia two-partner secretion proteins*, *Journal of molecular biology* **427** (2015), no. 23 3754–3765.

[99] B. Clantin, H. Hodak, E. Willery, C. Locht, F. Jacob-Dubuisson, and V. Villeret, *The crystal structure of filamentous hemagglutinin secretion domain and its implications for the two-partner secretion pathway*, *Proceedings of the National Academy of Sciences* **101** (2004), no. 16 6194–6199.

[100] S. K. Aoki, J. C. Malinverni, K. Jacoby, B. Thomas, R. Pamma, B. N. Trinh, S. Remers, J. Webb, B. A. Braaten, T. J. Silhavy, *et. al.*, *Contact-dependent growth inhibition requires the essential outer membrane protein bama (yaet) as the receptor and the inner membrane transport protein acrb*, *Molecular microbiology* **70** (2008), no. 2 323–340.

[101] T. M. Halvorsen, F. Garza-Sánchez, Z. C. Ruhe, N. L. Bartelli, N. A. Chan, J. Y. Nguyen, D. A. Low, and C. S. Hayes, *Lipidation of class iv cdia effector proteins promotes target cell recognition during contact-dependent growth inhibition*, *Mbio* **12** (2021), no. 5 e02530–21.

[102] N. L. Bartelli, S. Sun, G. C. Gucinski, H. Zhou, K. Song, C. S. Hayes, and F. W. Dahlquist, *The cytoplasm-entry domain of antibacterial cdia is a dynamic α-helical bundle with disulfide-dependent structural features*, *Journal of molecular biology* **431** (2019), no. 17 3203–3216.

[103] E. S. Danka, E. C. Garcia, and P. A. Cotter, *Are cdi systems multicolored, facultative, helping greenbeards?*, *Trends in microbiology* **25** (2017), no. 5 391–401.

[104] S. K. Aoki, E. J. Diner, C. t. de Roodenbeke, B. R. Burgess, S. J. Poole, B. A. Braaten, A. M. Jones, J. S. Webb, C. S. Hayes, P. A. Cotter, *et. al.*, *A widespread family of polymorphic contact-dependent toxin delivery systems in bacteria*, *Nature* **468** (2010), no. 7322 439–442.

[105] S. K. Aoki, S. J. Poole, C. S. Hayes, and D. A. Low, *Toxin on a stick: modular cdi toxin delivery systems play roles in bacterial competition*, *Virulence* **2** (2011), no. 4 356–359.

[106] Z. C. Ruhe, J. Y. Nguyen, J. Xiong, S. Koskiniemi, C. M. Beck, B. R. Perkins, D. A. Low, and C. S. Hayes, *Cdia effectors use modular receptor-binding domains to recognize target bacteria*, *MBio* **8** (2017), no. 2 e00290–17.

[107] Z. C. Ruhe, D. A. Low, and C. S. Hayes, *Bacterial contact-dependent growth inhibition*, *Trends in microbiology* **21** (2013), no. 5 230–237.

[108] E. Cascales, S. K. Buchanan, D. Duché, C. Kleanthous, R. Lloubes, K. Postle, M. Riley, S. Slatin, and D. Cavard, *Colicin biology*, *Microbiology and molecular biology reviews* **71** (2007), no. 1 158–229.

[109] D. F. Benítez-Chao, A. León-Buitimea, J. A. Lerma-Escalera, and J. R. Morones-Ramírez, *Bacteriocins: An overview of antimicrobial, toxicity, and biosafety assessment by in vivo models*, *Frontiers in Microbiology* **12** (2021) 630695.

[110] A. W. Negash, B. A. Tsehai, *et. al.*, *Current applications of bacteriocin*, *International Journal of Microbiology* **2020** (2020).

[111] S. Soelaiman, K. Jakes, N. Wu, C. Li, and M. Shoham, *Crystal structure of colicin e3: implications for cell entry and ribosome inactivation*, *Molecular cell* **8** (2001), no. 5 1053–1062.

[112] S. D. Zakharov, V. Y. Eroukova, T. I. Rokitskaya, M. V. Zhalnina, O. Sharma, P. J. Loll, H. I. Zgurskaya, Y. N. Antonenko, and W. A. Cramer, *Colicin occlusion of ompf and tolc channels: outer membrane translocons for colicin import*, *Biophysical journal* **87** (2004), no. 6 3901–3911.

[113] G. Kurisu, S. D. Zakharov, M. V. Zhalnina, S. Bano, V. Y. Eroukova, T. I. Rokitskaya, Y. N. Antonenko, M. C. Wiener, and W. A. Cramer, *The structure of btub with bound colicin e3 r-domain implies a translocon*, *Nature Structural & Molecular Biology* **10** (2003), no. 11 948–954.

[114] E. Bouveret, A. Rigal, C. Lazdunski, and H. Bénédetti, *The n-terminal domain of colicin e3 interacts with tolb which is involved in the colicin translocation step*, *Molecular microbiology* **23** (1997), no. 5 909–920.

[115] M. Haruhiko, A. Akiko, U. Takeshi, and O. Takahisa, *Identification of a unique specificity determinant of the colicin e3 immunity protein*, *Gene* **107** (1991), no. 1 133–138.

[116] B. T. Ho, T. G. Dong, and J. J. Mekalanos, *A view to a kill: the bacterial type vi secretion system*, *Cell host & microbe* **15** (2014), no. 1 9–21.

[117] A. Zoued, Y. R. Brunet, E. Durand, M.-S. Aschtgen, L. Logger, B. Douzi, L. Journet, C. Cambillau, and E. Cascales, *Architecture and assembly of the type vi secretion system*, *Biochimica et Biophysica Acta (BBA)-Molecular Cell Research* **1843** (2014), no. 8 1664–1673.

[118] A. B. Russell, S. B. Peterson, and J. D. Mougous, *Type vi secretion system effectors: poisons with a purpose*, *Nature reviews microbiology* **12** (2014), no. 2 137–148.

[119] J. M. Silverman, Y. R. Brunet, E. Cascales, and J. D. Mougous, *Structure and regulation of the type vi secretion system*, *Annual review of microbiology* **66** (2012) 453–472.

[120] M. Basler, *Type vi secretion system: secretion by a contractile nanomachine*, *Philosophical Transactions of the Royal Society B: Biological Sciences* **370** (2015), no. 1679 20150021.

[121] T. E. Wood, S. A. Howard, S. Wettstadt, and A. Filloux, *Paar proteins act as the 'sorting hat'of the type vi secretion system*, *Microbiology* **165** (2019), no. 11 1203.

[122] F. R. Cianfanelli, L. Monlezun, and S. J. Coulthurst, *Aim, load, fire: the type vi secretion system, a bacterial nanoweapon*, *Trends in microbiology* **24** (2016), no. 1 51–62.

[123] M. Basler, B. T. Ho, and J. J. Mekalanos, *Tit-for-tat: type vi secretion system counterattack during bacterial cell-cell interactions*, *Cell* **152** (2013), no. 4 884–894.

[124] A. M. Lasica, M. Ksiazek, M. Madej, and J. Potempa, *The type ix secretion system (t9ss): highlights and recent insights into its structure and function*, *Frontiers in cellular and infection microbiology* **7** (2017) 215.

[125] F. Thomas, J.-H. Hehemann, E. Rebuffet, M. Czjzek, and G. Michel, *Environmental and gut bacteroidetes: the food connection*, *Frontiers in microbiology* **2** (2011) 93.

[126] P. Veith, M. Glew, D. Gorasia, E. Cascales, and E. Reynolds, *The type ix secretion system and its role in bacterial function and pathogenesis*, *Journal of Dental Research* **101** (2022), no. 4 374–383.

[127] M. J. McBride, *Bacteroidetes gliding motility and the type ix secretion system*, *Protein Secretion in Bacteria* (2019) 363–374.

[128] D. G. Gorasia, G. Chreifi, C. A. Seers, C. A. Butler, J. E. Heath, M. D. Glew, M. J. McBride, P. Subramanian, A. Kjaer, G. J. Jensen, *et. al.*, *In situ structure and organisation of the type ix secretion system*, *BioRxiv* (2020) 2020–05.

[129] P. Leone, J. Roche, M. S. Vincent, Q. H. Tran, A. Desmyter, E. Cascales, C. Kellenberger, C. Cambillau, and A. Roussel, *Type ix secretion system porm and gliding machinery gldm form arches spanning the periplasmic space*, *Nature communications* **9** (2018), no. 1 429.

[130] K. Salimiyan Rizi, K. Ghazvini, and H. Farsiani, *Clinical and pathogenesis overview of enterobacter infections*, *Reviews in Clinical Medicine* **6** (2020), no. 4 146–154.

[131] G. Mancuso, A. Midiri, E. Gerace, and C. Biondo, *Bacterial antibiotic resistance: The most critical pathogens*, *Pathogens* **10** (2021), no. 10 1310.

[132] D. J. Brenner and J. Farmer Iii, *Enterobacteriaceae*, *Bergey's manual of systematics of archaea and bacteria* (2015) 1–24.

[133] D. L. Paterson, *Resistance in gram-negative bacteria: Enterobacteriaceae*, *American journal of infection control* **34** (2006), no. 5 S20–S28.

[134] J.-Y. Lim, J.-W. Yoon, and C. J. Hovde, *A brief overview of escherichia coli o157: H7 and its plasmid o157*, *Journal of microbiology and biotechnology* **20** (2010), no. 1 5–14.

[135] H. Passarelli-Araujo, J. K. Palmeiro, K. C. Moharana, F. Pedrosa-Silva, L. M. Dalla-Costa, and T. M. Venancio, *Genomic analysis unveils important aspects of population structure, virulence, and antimicrobial resistance in klebsiella aerogenes*, *The FEBS journal* **286** (2019), no. 19 3797–3810.

[136] C. Bornet, A. Davin-Regli, C. Bosi, J.-M. Pages, and C. Bollet, *Imipenem resistance of enterobacter aerogenes mediated by outer membrane permeability*, *Journal of clinical microbiology* **38** (2000), no. 3 1048–1052.

[137] A. Wesevich, G. Sutton, F. Ruffin, L. P. Park, D. E. Fouts, V. G. Fowler Jr, and J. T. Thaden, *Newly named klebsiella aerogenes (formerly enterobacter aerogenes) is associated with poor clinical outcomes relative to other enterobacter species in patients with bloodstream infection*, *Journal of clinical microbiology* **58** (2020), no. 9 e00582–20.

[138] T. J. Opperman and S. T. Nguyen, *Recent advances toward a molecular mechanism of efflux pump inhibition*, *Frontiers in microbiology* **6** (2015) 421.

[139] S. Kumar and M. F. Varela, *Biochemistry of bacterial multidrug efflux pumps*, *International journal of molecular sciences* **13** (2012), no. 4 4484–4495.

[140] A. Sharma, V. K. Gupta, and R. Pathania, *Efflux pump inhibitors for bacterial pathogens: From bench to bedside*, *The Indian journal of medical research* **149** (2019), no. 2 129.

[141] H. Venter, R. Mowla, T. Ohene-Agyei, and S. Ma, *Rnd-type drug efflux pumps from gram-negative bacteria: molecular mechanism and inhibition*, *Frontiers in microbiology* **6** (2015) 377.

[142] M. Mmatli, N. M. Mbelle, N. E. Maningi, and J. Osei Sekyere, *Emerging transcriptional and genomic mechanisms mediating carbapenem and polymyxin resistance in enterobacteriaceae: a systematic review of current reports*, *MSystems* **5** (2020), no. 6 e00783–20.

[143] T. Ferenci and K. Phan, *How porin heterogeneity and trade-offs affect the antibiotic susceptibility of gram-negative bacteria*, *Genes* **6** (2015), no. 4 1113–1124.

[144] J. Lee, D. Tomasek, T. M. Santos, M. D. May, I. Meuskens, and D. Kahne, *Formation of a β-barrel membrane protein is catalyzed by the interior surface of the assembly machine protein bama*, *Elife* **8** (2019) e49787.

[145] D. Bennion, E. S. Charlson, E. Coon, and R. Misra, *Dissection of β-barrel outer membrane protein assembly pathways through characterizing bama potra 1 mutants of escherichia coli*, *Molecular microbiology* **77** (2010), no. 5 1153–1171.

[146] N. Noinaj, A. J. Kuszak, C. Balusek, J. C. Gumbart, and S. K. Buchanan, *Lateral opening and exit pore formation are required for bama function*, *Structure* **22** (2014), no. 7 1055–1062.

[147] H. T. Bergal, A. H. Hopkins, S. I. Metzner, and M. C. Sousa, *The structure of a bama-bamd fusion illuminates the architecture of the β-barrel assembly machine core*, *Structure* **24** (2016), no. 2 243–251.

[148] A.-S. Delattre, B. Clantin, N. Saint, C. Locht, V. Villeret, and F. Jacob-Dubuisson, *Functional importance of a conserved sequence motif in fhac, a prototypic member of the tpsb/omp85 superfamily*, *The FEBS Journal* **277** (2010), no. 22 4755–4765.

[149] Z. C. Ruhe, A. B. Wallace, D. A. Low, and C. S. Hayes, *Receptor polymorphism restricts contact-dependent growth inhibition to members of the same species*, *MBio* **4** (2013), no. 4 e00480–13.

[150] H. Nikaido, *Molecular basis of bacterial outer membrane permeability revisited*, *Microbiology and molecular biology reviews* **67** (2003), no. 4 593–656.

[151] A. Baslé, G. Rummel, P. Storici, J. P. Rosenbusch, and T. Schirmer, *Crystal structure of osmoporin ompc from e. coli at 2.0 å*, *Journal of molecular biology* **362** (2006), no. 5 933–942.

[152] E. C. Garcia, *Contact-dependent interbacterial toxins deliver a message*, *Current opinion in microbiology* **42** (2018) 40–46.

[153] E. Yamashita, M. V. Zhalnina, S. D. Zakharov, O. Sharma, and W. A. Cramer, *Crystal structures of the ompf porin: function in a colicin translocon*, *The EMBO journal* **27** (2008), no. 15 2171–2180.

[154] C. M. Beck, J. L. Willett, D. A. Cunningham, J. J. Kim, D. A. Low, and C. S. Hayes, *Cdia effectors from uropathogenic escherichia coli use heterotrimeric osmoporins as receptors to recognize target bacteria*, *PLoS pathogens* **12** (2016), no. 10 e1005925.

[155] J. Ye and B. Van den Berg, *Crystal structure of the bacterial nucleoside transporter tsx*, *The EMBO journal* **23** (2004), no. 16 3187–3195.

[156] A. Nieweg and E. Bremer, *The nucleoside-specific tsx channel from the outer membrane of salmonella typhimurium, klebsiella pneumoniae and enterobacter aerogenes: functional characterization and dna sequence analysis of the tsx genes*, *Microbiology* **143** (1997), no. 2 603–615.

[157] H. Schneider, H. Fsihi, B. Kottwitz, B. Mygind, and E. Bremer, *Identification of a segment of the escherichia coli tsx protein that functions as a bacteriophage receptor area*, *Journal of bacteriology* **175** (1993), no. 10 2809–2817.

[158] X. Wang and P. J. Quinn, *Lipopolysaccharide: Biosynthetic pathway and structure modification*, *Progress in lipid research* **49** (2010), no. 2 97–107.

[159] E. L. Wu, O. Engström, S. Jo, D. Stuhlsatz, M. S. Yeom, J. B. Klauda, G. Widmalm, and W. Im, *Molecular dynamics and nmr spectroscopy studies of e. coli lipopolysaccharide structure and dynamics*, *Biophysical journal* **105** (2013), no. 6 1444–1455.

[160] T. C. Meredith, P. Aggarwal, U. Mamat, B. Lindner, and R. W. Woodard, *Redefining the requisite lipopolysaccharide structure in escherichia coli*, *ACS chemical biology* **1** (2006), no. 1 33–42.

[161] J. A. Yethon, D. E. Heinrichs, M. A. Monteiro, M. B. Perry, and C. Whitfield, *Involvement of waay, waaq, and waap in the modification of escherichia colilipopolysaccharide and their role in the formation of a stable outer membrane*, *Journal of Biological Chemistry* **273** (1998), no. 41 26310–26316.

[162] H. Lou, M. Chen, S. S. Black, S. R. Bushell, M. Ceccarelli, T. Mach, K. Beis, A. S. Low, V. A. Bamford, I. R. Booth, *et. al.*, *Altered antibiotic transport in ompc mutants isolated from a series of clinical strains of multi-drug resistant e. coli*, *PloS one* **6** (2011), no. 10 e25825.

[163] J. Vergalli, I. V. Bodrenko, M. Masi, L. Moynié, S. Acosta-Gutierrez, J. H. Naismith, A. Davin-Regli, M. Ceccarelli, B. Van den Berg, M. Winterhalter, *et. al.*, *Porins and small-molecule translocation across the outer membrane of gram-negative bacteria*, *Nature Reviews Microbiology* **18** (2020), no. 3 164–176.

[164] N. Liu and A. H. Delcour, *The spontaneous gating activity of ompc porin is affected by mutations of a putative hydrogen bond network or of a salt bridge between the l3 loop and the barrel.*, *Protein engineering* **11** (1998), no. 9 797–802.

[165] E. Dé, A. Baslé, M. Jaquinod, N. Saint, M. Malléa, G. Molle, and J.-M. Pagès, *A new mechanism of antibiotic resistance in enterobacteriaceae induced by a structural modification of the major porin*, *Molecular microbiology* **41** (2001), no. 1 189–198.

[166] A. B. Pacheco, B. E. Guth, K. C. Soares, D. F. De Almeida, and L. C. Ferreira, *Clonal relationships among escherichia coli serogroup o6 isolates based on rapd*, *FEMS Microbiology letters* **148** (1997), no. 2 255–260.

[167] T. A. Waller, S. A. L. Pantin, A. L. Yenior, and G. G. Pujalte, *Urinary tract infection antibiotic resistance in the united states*, *Primary Care: Clinics in Office Practice* **45** (2018), no. 3 455–466.

[168] A. W. Paton and J. C. Paton, *Detection and characterization of shiga toxigenic escherichia coli by using multiplex pcr assays for stx 1, stx 2, eaea, enterohemorrhagic e. coli hlya, rfb o111, and rfb o157*, *Journal of clinical microbiology* **36** (1998), no. 2 598–602.

[169] E. Scallan, R. M. Hoekstra, F. J. Angulo, R. V. Tauxe, M.-A. Widdowson, S. L. Roy, J. L. Jones, and P. M. Griffin, *Foodborne illness acquired in the united states—major pathogens*, *Emerg Infect Dis* **17** (2011), no. 1 7–15.

[170] S. R. Steyert, J. W. Sahl, C. M. Fraser, L. D. Teel, F. Scheutz, and D. A. Rasko, *Comparative genomics and stx phage characterization of lee-negative shiga toxin-producing escherichia coli*, *Frontiers in cellular and infection microbiology* **2** (2012) 133.

[171] T. Kaya and H. Koser, *Direct upstream motility in escherichia coli*, *Biophysical journal* **102** (2012), no. 7 1514–1523.

[172] P. Virtanen, M. Wäneskog, and S. Koskiniemi, *Class ii contact-dependent growth inhibition (cdi) systems allow for broad-range cross-species toxin delivery within the enterobacteriaceae family*, *Molecular microbiology* **111** (2019), no. 4 1109–1125.

[173] D. A. Relman, M. Domenighini, E. Tuomanen, R. Rappuoli, and S. Falkow, *Filamentous hemagglutinin of bordetella pertussis: nucleotide sequence and crucial role in adherence.*, *Proceedings of the national academy of sciences* **86** (1989), no. 8 2637–2641.

[174] A. Jamet and X. Nassif, *New players in the toxin field: polymorphic toxin systems in bacteria*, *MBio* **6** (2015), no. 3 e00285–15.

[175] K.-H. Choi, J. B. Gaynor, K. G. White, C. Lopez, C. M. Bosio, R. R. Karkhoff-Schweizer, and H. P. Schweizer, *A tn 7-based broad-range bacterial cloning and expression system*, *Nature methods* **2** (2005), no. 6 443–448.

[176] R. Balder, J. Hassel, S. Lipski, and E. R. Lafontaine, *Moraxella catarrhalis strain o35e expresses two filamentous hemagglutinin-like proteins that mediate adherence to human epithelial cells*, *Infection and immunity* **75** (2007), no. 6 2765–2775.

[177] M. Desvaux, L. M. Cooper, N. A. Filenko, A. Scott-Tucker, S. M. Turner, J. A. Cole, and I. R. Henderson, *The unusual extended signal peptide region of the type v secretion system is phylogenetically restricted*, *FEMS microbiology letters* **264** (2006), no. 1 22–30.

[178] I. Gentle, K. Gabriel, P. Beech, R. Waller, and T. Lithgow, *The omp85 family of proteins is essential for outer membrane biogenesis in mitochondria and bacteria*, *The Journal of cell biology* **164** (2004), no. 1 19–24.

[179] L. Sánchez-Pulido, D. Devos, S. Genevrois, M. Vicente, and A. Valencia, *Potra: a conserved domain in the ftsq family and a class of β-barrel outer membrane proteins*, *Trends in biochemical sciences* **28** (2003), no. 10 523–526.

[180] N. J. Bulleid, *Disulfide bond formation in the mammalian endoplasmic reticulum*, *Cold Spring Harbor perspectives in biology* **4** (2012), no. 11 a013219.

[181] J. M. Ravasco, H. Faustino, A. Trindade, and P. M. Gois, *Bioconjugation with maleimides: A useful tool for chemical biology*, *Chemistry–A European Journal* **25** (2019), no. 1 43–59.

[182] R. Lutz and H. Bujard, *Independent and tight regulation of transcriptional units in escherichia coli via the lacr/o, the tetr/o and arac/i1-i2 regulatory elements*, *Nucleic acids research* **25** (1997), no. 6 1203–1210.

[183] C. N. Vassallo, P. Cao, A. Conklin, H. Finkelstein, C. S. Hayes, and D. Wall, *Infectious polymorphic toxins delivered by outer membrane exchange discriminate kin in myxobacteria*, *Elife* **6** (2017) e29397.

[184] D. L. MacIntyre, S. T. Miyata, M. Kitaoka, and S. Pukatzki, *The vibrio cholerae type vi secretion system displays antimicrobial properties*, *Proceedings of the National Academy of Sciences* **107** (2010), no. 45 19520–19524.

[185] M. J. Casadaban and S. N. Cohen, *Analysis of gene control signals by dna fusion and cloning in escherichia coli*, *Journal of molecular biology* **138** (1980), no. 2 179–207.

[186] M. Emamalipour, K. Seidi, S. Zununi Vahed, A. Jahanban-Esfahlan, M. Jaymand, H. Majdi, Z. Amoozgar, L. Chitkushev, T. Javaheri, R. Jahanban-Esfahlan, *et. al.*, *Horizontal gene transfer: from evolutionary flexibility to disease progression*, *Frontiers in cell and developmental biology* **8** (2020) 229.

[187] R. M. Stubbendieck, C. Vargas-Bautista, and P. D. Straight, *Bacterial communities: interactions to scale*, *Frontiers in microbiology* **7** (2016) 1234.

[188] J. Mao, A. E. Blanchard, and T. Lu, *Slow and steady wins the race: a bacterial exploitative competition strategy in fluctuating environments*, *ACS synthetic biology* **4** (2015), no. 3 240–248.

[189] J. Sachs and A. Hollowell, *The origins of cooperative bacterial communities*, *MBio* **3** (2012), no. 3 e00099–12.

[190] M. B. Miller and B. L. Bassler, *Quorum sensing in bacteria*, *Annual Reviews in Microbiology* **55** (2001), no. 1 165–199.

[191] G. C. Williams, *Adaptation and natural selection: A critique of some current evolutionary thought*, vol. 61. Princeton university press, 2018.

[192] R. J. Redfield, *Is quorum sensing a side effect of diffusion sensing?*, *Trends in microbiology* **10** (2002), no. 8 365–370.

[193] J. Jumper, R. Evans, A. Pritzel, T. Green, M. Figurnov, O. Ronneberger, K. Tunyasuvunakool, R. Bates, A. Žídek, A. Potapenko, *et. al.*, *Highly accurate protein structure prediction with alphafold*, *Nature* **596** (2021), no. 7873 583–589.